# Investigation of the Efficacy of *in situ* Degradation Methods for Perfluorooctanoic Acid (PFOA) and Perfluorooctane Sulfonic Acid (PFOS) in Groundwater

by

Janice Marie Cooper

A thesis
presented to the University of Waterloo
in fulfillment of the
thesis requirement for the degree of
Master of Science
in
Earth Sciences (Water)
and
Civil Engineering (Water)

Waterloo, Ontario, Canada, 2018

© Janice Marie Cooper 2018

# Author's Declaration

This thesis consists of material all of which I authored or co-authored: see Statement of Contributions included in the thesis. This is a true copy of the thesis, including any required final revisions, as accepted by my examiners. I understand that my thesis may be made electronically available to the public.

# Statement of Contributions

Chapters 2, 3, and 4 of this thesis will be submitted as journal articles. The articles will be co-authored by myself, my supervisors – Dr. Carol Ptacek and Dr. Neil Thomson, and Rachel Baldwin. The majority of the contributions for these chapters was completed by myself (experiments, data analysis, writing). Rachel Baldwin assisted with the experimental work for the investigation of the fluoride-selective electrode in Chapter 2 and the experimental design for the persulfate and permanganate treatment system in Chapter 3. Co-authors made suggestions for the structure of the chapters and provided edits.

# Abstract

Per- and polyfluoroalkyl substances (PFASs) are a group of emerging contaminants that include perfluorooctanoic acid (PFOA) and perfluorooctane sulfonic acid (PFOS). PFASs can be released into groundwater through the application of fire-fighting foam, or effluent from industrial locations, wastewater facilities, and landfill leachate. Human exposure to PFASs should be limited due to the potential for human health implications; PFOA and PFOS are linked to liver, gastrointestinal, and thyroid toxic effects. Removal of PFASs from aqueous solutions can occur through capture, oxidation, reduction, or thermolysis. One of the most popular recent methods for the removal of aqueous PFOA in groundwater is thermally-activated persulfate. The goals of this thesis were to (1) evaluate the performance of a fluoride-selective electrode (FSE) in different matrix combinations that were representative of *in situ* groundwater remediation activities (2) investigate the removal of PFOA and PFOS with the addition of permanganate to thermally-activated or ambient persulfate, and (3) compare the removal of PFOA by thermally-activated or ambient persulfate in different sediment-slurry experiments.

A systematic investigation of the impacts of oxidant-based reagents and a quenching agent, aqueous geochemistry, and the presence of sediments was conducted for the FSE, in order to provide guidance on the use of this analytical tool. The hypothesis was that the quantification of fluoride ($F^-$) using an ultrapure water calibration curve would be inaccurate in some of the combinations tested. Using matrix spike recovery and electrode slope measured in the various matrices as indicators, permanganate, ascorbic acid, and sediments were flagged as components of concern. While either a matrix-matched calibration curve or the standard addition method could be used for samples containing permanganate, the presence of sediments or ascorbic acid should

be avoided for $F^-$ quantification with the FSE. Matrix spike recovery was within the acceptable bounds defined by the USEPA, and the electrode slopes were consistent with the slope of the calibration curve in the presence of persulfate and in different geochemical aqueous phases.

The impact of adding permanganate to both thermally-activated (60 °C) and ambient (20 °C) persulfate treatment systems for the removal of PFOA and PFOS was investigated using a 1:100 molar ratio of permanganate: persulfate. It was hypothesized that permanganate, or the manganese dioxide produced from permanganate in the presence of water, might be able to activate persulfate. Sacrificial, aqueous batch reactors prepared in the laboratory were used in this experiment. Analysis was conducted for pH using a pH probe, aqueous $F^-$ using the FSE, and aqueous PFASs using solid-phase extraction preparation and liquid-chromatography tandem mass spectrometry. PFASs with carbon chain lengths from four to eight were quantified. PFOA was successfully removed (> 99 %) in the thermally-activated persulfate with permanganate (dual-oxidant) and thermally-activated persulfate systems in both ultrapure and sodium bicarbonate simulated groundwater after seven days. Both short-chain PFCAs and aqueous $F^-$ were generated and indicated that PFOA was degraded in these experiments. The removal of PFOA was not evident in the ambient dual-oxidant and heated permanganate systems. The mass balance calculations for the PFOA systems accounted for nearly all of the initial PFOA (81 – 142 %). There was no indication of removal of PFOS by any combination of oxidants, and no degradation products were generated. Removal of PFOA or PFOS was not improved in the thermally-activated or ambient persulfate systems with the addition of permanganate at the tested ratio.

The challenges for the implementation of thermally-activated persulfate for the removal of PFOA in groundwater settings include the interaction of persulfate and PFOA with the aquifer sediments. The hypothesis of this experiment was that PFOA would be removed and converted

into PFCAs and $F^-$ with thermally-activated persulfate treatment, even in the presence of sediments. The removal of PFOA by thermally-activated (60 °C) persulfate (50 mM, 9.6 g $L^{-1}$) was compared using three different sediments in sacrificial sediment-slurry batch reactors. For each reactor, pH, aqueous $F^-$, and aqueous PFCAs were determined, similar to the dual-oxidant experiment. In addition, liquid-solid extraction was used to quantify the sorbed PFASs in the solid phase. At least 60 % of the initial PFOA was removed after seven days in all three sediment slurries using thermally-activated persulfate. Removal of PFOA in all slurry reactors was lower than in aqueous reactors (99 % after 7 days). The detection of degradation products (short-chain PFCAs and $F^-$) was also altered in sediment slurries compared to aqueous reactors. Short-chain PFCAs were retained within the systems longer when sediments were present. The decreased amount of PFCA removal led to the production of less $F^-$. Furthermore, less $F^-$ could be measured in the sediments with high carbonate or organic carbon content. PFOA was extracted at higher concentrations from the sediment with the highest organic carbon content under acidic pH conditions. No removal of PFOA was measured under ambient persulfate treatment conditions. Thermally-activated persulfate was still effective for the removal of PFOA from soil-slurry reactors, but at decreased removal efficiency.

Thermally-activated persulfate can be considered as a potential remediation method for use in the removal of PFOA in groundwater settings. At the ratio tested, permanganate did not improve the effectiveness of persulfate under thermally-activated or ambient conditions. However, the investigation of a wider range of persulfate to permanganate ratios could provide further information. PFOS removal was not observed in thermally-activated or ambient persulfate treatment conditions. The quantification of degradation products, such as short-chain PFASs and

F$^-$, should be included in the analytical suite for any PFAS degradation project. The FSE is a valuable tool for the measurement of aqueous F$^-$ concentrations.

# Acknowledgements

First, I am grateful to my supervisors, Dr. Carol Ptacek and Dr. Neil Thomson, for their patience and assistance through the completion of this project. The additional support from the members of my committee, Dr. Sigrid Peldszus and Dr. David Blowes, is sincerely appreciated.

Second, I am indebted to all the technicians who provided guidance during the extensive method development phase of this thesis: Dr. Julie Marr, Laura Groza, Paul Campanelli, Krista Paulson, and Brian Smith. Many fellow students were invaluable for troubleshooting assistance: Rachel Baldwin, YingYing Liu, Chuan Liu, Sabrina Bedjera, Maria Digaletos, Emily Saurette, and Sara Fellin. Steven Baldwin designed the Arduino control for the hot water bath used in these experiments. I am grateful to all who assisted with fluoride measurements and experiment preparations: Lisa Kester, Viktoriya Bardal, Nicole Russell, Reagan McKinney, Anne Allen, and William McLaren. And to the past and present members of the Groundwater Geochemistry and Remediation group – thank you for your friendship!

Finally, thank you to the family and friends who listened willingly to my incoherent babbling over the past few years. I promise I'll find something else to talk about now.

# Table of Contents

# List of Tables

# List of Figures

# List of Abbreviations

| | |
|---|---|
| AA | Ascorbic acid |
| AC | Activated carbon |
| AOP | Advanced oxidation processes |
| BS | Borden sand |
| C- | Control system |
| CCC | Continuous calibration check |
| CDTA | 1,2-cyclohexane diamine tetra acetic acid |
| DF | Defluorination |
| FA | Filtered after spike |
| FB | Filtered before spike |
| FSE | Fluoride-selective electrode |
| G | Simulated groundwater |
| IC | Ion chromatography |
| IG | PFAS-impacted groundwater |
| IS | PFAS-impacted sediment and tap-water slurry |
| LC-MS/MS | Liquid-chromatography tandem mass spectrometry |
| LSE | Liquid-solid extraction |
| MDL | Method detection limit |
| MeOH | Methanol |
| MRL | Minimum reporting level |
| N | Ultrapure water with NaCl |
| NOM | Natural organic matter |
| OSS | Ottawa silica sand |
| PFASs | Per- and polyfluoroalkyl substances |
| PFBA | Perfluorobutanoic acid |
| PFBS | Perfluorobutane sulfonic acid |
| PFCAs | Perfluorocarboxylic acids |
| PFHpA | Perfluoroheptanoic acid |

| | |
|---|---|
| PFHpS | Perfluoroheptane sulfonic acid |
| PFHxA | Perfluorohexanoic acid |
| PFHxS | Perfluorohexane sulfonic acid |
| PFOA | Perfluorooctanoic acid |
| PFOS | Perfluorooctane sulfonic acid |
| PFPeA | Perfluoropentanoic acid |
| PFSAs | Perfluorosulfonic acids |
| PM | Permanganate |
| PP | Polypropylene |
| PS | Persulfate |
| RO | Reverse osmosis |
| SPE | Solid-phase extraction |
| SRS | South River sediment |
| TCE | Trichloroethylene |
| TISAB II | Total ionic strength adjustment buffer |
| U | Ultrapure water |
| UF | Unfiltered |
| USEPA | United States Environmental Protection Agency |
| UV | Ultraviolet |
| ZVI | Zero-valent iron |

# Chapter 1:  Introduction

Perfluorooctanoic acid (PFOA) and perfluorooctane sulfonic acid (PFOS) are two fully-fluorinated long-chain members of the per- and polyfluoroalkyl substances (PFASs) group present in a variety of manufacturing and industrial materials (Pancras et al. 2016). They are fire resistant (USEPA 2014a) and have both hydrophobic and oleophobic properties (US Department of Health and Human Services 2015). The use and production of PFOA and PFOS has been restricted in Europe (European Union 2006), they have appeared on the Stockholm Convention on Persistent Organic Pollutants (United Nations Environmental Program 2009), and were phased out of production in North America (USEPA 2014a). PFOA and PFOS are the PFASs that were produced in the largest quantities in the United States (USEPA 2014a).

PFOA and PFOS are found in surface water, sediment, sewage effluent, and sludge (Zareitalabad et al. 2013). The highest measured concentrations of PFOA and PFOS are detected in groundwater near military bases (Schultz et al. 2003), fire-training facilities, and emergency response locations (Moody and Field 1999), since these chemicals were used in aqueous film-forming foams to fight fires (Kuroda et al. 2014). PFOA and PFOS have been detected >20 years after the facility or site has been vacated (McGuire 2013). The environmental persistence of PFOA and PFOS is a result of their resistance to biological degradation (Zareitalabad et al. 2013) and low volatility (USEPA 2014a). Furthermore, high water solubility has resulted in the widespread distribution of PFASs in the natural environment (Zareitalabad et al. 2013).

Exposure to PFOA and PFOS may impact human health (Lin et al. 2012). PFOA and PFOS bioaccumulate in organisms, and elevated levels have been linked to kidney and testicular cancer (Rahman et al. 2014), as well as liver, gastrointestinal, and thyroid impacts (Pancras et al. 2016). Groundwater concentrations of PFOA and PFOS have been measured at the threshold limit for

adverse impacts (Kuroda et al. 2014). There is a need to address these emerging contaminants. This introductory chapter provides background on the physical and chemical properties, groundwater concentrations, and potential treatment methods of PFOA and PFOS, as well as describes the specific goals of this thesis.

## 1.1  Physical and Chemical Properties of PFOA and PFOS

The structure of PFOA and PFOS results in elevated resistance to chemical reactions. PFOA and PFOS have fully fluorinated, hydrophobic carbon tails (Table 1.1). The complete fluorine substitution in the carbon chain means that electrons are highly retained (Vecitis et al. 2009); fluorine is the most electronegative element, with a Pauling electronegativity value almost two times larger than hydrogen (O'Hagan 2008). The carbon-fluorine bond is one of the strongest known chemical bonds, with a bond dissociation energy of 105.4 kcal mol$^{-1}$; the carbon-hydrogen bond has a dissociation energy of 98.8 kcal mol$^{-1}$ (O'Hagan 2008). Furthermore, the carboxylic acid and sulfonic acid functional groups attached to the carbon tails are highly resistant to oxidation (Rahman et al. 2014).

The behavior of PFOA and PFOS in water is controlled by other physical and chemical properties. Both PFOA and PFOS have low acid dissociation constants (pKa < 3.8) (Goss 2008; Burns et al. 2008; Cheng et al. 2009), which indicates that they are strong acids. A polar, negatively charged functional group is produced through dissociation of the hydrogen atom (Shimadzu 2015), which allows PFOA and PFOS to be water soluble. However, the non-polar, fluorinated chain repels water. Therefore, PFOA and PFOS are most stable at an interface between non-polar and polar substances, hence the use of these compounds as surfactants (Rahman et al. 2014). The accumulation of PFOA and PFOS at interfaces makes the octanol/water partition coefficient (log $K_{ow}$) difficult to quantify (Rahman et al. 2014). The soil organic carbon-water partitioning

coefficients (log $K_{oc}$) for PFASs increase with the length of the fluorocarbon chain. Log $K_{oc}$ values tend to be larger for perfluorosulfonic acids (PFSAs), compared to the equivalent perfluorocarboxylic acids (PFCAs) (Higgins and Luthy 2006). PFOA and PFOS are essentially non-volatile and anionic under typical groundwater pH conditions (USEPA 2014a). These factors contribute to their long half-lives in water: over 92 years for PFOA and over 41 years for PFOS (USEPA 2014a).

## 1.2 Groundwater Occurrences of PFOA and PFOS

Although there is interest in the concentrations of PFOA and PFOS in all environmental media, this research effort is focused on groundwater. The concentrations observed in the environment are usually low (Table 1.2). Background concentrations range from 0.011 – 0.230 µg $L^{-1}$ for PFOA, and from 0.01 – 0.097 µg $L^{-1}$ for PFOS (Atkinson et al. 2008; Quiñones and Snyder 2009; Plumlee et al. 2008; Schaider et al. 2014). For industrial-impacted sites, most locations also have low concentrations (< 0.99 µg $L^{-1}$) of both compounds (Falkenberg et al. 2015; Weiß et al. 2012; Kuroda et al. 2014; Atkinson et al. 2008; Xiao et al. 2015). However, when sampling is conducted within a known release area, concentrations can range up to 6570 µg $L^{-1}$ for PFOA and 2300 µg $L^{-1}$ for PFOS (Schultz et al. 2004).

## 1.3 Potential Treatment Methods

A review of research concerning the treatment of PFASs over the last fifteen years was conducted (Appendix A). In general, PFASs are highly resistant to microbial transformation and other typical environmental degradation processes (USEPA 2014a). Therefore, physical or chemical treatment is required to remove PFOA and PFOS from water. There are four major categories of methods that can remove PFASs: capture, oxidation, reduction, and thermolysis.

Capture methods separate PFASs from the aqueous media, but require further treatment to degrade PFASs. Examples of capture methods include reverse osmosis (RO), nano- and microfiltration, activated carbon (AC) (Vecitis et al. 2009), and ion exchange resins (Rahman et al. 2014). Electrostatic attraction or hydrophobic interaction form the basis of removal via sorption (Pancras et al. 2016). Therefore, pH is important, as positively-charged functional groups on the sorptive material will attract the negatively charged PFASs (Yu et al. 2008). PFOS is more hydrophobic than PFOA, due to the additional fluorinated carbon (Yan et al. 2014). PFSAs also have higher affinity for organic carbon than PFCAs (Higgins and Luthy 2006). Most studies using capture methods remove > 80 % of the aqueous PFOA and PFOS. When both PFOA and PFOS are measured, higher removal of PFOS occurs in capture methods than PFOA (Li et al. 2011; Thompson et al. 2011; Yan et al. 2014; Zhou et al. 2010b; Arvaniti et al. 2014a; Hansen et al. 2010).

PFASs are resistant to oxidation, as fluorine atoms strongly retain their associated electrons (Vecitis et al. 2009). Conventional advanced oxidation processes, using the hydroxyl radical ($^\bullet$OH), ozone ($O_3$), or oxygen ($O_2$) atoms, are not expected to degrade PFOA or PFOS (Stratton et al. 2017; Cummings et al. 2015; Jin et al. 2014; Yang et al. 2013; Tang et al. 2012; Park et al. 2009; Vecitis et al. 2009; Cheng et al. 2008). However, certain advanced oxidation processes (AOP) have potential, such as sulfate radicals ($SO_4^{\bullet-}$) from activated persulfate or advanced photolytic methods (Vecitis et al. 2009). The mechanism for oxidative treatment of PFASs is hypothesized to involve the formation of a perfluorinated radical, removal of the functional group, and then removal of fluorine through hydrolysis reactions (Park et al. 2016; Lee et al. 2012a; Tang et al. 2012; Yamamoto et al. 2007). The oxidative mechanism is summarized schematically (Appendix B), based on hypotheses from the literature (Tang et al. 2012; Hori et al. 2008). PFOA

4

is the compound of interest for over half of the reported oxidative studies; PFOS has only rarely been studied individually. When both PFOA and PFOS are measured, greater removal of PFOA is observed compared to PFOS in all but one study (Lin et al. 2012; Schaefer et al. 2015; Yates et al. 2014; Quinnan et al. 2013; Strajin and Kerfoot 2012; Pancras et al. 2013). The most popular oxidant was persulfate with thermal activation to produce $SO_4^{\cdot-}$ (Houtz and Sedlak 2012; Lee et al. 2013; Lee et al. 2012a; Lee et al. 2012b; Yin et al. 2016; Liu et al. 2012a; Park et al. 2016a; Hori et al. 2008; Yang et al. 2013; Lee et al. 2009; Santos et al. 2016; Lee et al. 2010; Hori et al. 2005; Chen and Zhang 2006; Pancras et al. 2013). The largest barrier to the use of persulfate is that it is not consistently shown to effectively degrade PFOS (Park et al. 2016). In an unbuffered system, the pH of an activated persulfate system can drop below pH 3 (Park et al. 2016). In persulfate treatment under alkaline pH conditions, the hydroxide ($OH^-$) present can scavenge the $SO_4^{\cdot-}$ to produce $^{\cdot}OH$, which is less effective for PFAS degradation (Houtz and Sedlak 2012; Vecitis et al. 2009). Besides persulfate, high removal (> 89 %) of PFOA and PFOS, with high associated defluorination (DF, > 50 %), is reported for electrochemical degradation, ferric iron ($Fe^{3+}$) with hydrogen peroxide ($H_2O_2$), $Fe^{3+}$ with ultraviolet (UV) light, and catalysed photolysis studies (Schaefer et al. 2015; Jin et al. 2014; Mitchell et al. 2014; Vecitis et al. 2009). Permanganate, another oxidant, led to removal of just under 50% of PFOS under high heat conditions.

For a reductive reaction with PFOA or PFOS to proceed, a reduction potential < -2.7 V is required based on the carbon-fluorine bond (Vecitis et al. 2009). This large reduction potential required for effective reduction of PFOA or PFOS can be achieved through the use of hydrated electrons, and elemental alkali/ alkaline metals (Vecitis et al. 2009). Reductive methods are hypothesized to dehalogenate PFASs by replacing the fluorine atoms closest to the functional

group with hydrogen atoms; the $CH_2$ group is then removed to form a shorter chain compound (Appendix B) (Song et al. 2013). Reduction is thermodynamically favorable in anaerobic conditions (Rahman et al. 2014). The removal of PFOS is usually reported as > 90 % from studies using reductive methods (Arvaniti et al. 2015; Ochoa-Herrera et al. 2008; Hori et al. 2006). However, when branched and linear isomers of PFOS are compared, branched isomers have higher DF (78 %) than the linear isomers (18 %) (Ochoa-Herrera et al. 2008). The reductive treatment of PFOA has been shown to have mixed results; complete removal of PFOA occurs with sulfite and UV (Song et al. 2013), but minimal PFOA is removed (38 %) with magnesium-aminoclay coated zero valent iron (ZVI) (Arvaniti et al. 2015). There are fewer pertinent studies for reductive methods (6), compared to oxidative methods (29).

Thermal degradation has been applied to treat solid and aqueous PFASs. Incineration has been used to destroy PFOA and PFOS, with temperatures > 600 °C (Vecitis et al. 2009; Wang et al. 2015). Sonolysis and sonozone can also be classified as thermolytic processes. Micro-bubbles are formed from cavitation after the application of an acoustic field. When these bubbles collapse, high temperature occurs and ˙OH are released. Any contaminants, such as PFASs, that adhere to the bubble surfaces can be pyrolyzed or oxidized (Vecitis et al. 2009). PFOA and PFOS has been removed in less than 3 hours in sonochemical experiments (Cheng et al. 2008; Vecitis et al. 2008; Moriwaki et al. 2005). PFOA has higher removal and DF than PFOS, which could be a result of the secondary oxidation processes occurring at the interface of the bubble (Vecitis et al. 2009). An increase in the power delivered per area increases the removal and defluorination of PFOA and PFOS during sonochemical degradation (Vecitis et al. 2008; Moriwaki et al. 2005). All thermolytic studies have reported high DF values (> 50 %) (Wang et al. 2015; Cheng et al. 2008; Vecitis et al. 2008; Moriwaki et al. 2005).

## 1.4 Research Objectives

Despite the breadth of research surrounding PFASs, many of the proposed remediation alternatives are not viable or require secondary treatment. Research gaps exist around thermally-activated persulfate, specifically relating to the presence of permanganate in persulfate systems, and the removal of PFASs by thermally-activated persulfate in the presence of sediments. Specifically, this thesis aimed to:

1. Investigate the matrix spike recovery and electrode slope for fluoride quantification with a fluoride-selective electrode in matrices representative of field-based remediation conditions,

2. Quantify the degradation of PFOA and PFOS in thermally-activated and ambient dual-oxidant (permanganate and persulfate) conditions, and

3. Evaluate the impact of the presence of different aquifer materials on the degradation of aqueous PFOA by ambient and thermally-activated persulfate systems.

## 1.5 Thesis Organization

This thesis is structured as a collection of research papers covering the body of work completed. The first paper, Chapter 2, describes an investigation that evaluates the use of a fluoride-selective electrode for fluoride detection in samples containing different geochemical compositions, oxidants and quenching agents, and the presence of sediments. Chapter 3 presents the results of a study where permanganate was added to thermally-activated and ambient persulfate systems to remove PFOA and PFOS. Chapter 4 describes the results from an investigation into the ability of thermally-activated persulfate to treat PFOA in the presence of different types of aquifer sediments. The final chapter, Chapter 5, summarizes the major findings from this research.

Table 1.1 : Summary of physical and chemical properties of PFOA and PFOS.
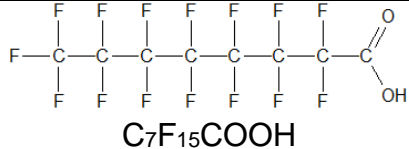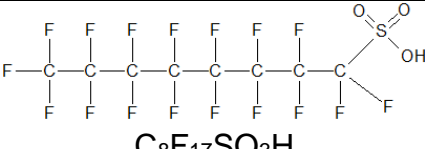
| Name | PFOA | PFOS |
|---|---|---|
| Structure[1] |  $C_7F_{15}COOH$ |  $C_8F_{17}SO_3H$ |
| Molecular Weight (g mol$^{-1}$)[2] | 414.1 | 500.1 |
| pKa | $0^3 - 3.8^4$ | $< 1^5$ |
| Solubility (mg L$^{-1}$) | 4340 (24 °C)[6] | 570[7] |
| Log K$_{oc}$ (L kg$^{-1}$) | $1.47^8 - 2.23^9$ | $2.10^8$ |
| Vapour Pressure (Pa) | 4.17 (25 °C)[10] | $3.31 \times 10^{-4}$ (25 °C)[7] |
| Half- Life (years)[11] | > 92 (25 °C) | > 41 (25 °C) |

1 Linear isomer structure was created in ChemSketch.
2 (United States National Library of Medicine 2011)
3 Goss (2008)
4 Burns et al. (2008)

5 Cheng et al. (2009)
6 Kaiser et al. (2006)
7 Stock et al. (2007)
8 Awad et al. (2011)
9 Park et al. (2016)
10 Bhhatarai and Gramatica (2011)
11 USEPA (2014)

Table 1.2 : Groundwater concentrations of PFOA and PFOS at non-impacted, industrial-impacted, and known-release sites.

| Site | PFOA ($\mu$g L$^{-1}$) | PFOS ($\mu$g L$^{-1}$) | Source |
|---|---|---|---|
| **Non-Impacted Sites** | | | |
| UK (Various) | < 0.024 - 0.230 | < 0.011 | (Atkinson et al. 2008) |
| USA (Arizona) | 0.01 | 0.01 | (Quinones and Snyder 2009) |
| USA (California) | < 0.018 | 0.019 – 0.087 | (Plumlee et al. 2008) |
| USA (Massachusetts) | < 0.022 | < 0.097 | (Schaider et al. 2014) |
| **Industrial-impacted Risk Sites** | | | |
| Denmark (Airfield) | < 0.01 – 7.5 PFASs (Mostly C6, C7) | | (Falkenberg et al. 2015) |
| Germany (Fire-Fighting Activities) | < 0.01 – 0.16 | 0.02 – 8.35 | (Weiß et al. 2012) |
| Japan (Various Impacts) | < 0.00025 – 1.8 | < 0.00025 – 0.99 | (Kuroda et al. 2014) |
| UK (Airfield) | < 0.024 – 0.070 | < 0.011 – 0.154 | (Atkinson et al. 2008) |
| UK (Fire-Fighting Activities) | 0.027 – 0.036 | < 0.011 – 0.040 | (Atkinson et al. 2008) |
| UK (Industrial) | 0.024 – 0.064 | < 0.011 - 0.015 | (Atkinson et al. 2008) |
| USA (Old Disposal Site) | < 0.1 – 20 | < 2 | (Xiao et al. 2015) |
| **Known-Release Area** | | | |
| USA (Airfield) | < 6570 | < 2300 | (Schultz et al. 2004) |
| USA (Airfield) | < 105 | 4 – 110 | (Moody et al. 2003; Schultz et al. 2004) |

# Chapter 2: Evaluation of Direct Measurement of Fluoride Concentration with a Fluoride-Selective Electrode for Applications in Advanced Oxidation Remediation of Sites Contaminated by Per- and Polyfluoroalkyl Substances

## 2.1 Executive Summary

Determinations of fluoride ($F^-$) concentration in groundwater can be used as an independent method to evaluate degradation of per- and polyfluoroalkyl substances (PFASs) at contaminated sites. In this study, different combinations of groundwater matrices, oxidant reagents and a quenching agent, and sample-handling procedures for the presence of sediments were utilized to assess their impact on determinations of $F^-$. The quantification of $F^-$ was evaluated for the fluoride-selective electrode (FSE) for each of the combinations using matrix spike recovery (acceptable range 75 – 125 %) and electrode slope performance (ideal range -54 – -60 mV). For all of the unaltered aqueous matrices considered, ultrapure water, ultrapure water with sodium chloride, and simulated groundwater, matrix spike recoveries were above 93 % and acceptable electrode slopes ($-59.5 \pm 0.2$ mV) were measured. The addition of two oxidants resulted in matrix spike recoveries and electrode slopes of: persulfate (87 %, $-58.4 \pm 1.3$ mV), and permanganate (93 %, $-47.3 \pm 2.2$ mV). To quantify $F^-$ using the FSE in matrices containing permanganate, either a matrix-matched calibration curve or the method of standard additions should be used. The addition of ascorbic acid, a preservative used in oxidant-based treatment systems, resulted in a decrease in matrix spike recoveries to < 74 %. The presence of ascorbic acid in $F^-$ samples for the FSE should be avoided in favour of alternate quenching procedures. Removal of sediments by filtration prior to the addition of fluoride led to improved matrix spike recoveries (> 96 %); otherwise fluoride spikes

added in the presence of sediments were underestimated using the FSE. The use of a FSE at remediation field sites utilizing oxidant-based reagents should be approached with care to ensure accurate results are obtained.

## 2.2 Introduction

Contamination of groundwater by per- and polyfluoroalkyl substances (PFASs) is an emerging global issue (Moody and Field 1999; Zareitalabad et al. 2013; Kuroda et al. 2014), since potential threats to human and environmental health have been identified (USEPA 2014a). In response, there has been a growing interest in technologies to treat groundwater impacted with PFASs (Park et al. 2016; Yin et al. 2016; Schaefer et al. 2015). Chemical oxidation using persulfate and permanganate has shown some promise, as demonstrated in recent studies (Park et al. 2016; Yin et al. 2016; Liu et al. 2012b). To evaluate the effectiveness of degradation processes, it is standard practice to quantify degradation products, in addition to the concentration of the parent compounds (Song et al. 2017). Increased aqueous fluoride ($F^-$) concentration during treatment is a strong indicator of PFAS degradation (Vecitis et al. 2009).

A variety of techniques can be used to quantify aqueous $F^-$ concentration, including a fluoride-selective electrode (FSE) (*e.g.*, Frant and Ross 1968; Harwood 1969; Kauranen 1977; Nicholson and Duff 1981; Barnard and Nordstrom 1982; Kissa 1983), colorimetry (Crosby et al. 1968), ion chromatography (IC) (Saha and Kundu 2003), and proton-induced gamma emission (Fazlul Hoque et al. 2002). The USEPA recommends the use of the FSE and IC in their standard methods (USEPA 1997; USEPA 1996). The FSE is a portable and inexpensive option (Sousa and Trancoso 2005) that may be suitable for a wider range of users than the IC. In addition, elevated concentrations of other ionic species can overload the analytical column on the IC, and impact quantification of other ions (Chromatography Today 2014). The FSE has been shown to be less

11

sensitive to interfering species than traditional colorimetric methods (Crosby et al. 1968). Therefore, the FSE can be considered an attractive method for quantifying $F^-$ in field samples containing oxidant-based reagents.

The FSE measures the activity of $F^-$ ions in aqueous solutions and links the $F^-$ activity to concentration through a calibration curve. FSEs are available from many different manufacturers, and all operate using the same principles (*e.g.*, Cole-Parmer Company 2008; Thermo Scientific 2011; Hanna Instruments, n.d.). The potential across a lanthanum fluoride crystal is measured when the electrode is submerged in a solution containing $F^-$ ions; only $F^-$ ions are mobile across the crystal (Mikhelson 2013). A pH/ mV meter is used to measure the solution potential from the electrode against an external constant reference potential, which is reported in mV (Mikhelson 2013; Cole-Parmer Company 2008; United States Environmental Protection Agency 1974). A total ionic strength adjustment buffer (TISAB II), is added to samples to produce a uniform ionic strength of background ions, which is important for the $F^-$ ion activity to be measured consistently in different samples (Nicholson and Duff 1981; USEPA 1996; Frant and Ross 1968). The buffer also maintains the sample pH between 5 and 5.5, and breaks fluoride ion complexes, which occur with hydrogen, hydroxide, and multivalent cations (Nicholson and Duff 1981; USEPA 1996; Frant and Ross 1968). Calibration curves are generated using a best-fit linear regression fit between the FSE response and a set of standards.

Many studies that use the production of $F^-$ as an indicator of the degradation of PFASs obtain $F^-$ measurements using a FSE (Park et al. 2016; Yin et al. 2016; Santos et al. 2016; Song et al. 2013; Tang et al. 2012). However, few details regarding the methods used for $F^-$ measurement are provided in these studies, and there have been no accompanying studies to investigate the response of $F^-$ measured by a FSE in similar samples. To support the use of the FSE as a tool to

evaluate the remediation of PFASs in groundwater, a systematic evaluation of FSE quantification with different aqueous matrices (ultrapure water, ultrapure water with sodium chloride, simulated groundwater, PFAS-impacted field matrices), oxidant-based reagents and a quenching agent (persulfate, permanganate, ascorbic acid), and filtration of particulate matter was conducted. A bench scale study was used to test these combinations, as it was hypothesized that the measurement of $F^-$ ionic activity by the FSE would be impacted.

## 2.3 Materials and Methods

### 2.3.1 Reagents

All reagents were analytical grade and used as received. Sodium hydroxide (99.2 %) and glacial acetic acid (99.7 %) were purchased from Fisher Scientific (Fair Lawn, NJ, US, and Nepean, ON, CA, respectively). Sodium chloride (NaCl, certified ACS grade) was purchased from Merck (Darmstadt, Germany). Powdered sodium fluoride (99 %), L-ascorbic acid (99 %), and 1, 2-cyclohexane diamine tetra acetic acid (CDTA, 98 %) were obtained from Anachemia (Montréal, QC, CA), along with sodium persulfate (Mississauga, ON, CA). Sodium permanganate monohydrate (> 97 %) was purchased from Sigma-Aldrich (St. Louis, MO, US). All water used for rinsing and preparation of solutions was ultrapure water generated by a Milli-Q® direct water purification system (EMD Millipore, 18.2 MΩ·cm at 25 °C), unless otherwise stated.

### 2.3.2 Batch Experiments

Three laboratory aqueous matrices and two field-based matrices were compared for different combinations of reagents and/or filtration (Figure 2.1). The laboratory matrices were selected as clean and controlled aqueous phases with a range of ionic strengths. The laboratory matrices included: ultrapure water (U), ultrapure water with NaCl (N; 20 mg $L^{-1}$ NaCl), and simulated groundwater (G; 80 – 100 mg $L^{-1}$ calcium carbonate in argon-purged ultrapure water,

13

allowed to equilibrate with atmosphere for 2 weeks). The field-based matrices were available as a comparison for real field conditions and included PFAS-impacted groundwater (IG), and a 10:1 (w: w) mixture of tap water and PFAS-impacted sediments from the fire-fighting training area at Canadian Forces Base Borden in Ontario (IS).

The presence of two common chemical oxidants (persulfate (PS, 50 g $L^{-1}$), and permanganate (PM, 0.26 g $L^{-1}$)), and a common quenching reagent (ascorbic acid (AA) at a 4:1 molar ratio AA: PS) were also considered. Persulfate and permanganate were evaluated for their impact on the electrode response due to their potential use as oxidants for the remediation of PFASs (Park et al. 2016; Yin et al. 2016; Liu et al. 2012b). Sulfate and sulfate radicals ($SO_4^{\cdot-}$) are produced from PS (Park et al. 2016), while PM reacts in the presence of water to produce $MnO_{2(s)}$ or $Mn^{2+}$ (Jin 2017). Since the quantification of these products was not conducted as part of this investigation, the matrix-effects determined in solutions containing these oxidants will be attributed to the parent oxidant, with the understanding that a mixture is present. Ascorbic acid was tested as well, as it can be used to quench persulfate and permanganate activity for sample preservation (Liu et al. 2012b; Huling et al. 2011). When AA is added to an aqueous solution containing PS, it acts as a reductant to consume the PS and $SO_4^{\cdot-}$ (Huling et al. 2011). For PM, the addition of AA reduces the manganese species in the solution to $Mn^{2+}$ (Liu et al. 2012b; Babatunde 2008). Each reagent was tested individually, as well as within mixtures (PS + PM, PS + PM + AA), in the laboratory matrices.

For the PFAS-impacted groundwater (IG) and PFAS-impacted sediments mixed with tap water (IS), filtration was tested as a result of the presence of particulates, which included soil and manganese dioxide ($MnO_{2(s)}$) precipitates from the permanganate reaction (Cha et al. 2012). For the field-based matrices, some were left unfiltered over the entire procedure (UF), allowing for the

evaluation of FSE performance in samples where the F$^-$ ions from the matrix spike had time to interact with particulates and when measurements of F$^-$ were taken in aqueous samples containing particulates. Others were spiked with the F$^-$ standard and then filtered (FA), which would identify the change in behaviour of the FSE when the F$^-$ ions interacted with the particulates, but these particulates were removed prior to measurement. Finally, the last group of field-based matrix samples were filtered prior to the addition of the F$^-$ standard (FB); no interaction between the F$^-$ matrix spike or the FSE and particulate matter occurred. Acrodisc® 25 mm syringe filters with 0.45 µm GH Polypro membrane (Life Sciences, Mississauga, ON, CA) were used for the filtering of F$^-$ samples in the IG and IS matrices.

For each of the laboratory matrices, 45 mL of the stock aqueous phase was massed into a clean 50 mL polypropylene (PP) centrifuge tube (VWR, Radnor, PA, US). If applicable, solid PS, PM, and/ or AA was massed and added to the centrifuge tube. As part of a separate investigation, all three reagents (PS, PM, AA) were added to the two field-based matrices at the same initial concentrations as the laboratory matrix samples. Controls without the addition of chemical oxidants and the quenching reagent were evaluated for both the laboratory and field-based matrices. Thus, the focus of this study was on the impact of the remnants of these three reagents on the determination of F$^-$ concentration by the FSE. A sufficient volume of the treated (PS + PM + AA) and untreated (Control) field-based matrices was available for use in this study. These matrices were shaken to homogenize the mixture (aqueous and solids), and then 45 mL was decanted into clean 50 mL PP centrifuge tubes.

For both laboratory and field-based matrices, three separate 10 mL aliquots were removed from the centrifuge tube with a pipette after thorough shaking, filtered if necessary, and then placed into clean 30 mL high density polyethylene bottles (Nalgene, Rochester, NY, US). These three

bottles were used for a blank, low $F^-$ matrix spike (0.2 mg $L^{-1}$ $F^-$), and high $F^-$ matrix spike (2.0 mg $L^{-1}$ $F^-$). The $F^-$ matrix spike was added by pipetting an appropriate volume of aqueous $F^-$ standard. Ultrapure water was added to the blank or low $F^-$ matrix spike as required to ensure a uniform final volume in all three bottles. Further filtration was conducted after the matrix spike, if required for the IG and IS matrices.

### 2.3.3   Fluoride Analysis

A RK-27502-19 FSE (Cole-Parmer) was used in conjunction with an Orion Star A321 pH meter (Thermo Scientific). The TISAB II was prepared using 500 mL ultrapure water, 57 mL glacial acetic acid, 58 g NaCl, and 4.0 g CDTA. Solid sodium hydroxide was added to adjust the pH of the buffer to between 5.3 and 5.5, and then ultrapure water topped the total TISAB II volume up to 1 L. Calibration curve standards and samples were prepared to a total volume of 20 mL with a 1:1 volumetric ratio to TISAB II. After adding the TISAB II, samples and standards were left for at least 20 minutes to allow for decomplexation and stabilization. A mini Teflon stir bar (Fisherbrand, Ottawa, ON, CA) was placed inside the bottle, and the bottle was placed on a Thermolyne Climarec™ magnetic stir plate (Thermo Scientific). While the sample or standard was constantly and slowly stirred, the electrode was suspended in the container so that the tip was fully submerged. Readings were taken every minute, for at least 5 minutes, or until 2 consecutive readings were within 0.1 mV of each other. The electrode tip was rinsed with ultrapure water and blotted with a delicate task wipe (KimTech, Mississauga, ON, CA) between each standard or sample to prevent cross-contamination. A calibration curve spanning 0.2 to 2.0 mg $L^{-1}$ F was used for quantification. The materials and method used in this study for the FSE were selected from the manufacturer's guidelines (Cole-Parmer Company 2008), published scientific methods (USEPA

1974; USEPA 1996), and pertinent literature (Frant and Ross 1968; Harwood 1969; Nicholson and Duff 1981).

Quality assurance and control was conducted using continuing calibration checks (CCC) conducted approximately every 2 hours with random calibration standards to ensure that the FSE readings were consistent over time. Select samples were also analyzed on an IC to compare to F$^-$ measurements determined by the FSE. A Dionex™ ICS-5000$^+$ high-pressure IC system (Thermo Scientific) with an IonPac® AS18 anion-exchange column (Thermo Scientific) was used. The method detection limit (MDL) for F$^-$ on the IC was determined by the analysis of seven separate 0.08 mg L$^{-1}$ standards and was calculated to be 0.007 mg L$^{-1}$. Acrodisc® CR 13 mm syringe filters with 0.2 µm polytetrafluoroethylene membrane (Life Sciences, Mississauga, ON, CA) were used to filter samples prior to IC analysis.

## 2.4  Results and Discussion

### 2.4.1   FSE Calibration and Quality Control

The Nernst equation is used for the FSE to relate differences in potential to a logarithmic scale of F$^-$ activity as given by

$$E(T) - E_o(T) = S(T) \cdot \log X \hspace{4cm} \text{Equation 2.1}$$

where $E$ is the measured potential (mV), $E_o$ is the constant reference potential (mV), $S$ is the electrode slope (mV), $X$ represents the F$^-$ ionic activity, and $T$ shows terms with temperature dependence (Mikhelson 2013; Cole-Parmer Company 2008). As long as the ionic strength of the solution is high and constant, compared to the F$^-$ ionic strength, the activity of F$^-$ can be considered to be proportional to the free F$^-$ concentration (Thermo Scientific 2011; Cole-Parmer Company 2008). The electrode slope in Equation 2.1 can be determined by taking the difference in potential between readings at a 10 times difference in F$^-$ concentration (*i.e.*, high and low F$^-$ matrix spikes)

17

(Thermo Scientific 2011; Cole-Parmer Company 2008). The slope measured by the FSE should range from -54 to -60 mV for a solution temperature between 20 and 25 °C (Thermo Scientific 2011b; USEPA 1996).

The electrode potential for the calibration curve standards were measured each day of sample analysis and these data were consistent for up to 10 days (Figure 2.2). The pooled regression for the calibration curve standards produced an electrode slope of -58.7 mV ($R^2 =$ 0.9989). The limited variation in slope is deemed acceptable considering the minor temperature fluctuations in the laboratory. Cole-Parmer Company (2008) reports that the slope value for this FSE can vary up to 1 mV with a 5 °C temperature change. Ten CCC were preformed over the course of the experiment, and the differences were < 5 % from the initial measurement of the calibration standard. The FSE potential readings stabilized more rapidly in solutions with higher $F^-$ concentration with stabilization times ranging from ~ 20 mins for blank samples to 5 mins for the 0.2 mg $L^{-1}$ $F^-$ standard.

The concentration of $F^-$ in the laboratory matrix controls (without any reagent addition) was measured on the IC and the results were compared to the FSE values calculated from the ultrapure water calibration curve. The $F^-$ concentrations measured by the FSE and IC were within 15 % of each other. The high concentrations of sulfate and ascorbic acid impacted the detection of the $F^-$ peak on the IC by overloading the column and producing distorted peak shapes.

Two parameters were used in this investigation to identify potential matrix effects on the FSE: matrix spike analysis and comparison of electrode slope. Matrix spike analysis can be used to identify potential interferences and method bias for sample matrices (USEPA 2014b); a sample is measured before and after a known mass of an analyte, referred to as the matrix spike, is added. The difference between the two measurements is compared to the theoretical concentration from

the matrix spike and used to calculate the matrix spike recovery (USEPA 2014b). The accepted range for matrix spike recovery is usually between 75 – 125 % (USEPA 1996). For electrodes, the slope in the sample matrix needs to match the slope of the calibration curve (*i.e.*, 54 – 60 mV) for direct measurement using the calibration curve. The electrode slope changes if the FSE does not effectively respond to potential differences, as a result of impeded reference surface potentials or interfering species (Sousa and Trancoso 2005). If both conditions are met, quantification of $F^-$ concentration in the new matrix can be conducted using the calibration curve without adverse effects.

## 2.4.2   Laboratory Matrices

The matrix spike recovery for the three laboratory matrices (U, N, G) with the presence of oxidants PS and/or PM, and/or AA as the quenching reagent, was compared to the laboratory matrix control (Figure 2.4). Two matrix spike recoveries (low $F^-$ spike and high $F^-$ spike) were calculated for each combination of reagents and aqueous matrices, and the average was reported. The matrix spike recoveries determined for all the laboratory matrices were acceptable (> 75 %), except when AA was present (58 – 74 %). The matrix spike recoveries reported for AA only were at least 13 % lower than reported for PS or PM only. The decrease in matrix spike recovery indicates that the presence of AA in samples impacts the measurement of $F^-$ activity by the FSE, whether through a change in ionic strength or the release of $F^-$ complexing agents. The matrix spike recoveries for each separate combination of reagents were consistent (within 5 %) between the three laboratory matrices.

The electrode slopes in the matrix combinations were calculated by taking the difference in electrode potential readings between the high and low $F^-$ matrix spikes. For all laboratory matrices, the PS, AA, and control samples had electrode slopes that were between -57 and -60 mV

(Table 2.1), or within the acceptable range to use the direct measurement method with the calibration curve. The electrode slopes for samples containing PM (PM, PS + PM, PS + PM + AA) were < -50 mV, which would be too low for the use of direct measurement with an ultrapure water calibration curve.

Therefore, in the laboratory matrices, matrix effects caused by AA and PM were identified through matrix spike recovery and comparison of electrode slopes. The presence of AA led to decreased matrix spike recovery, but the electrode slope matched the slope of the calibration curve. The effect observed in samples containing AA can be considered a translational matrix effect, where the intercept is different than the calibration curve as a result of background interference (Ellison and Thompson 2008). In order to measure $F^-$ concentrations in such a matrix, matrix-matched calibration curve standards can be prepared with the same composition of reagents or solution ionic strength, instead of ultrapure water (Stüber and Reemtsma 2004). Other quenching procedures (*e.g.*, ice bath) for PS and PM (Wang et al. 2017a), or immediate measurement of $F^-$ samples could be conducted to eliminate the impacts of AA where quantification of $F^-$ uses the FSE. For samples containing PM, the electrode slopes measured in the PM-containing matrices were < -50 mV. A decreased slope is a rotational matrix effect, which can be corrected using the method of standard additions (Ellison and Thompson 2008). The original $F^-$ concentration can be back-calculated from measurements of $F^-$ matrix spikes in the solution (Skoog et al. 2014). A matrix-matched calibration curve for PM would still be an acceptable method of quantification. Therefore, alternative quantification procedures can be used to quantify $F^-$ using a FSE in samples with matrix effects.

### 2.4.3   Field-Based Matrices

The matrix spike recoveries and electrode slopes for the field-based matrices (IG and IS) were evaluated using the same criteria as the laboratory matrices. The filters used for the field-based matrices were tested for $F^-$ recovery prior to use. Duplicated 0.1 mg $L^{-1}$ and 1.0 mg $L^{-1}$ $F^-$ spikes in ultrapure water were filtered and spike recoveries were > 86 %.

The matrix spike recoveries for the impacted groundwater (IG) samples were almost all acceptable (> 74 %), with the highest recovery observed for the FB conditions (> 99 %) (Figure 2.5). The only particulate matter present in the IG samples would have been the $MnO_{2(s)}$ particles. Since the matrix spike recovery was acceptable in the unfiltered (UF) sample, the presence of $MnO_{2(s)}$ particulates alone does not appear to be an issue for measurement with the FSE. The treatment mixture, including AA, had less of a detrimental impact on the matrix spike recovery in IG compared to the laboratory matrices; the PS + PM + AA matrix spike recoveries were < 8 % lower than the control matrix spike recoveries in IG (compared to < 39 % lower in the laboratory matrices). The PS + PM + AA samples for the field-based matrices were older than the corresponding samples for the laboratory matrices, allowing for additional time for reaction between the quenching agent (AA) and the sulfate and manganese species.   Therefore, the concentration of AA present in these samples might be less than in the fresh laboratory samples, which could be the reason for the decreased impact on matrix spike recovery. The electrode slopes measured in the control IG samples were acceptable to use direct measurement from the calibration curve (-56 to -59 mV; Table 2.2). The slope decreased < -44 mV with the addition of PS + PM + AA. Based on the laboratory matrix results, the decrease in electrode slope can be attributed to the presence of permanganate. As discussed for the laboratory matrices, the decreased slope would

21

prevent the use of direct measurement using the ultrapure water calibration curve for these samples.

For impacted sediment and tap-water slurry (IS) samples, the matrix spike recoveries were all low ($< 38\%$), except for when filtered before the spike (FB $> 96\%$; Figure 2.5). Fluoride spikes that were added in the presence of the sediments from the IS samples (*i.e.*, UF, FA) were not recovered. Furthermore, electrode slope was not acceptable ($< -38$ mV; Table 2.2) for either the control or PS + PM + AA samples. Therefore, direct measurement from the calibration curve could not be used for any of the IS samples. When matrix spike recovery was very low, sorption and/or complexation reactions with $F^-$ likely occurred in the presence of solids. Fluoride can be found in its free, anionic form in environments with low dissolved calcium, few complexation agents (*e.g.,* $Al^{3+}$, $Fe^{3+}$, etc.), slightly alkaline pH, and sandy soils (Edmunds and Smedley 2013). Characterization of the sediment would assist in determining which of these conditions may have contributed to the sorption of $F^-$ in the UF and filtered after the spike (FA) samples. The addition of the TISAB II buffer can assist in the recovery of aqueous $F^-$, as it contains a chelating agent to complex aluminum and iron (USEPA 1974). However, it has not been reported to have any impact on calcium fluoride, and maintains pH within the mixed sample between 5 and 5.5 (Nicholson and Duff 1981; USEPA 1996; Frant and Ross 1968). At a solution pH of $5 - 5.5$, $F^-$ could sorb to the sediments in the sample (Edmunds and Smedley 2013). When oxidative remediation of PFASs occurs in groundwater, the $F^-$ released from degradation is released into aqueous solutions in the presence of aquifer solids. Site conditions must be analyzed to determine the likelihood that $F^-$ ions will remain in the aqueous phase at a specific field site. Therefore, aqueous $F^-$ measurements may be underestimated in field samples, and should be interpreted carefully.

## 2.5 Conclusions and Implications

The FSE accurately measured $F^-$ concentration in laboratory matrices in the absence of reagents as confirmed by the consistency with results from the IC (within 15 % when above MDL). With the use of the buffer under stirred conditions, concentrations of $> 0.2$ mg L$^{-1}$ F$^-$ were measured in ~ 5 mins. The measured electrode potentials for the calibration standards were consistent for 10 days. Matrix spike recoveries and electrode slopes were consistent ($< 5$ % deviation) and within the acceptable limits for the three laboratory aqueous matrix controls investigated (ultrapure water, NaCl water, and simulated groundwater). The matrix recovery in the laboratory matrices in the presence of either persulfate (87 %) or permanganate (93 %) was acceptable; however, the addition of ascorbic acid resulted in matrix spike recovery was $< 75$ %. Electrode slopes measured in laboratory-matrix samples containing persulfate were within the bounds required for direct measurement with the calibration curve, but the electrode slopes measured in samples containing permanganate were $< 50$ mV. For the field-based matrices (PFAS-impacted groundwater and PFAS-impacted sediment and tap water slurry), matrix spike recovery was highest ($> 96$ %) in samples that were filtered before the addition of the F$^-$ spike. When the F$^-$ spike was added in the presence of sediments in the IS samples, matrix spike recovery was very low ($< 38$ %). Direct measurement of samples using the calibration curve could only be conducted with the control IG samples, as the electrode slopes were between -56 and -59 mV. The electrode slopes measured in the presence of the treatment combination (PS + PM + AA) and IS matrix were too low ($< - 43$ mV) to use the ultrapure water calibration curve.

Measurements of F$^-$ using a FSE should not be used for field samples without full awareness of the limitations of this tool. First, the FSE can only be used to measure aqueous F$^-$ concentrations, which is an important limitation in field sites. The presence of sediments was

linked to the removal of aqueous $F^-$ through the experiments in this project. Second, complicated sample matrices can impact the measurement of $F^-$ activity in aqueous samples. This study identified ascorbic acid and permanganate as reagents that would impact the measurement of $F^-$ by the FSE. The adverse effects from the presence of ascorbic acid in the sample matrix can be avoided through the use of alternate quenching procedures or preforming $F^-$ analysis immediately after sampling. Direct measurement of samples containing permanganate using an ultrapure water calibration curve would not produce accurate results, but quantitation could be obtained using a matrix-matched calibration curve or known $F^-$ additions. Bearing these caveats in mind, the FSE can be considered a quick, mobile, and reliable tool for the determination of $F^-$ in aqueous matrices as part of the investigation of PFAS remediation projects.

Table 2.1. Electrode slopes (mV) recorded in different combinations of reagents (persulfate (PS), permanganate (PM), and ascorbic acid (AA)) in all three laboratory matrices (ultrapure water (U), ultrapure water with NaCl (N), and simulated groundwater (G)).

| Reagents | Electrode Slope (mV) | | |
|---|---|---|---|
| | U | N | G |
| Control | -59.3 | -59.7 | -59.4 |
| PS | -58.8 | -57.1 | -59.7 |
| PM | -49.5 | -46.5 | -45.1 |
| AA | -59.8 | -59.3 | -59.8 |
| PS + PM | -44.3 | -46.3 | -45.8 |
| PS + PM + AA | -45.3 | -44.1 | -44.9 |

Table 2.2. Electrode slopes (mV) recorded for the control and treatment (persulfate (PS), permanganate (PM), ascorbic acid (AA)) combinations in the two field-based matrices (impacted groundwater (IG) and impacted sediments and tap water slurry (IS)) under different filtration conditions (unfiltered (UF), filtered after the matrix spike (FA), and filtered before the matrix spike (FB)).

| Reagents | Electrode Slope (mV) | |
| --- | --- | --- |
| | IG | IS |
| Control, UF | -58.3 | -21.6 |
| Control, FA | -57.7 | -34.2 |
| Control, FB | -56.3 | -37.8 |
| PS + PM + AA, UF | -34.3 | -12.2 |
| PS + PM + AA, FA | -20.3 | -6.4 |
| PS + PM + AA, FB | -43.2 | -35.8 |
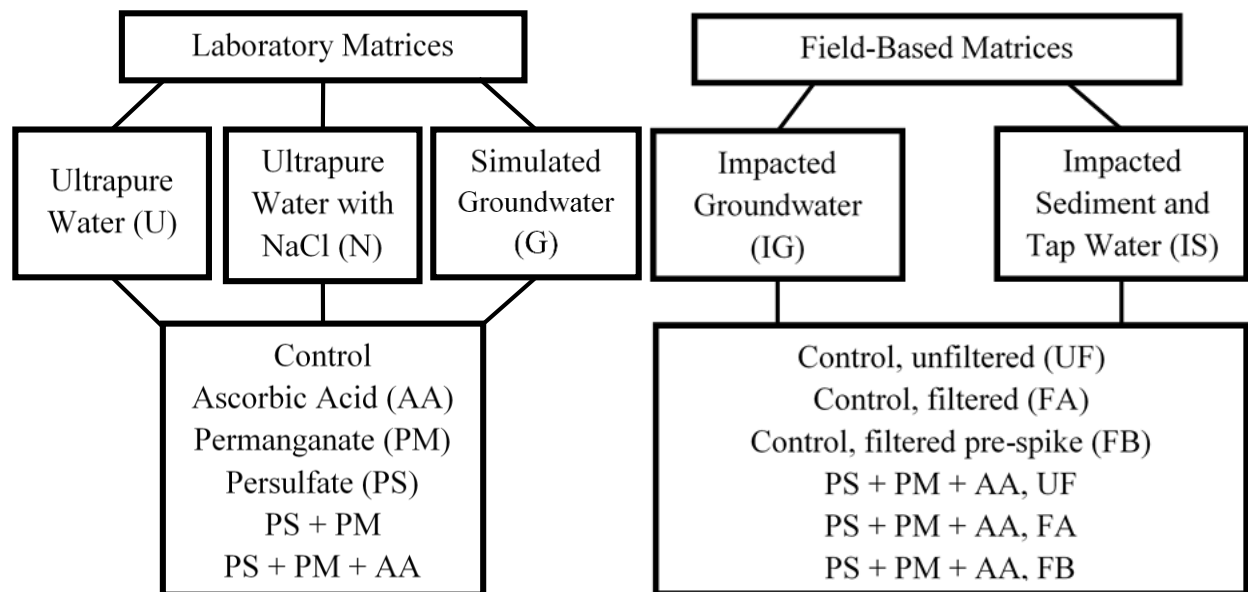
Figure 2.1. Structure of the various combinations used to evaluate each of the laboratory matrices and field-based matrices.
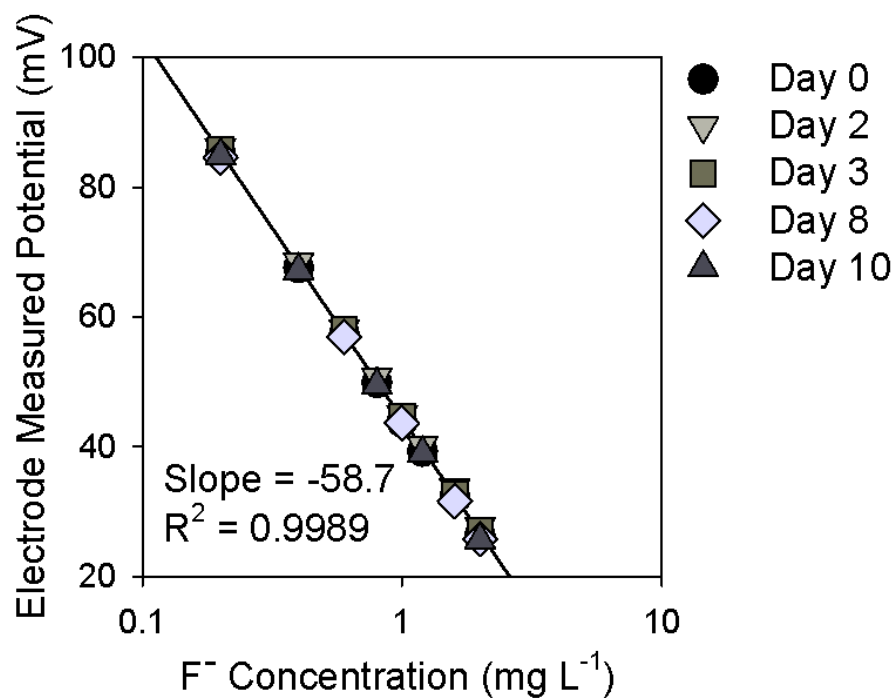
Figure 2.2. FSE calibration curve data for calibration standards used over 10 days of analysis. The $R^2$ value for the pooled data regression for the calibration curves was 0.9989 (Slope = -58.7).
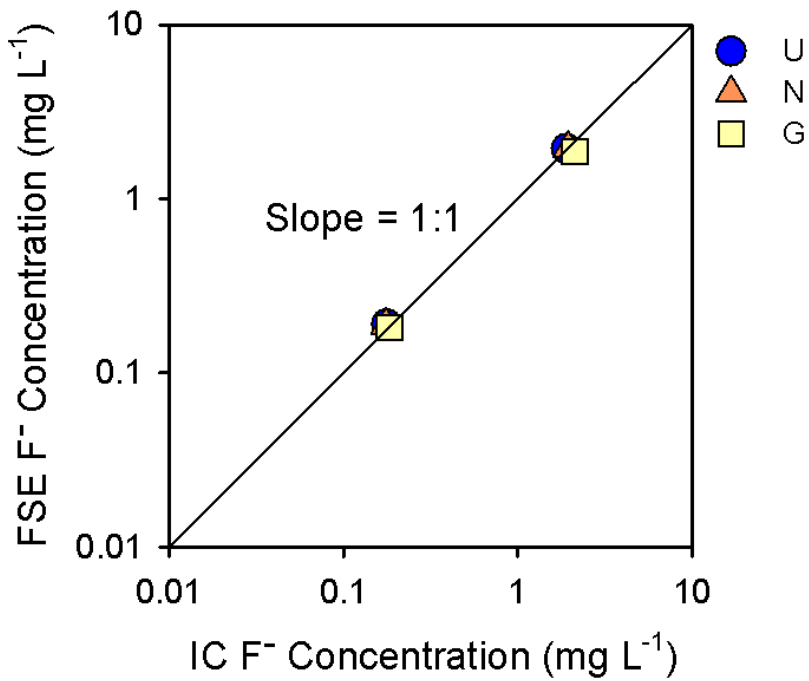
Figure 2.3. Comparison of fluoride concentrations determined by ion chromatography (IC) and the fluoride-selective electrode (FSE) for the 0.2 mg L$^{-1}$ F$^-$, and 2.0 mg L$^{-1}$ F$^-$ samples in the laboratory matrix control samples (no reagents present).
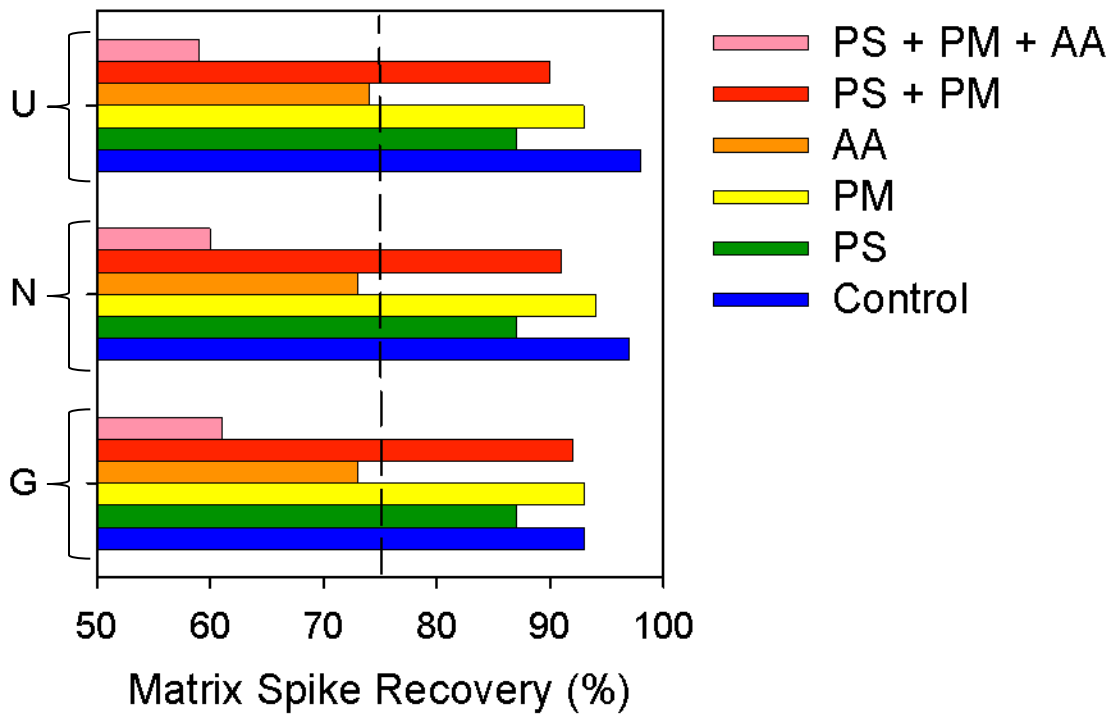
Figure 2.4. Matrix spike recovery (%) for the laboratory matrices (ultrapure water (U), NaCl water (N), and simulated groundwater (G)), in the presence of ascorbic acid (AA), permanganate (PM), and/or persulfate (PS). The Control is the laboratory matrix without any reagents. The vertical dashed line is the lower limit of acceptable matrix spike recovery (75 %), as suggested by the USEPA (1996).
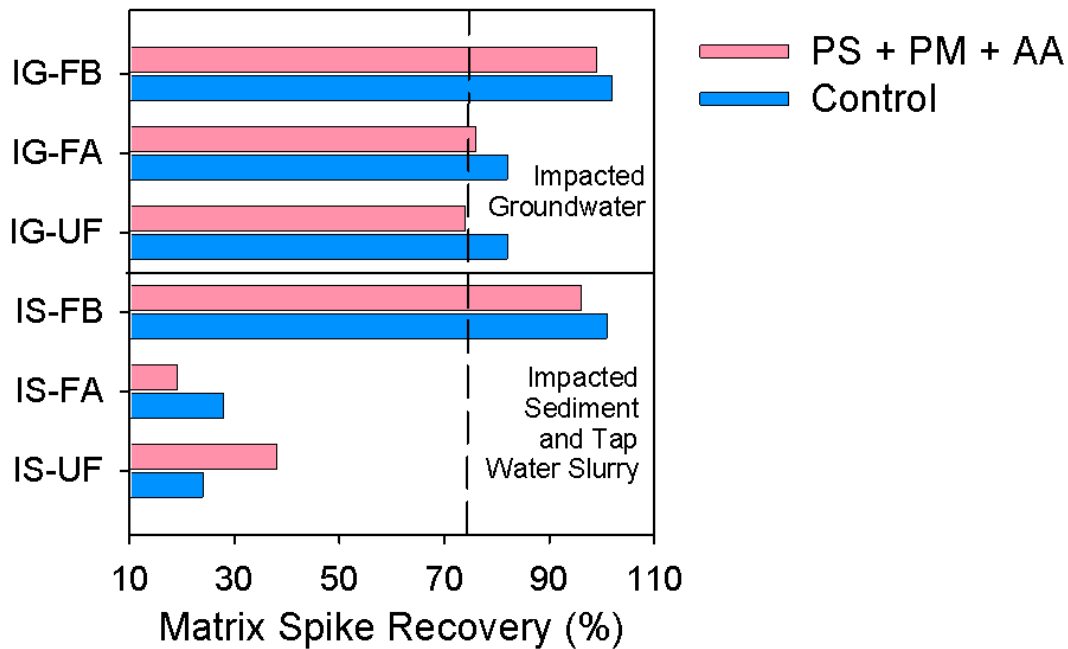
Figure 2.5. Matrix spike recovery (%) for field-based matrices, impacted sediments and tap water slurry (IS), and impacted groundwater (IG). These matrices were prepared as a Control (no reagents added), or with all three reagents added (persulfate (PS), permanganate (PM), and ascorbic acid (AA)). Samples were either unfiltered (UF), filtered before the matrix spike was added (FB), or filtered after the matrix spike was added (FA). The vertical dashed line is the lower limit of acceptable matrix spike recovery (75 %), as suggested by the USEPA (1996).

# Chapter 3: Evaluation of a Thermally-Activated Persulfate System with Added Permanganate for the Treatment of Perfluorooctanoic Acid (PFOA) and Perfluorooctane Sulfonic Acid (PFOS) in Different Aqueous Phases

## 3.1 Executive Summary

Perfluorooctanoic acid (PFOA) and perfluorooctane sulfonic acid (PFOS) are two emerging contaminants with potential human health impacts. A thermally-activated persulfate system with the addition of permanganate (dual-oxidant) was investigated for the treatment of PFOA and PFOS. A molar ratio of 100:1 persulfate: permanganate was used in aqueous treatment experiments heated to 60 °C. Concentrations of short-chain perfluorocarboxylic acids, short-chain perfluorosulfonic acids, and fluoride were measured as indicators of degradation. PFOA removal was observed in ultrapure water in both the thermally-activated dual-oxidant (99.9 %, defluorination of 90 %) and persulfate (99.8 %, defluorination of 91 %) systems after 7 days. A higher initial decrease in PFOA concentrations was observed in simulated groundwater than in ultrapure water for the thermally-activated dual-oxidant and persulfate systems. Slightly less defluorination was observed in the simulated groundwater system (84 – 86 %) at the end of 7 days. No removal of PFOA occurred in systems without heat-activation or persulfate over the experimental period (7 days). PFOS concentrations did not decrease with any combination of oxidants or heat, and no degradation products were detected over an experimental period of 21 days.

## 3.2  Introduction

Per- and polyfluoroalkyl substances (PFASs) are emerging contaminants that include environmentally stable perfluorocarboxylic acids (PFCAs) and perfluorosulfonic acids (PFSAs). The most well-known PFASs are perfluorooctanoic acid (PFOA) and perfluorooctane sulfonic acid (PFOS). Toxicological studies link PFOA and PFOS to health impacts; exposure is associated with impacts to the liver, thyroid, uric acid production, and birth weight (US Department of Health and Human Services 2015; Pancras et al. 2016). Health Canada reports a probable link between PFOA and certain cancers (Health Canada 2016b), while the link between PFOS and cancer requires further study (Health Canada 2016a). Environmental quality standards for PFASs in drinking water recommend concentrations of $0.2 - 0.4$ µg $L^{-1}$ for PFOA (Health Canada 2016b; US Department of Health and Human Services 2015) and $0.2 - 0.6$ µg $L^{-1}$ for PFOS (Health Canada 2016a; US Department of Health and Human Services 2015) to prevent harmful impacts.

PFOA, PFOS, and other PFASs are used in aqueous film-forming foam, surfactants, and lubricants (Pancras et al. 2016); they can enter groundwater through various pathways, such as industrial discharge, fire-fighting activities, wastewater treatment effluent, and landfill leachate (Pancras et al. 2016; Oliaei et al. 2013; Ahrens and Bundschuh 2014). Fighting fires with aqueous film-forming foams containing PFASs can lead to elevated concentrations of PFASs in the environment. For example, Schultz et al. (2004) reported groundwater concentrations as high as 6570 µg $L^{-1}$ for PFOA and 2300 µg $L^{-1}$ for PFOS. These source areas often generate large plumes with low concentrations PFASs ($3 - 120$ µg $L^{-1}$) (Moody and Field 2000; Moody et al. 2003). As a result of the recalcitrant nature of PFASs, these source areas and plumes persist for many years (Moody et al. 2003; McGuire 2013). Thus, to protect human health, sites impacted by PFASs need to be addressed.

Treatment of PFOA and PFOS is complicated by the physicochemical properties of these compounds, including strong C-F bonds, low volatility, and high aqueous solubility (US Department of Health and Human Services 2015; Post et al. 2012). Microbial degradation and environmental photolysis are relatively ineffective for the treatment of PFOA or PFOS in the environment (USEPA 2014a). Pump-and-treat systems using activated carbon can reduce aqueous concentrations of both PFOA and PFOS (Merino et al. 2016; Cummings et al. 2015), but post-treatment incineration of the spent activated carbon is required (USEPA 2014a; Wang et al. 2017b). The desire to degrade PFASs in groundwater has led to the investigation of *in situ* oxidative and reductive technologies, such as electrochemical oxidation, and use of aqueous iodide, dithionite, sulfite, and activated persulfate (PS) (Merino et al. 2016). One of the most often researched technologies for the degradation of PFASs has been thermally-activated persulfate (Park et al. 2016; Yin et al. 2016; Santos et al. 2016; Yang et al 2013; Lee et al. 2012a; Lee et al. 2012b; Liu et al. 2012a; Lee et al. 2010; Lee et al. 2009; Hori et al. 2008).

For the removal of PFOA, thermal-activation of persulfate has been shown in numerous studies to be very successful, with > 80 % removal of PFOA (Park et al. 2016; Yin et al. 2016; Santos et al. 2016; Lee et al. 2012a; Lee et al. 2012b; Liu et al. 2012a; Lee et al. 2010; Lee et al. 2009; Hori et al. 2008). Persulfate dosages range from 2 to 200 mM ($0.5 - 54.1$ g $L^{-1}$) with temperatures ranging from 40 to 90 °C (Park et al. 2016; Yin et al. 2016; Santos et al. 2016; Lee et al. 2012a; Lee et al. 2012b; Liu et al. 2012a; Lee et al. 2010; Lee et al. 2009; Hori et al. 2008). Most studies have used very high input concentrations of PFOA, between 8200 and 155000 µg $L^{-1}$ (Yin et al. 2016; Santos et al. 2016; Lee et al. 2012a; Lee et al. 2012b; Lee et al. 2009; Hori et al. 2008), but thermally-activated PS is also effective at treatment of PFOA at concentrations < 500 µg $L^{-1}$ (Park et al. 2016; Liu et al. 2012a). It is hypothesized that persulfate produces primarily

sulfate radicals ($SO_4^{\bullet-}$) under thermal-activation at pH < 7 (Liang and Su 2009) that are able to degrade PFOA through a step-wise procedure that forms shorter-chain PFCAs and releases $F^-$ each iteration (Park et al. 2016; Yin et al. 2016).

$$S_2O_8^{2-} \xrightarrow{heat} 2SO_4^{\bullet-} \hspace{4cm} \text{Equation 3.1}$$

PFOS is generally more resistant to oxidative degradation than PFOA (Lin et al. 2012; Schaefer et al. 2015; Yates et al. 2014; Quinnan et al. 2013; Strajin and Kerfoot 2012; Pancras et al. 2013). For thermally-activated persulfate, studies have reported conflicting results for the removal of PFOS. At an unreported temperature, 26 % DF of ~ 100000 $\mu$g $L^{-1}$ PFOS occurred in the presence of 18.5 mM thermally-activated PS after 12 hours (Yang et al. 2013). In a different study, at 90 °C with 84 mM PS, no decrease in PFOS was detected from an initial concentration of 450 $\mu$g $L^{-1}$ (Park et al. 2016). Permanganate (PM) has been used as an oxidant to treat PFOS; heated PM (~ 8 $\mu$M, 60 °C) can remove 46 % aqueous PFOS (10:1 PM:PFOS) and the presence of manganese dioxide solid particles ($MnO_{2(s)}$) increases the decomposition of PFOS by PM (Liu et al. 2012b). Different oxidative degradation mechanisms have been proposed for PFOS, which includes the potential formation of PFOA and other PFCAs (Jin et al. 2014; Yamamoto et al. 2007). Removal of PFOA by reductive methods, such as B12-citrate-heat and zero-valent iron, is usually > 90 % (Arvaniti et al. 2015; Ochoa-Herrera et al. 2008; Hori et al. 2006). As PFOA and PFOS are found together in the environment, the identification of a remediation technique that could degrade them both is highly desirable.

A combination of PS and PM is reported to remove both PFOA and PFOS at near ambient temperatures (< 45 °C) (Pancras et al. 2013). Removal of PFOA and PFOS was high (50 – 95 %) after two weeks, even when tested in less than ideal conditions (*i.e.*, concentrations < 30 $\mu$g $L^{-1}$, sediment slurries) (Pancras et al. 2013). Reduction of permanganate occurs in the presence of water

to generate manganese dioxide ($MnO_{2(s)}$) between pH 3.5 and 12 (Watts and Teel 2006; Jin 2017); dissolved $Mn^{2+}$ is formed at pH < 3.5 (Jin 2017). Persulfate can be activated in ambient conditions by electron transfer from transition metals, such as Mn (Sra et al. 2007).

$$S_2O_8^{2-} + M^{n+} \rightarrow SO_4^{\cdot-} + SO_4^{2-} + M^{n+1}$$

Equation 3.2

In a study that looked at a combined permanganate and persulfate system for the removal of organic chemicals such as trichloroethylene (TCE), benzene, and 1-methylnaphthalene, persulfate was hypothesized to be activated by the $MnO_{2(s)}$ (Jin 2017).

$$2S_2O_8^{2-} \xrightarrow{MnO_{2(s)}} SO_4^{\cdot-} + SO_4^{2-} + S_2O_8^{\cdot-}$$

Equation 3.3

In several treatment studies, $SO_4^{\cdot-}$ and hydroxyl ($\cdot OH$) radicals are formed from the activation of PS by manganese (IV) oxides and birnessite ($\delta$-$MnO_2$) (Liu et al. 2014; Ahmad et al. 2010). Therefore, the dual-oxidant system (PS and PM) appears to have conditions suitable for the treatment of both PFOA and PFOS, in addition to removing the requirement for high temperature activation.

The objective of this investigation was to determine whether the presence of PM offers any enhancement to the removal of PFOA or PFOS in a thermally-activated PS treatment system. The PS concentration of 50 mM (9.6 g $L^{-1}$) used is approximately the average of that used by others for a thermally-activated PS system (Yin et al. 2016; Park et al. 2016; Santos et al. 2016). A molar ratio of 100:1 PS: PM in the dual-oxidant systems was used based on the midpoint provided by Pancras et al. (2013). A moderate temperature (60 °C) was selected for this investigation to increase the potential feasibility for *in situ* application; in a critical evaluation of thermal *in situ* heating techniques, temperatures between 80 and 110 °C were often achieved (Kingston 2008). Defluorination (DF), or the moles of fluoride ($F^-$) produced, divided by the total moles of fluoride contributed from the initial PFASs can be tracked as a means of evaluating degradation, in addition

to the formation of short-chain PFASs (Park et al. 2016; Yin et al. 2016; Santos et al. 2016; Hori et al. 2008). A high initial concentration of PFOA or PFOS ($15000$ µg L$^{-1}$) was used to reflect source zone concentrations, as well as improve detection of degradation products. Mass balances that considered the contributions of aqueous PFOA or PFOS, aqueous PFCA or PFSA short-chains, and aqueous F$^-$ were used to summarize and evaluate the extent of degradation.

## 3.3  Materials and Methods

### 3.3.1  Reagents

Methanol-based standards for the PFAS analytes were purchased from Wellington Laboratories (Guelph, ON, CA) and are listed in Table 3.1. PFOA salt ($C_7F_{15}COOH$, 96 %), PFOS salt ($C_8F_{17}SO_3H$, > 98 %), sodium permanganate monohydrate ($MnNaO_4 \cdot H_2O$, > 97 %), and methanol (HPLC grade, > 99.9 %) were obtained from Sigma-Aldrich (St. Louis, MO, US), as well as ammonium acetate ($C_2H_7NO_2$, 99.999 %) (Tokyo, Japan). Sodium persulfate ($Na_2S_2O_8$), sodium fluoride (NaF, 99 %), and 1,2 cyclohexane diamine tetra acetic acid (98 %) were purchased from Anachemia (Montreal, QC, CA). Sodium hydroxide (NaOH, 99.2 %) was obtained from Fisher Scientific (Fair Lawn, NJ, US); glacial acetic acid was also obtained from Fisher Scientific (Nepean, ON, CA). Sodium chloride (NaCl) was purchased from Merck (Darmstadt, Germany). Sodium bicarbonate ($NaHCO_3$, > 99.7 %) was obtained from BDH, VWR Analytical (Radnor, PA, US). All reagents were used as received. Ultrapure water was produced using a Milli-Q® direct water purification system (EMD Millipore, 18.2 MΩ·cm at 25 °C).

### 3.3.2  Treatment Experiments

The removal of PFOA was determined in ultrapure water and simulated groundwater, while PFOS removal was investigated in ultrapure water only (Figure 3.1). For each of these experiments, there were four treatment systems, and three control systems. The treatment systems

37

consisted of thermally-activated dual-oxidant (T-PS/PM/60°C), ambient dual-oxidant (T-PS/PM/20°C), thermally-activated PS (T-PS/60°C), and heated PM (T-PM/60°C), while the control systems consisted of PFOA or PFOS in heated conditions (C-PFOA/60°C or C-PFOS/60°C), thermally-activated PS and PM (C-PS/PM/60°C), and heated blanks (C-BLANK/60°C). The PFOA experiments were run for 7 days, while the PFOS experiment was run for 21 days.

Aqueous batch tests were used in this investigation for increased control and ease of replication. Fifty mL polypropylene (PP) centrifuge tubes (VWR, Radnor, Pennsylvania, US) were used as sacrificial reactors. Ultrapure water or simulated groundwater was added by mass to each reactor. A PFOA aqueous stock solution (100000 µg L$^{-1}$) was prepared in ultrapure water and pipetted into the reactors to an initial PFOA concentration of 15000 µg L$^{-1}$ and a reactor volume of 40 mL. For reactors that did not contain PFOA, a separate ultrapure water spike was used to ensure all reactors had the same total volume. For the experiments run to investigate the removal of PFOS, a large volume of 15000 µg L$^{-1}$ PFOS aqueous solution was prepared, and 40 mL was massed into each reactor, as applicable. Solid sodium permanganate monohydrate was massed and transferred to the reactor to an initial PM concentration of 500 µM. After shaking, solid sodium persulfate was then added to an initial target PS concentration of 50 mM. Both solid oxidants were completely dissolved in all reactors. The reactors were then vortexed (Fisher Scientific, MN 945404) for 30 s and placed in a microcontrolled (Arduino) water bath set at 60 °C on an orbital platform shaker (Lab Line, MN 3520). Ambient reactors were placed on a different orbital shaker (Lab Line) and mixed at room temperature (~ 20 °C).

At each sampling time (Figure 3.1), heated reactors were first quenched in an ice bath. After cooling to ambient temperature, the reactors were vortexed for 30 s. A 5 mL aliquot was removed

for immediate pH measurements using a pH probe (Orion 3 Star, Thermo Scientific). Another aliquot (5 – 10 mL) required for $F^-$ analysis was pipetted into a separate container before the remaining sample was preserved at a 1:1 volumetric ratio of methanol to sample volume. Methanol was also added to quench $SO_4^{\cdot-}$ (Park et al. 2016; McKenzie et al. 2015a). Preserved samples were vortexed and stored at 4 °C after being processed for $F^-$ and PFAS analysis within the same day of sampling.

### 3.3.3   Fluoride Analysis

A fluoride-selective electrode (FSE, RK-27502-19, Cole Parmer) was used in conjunction with a pH meter (Orion Star A321, Thermo Scientific) to determine aqueous $F^-$ concentrations. Total ionic strength adjustment buffer (TISAB II) was used at a 1:1 volumetric ratio with the sample and standards to maintain pH between 5 – 5.5, and minimize $F^-$ complex formation and other interferences (USEPA 1996). Samples and standards were prepared in clean 30 mL high density polyethylene bottles (Nalgene, Rochester, NY, US). After adding TISAB II and mixing thoroughly, samples were left for at least an hour to ensure complete decomplexation (Nicholson and Duff 1981). A mini Teflon stir bar (Fisherbrand, Ottawa, ON, CA) was placed inside the sample container, and the container was placed on a PC-353 magnetic stir plate (Corning). Under constant stirring, the electrode was suspended in the container so that the tip was fully submerged. Readings were taken every minute, for at least 5 minutes, or until two consecutive readings were within ± 0.1 mV (Cole-Parmer Company 2008). A calibration curve spanning $0.2 – 2.0$ mg $L^{-1}$ $F^-$ was used for quantification. Seven matrix matched calibration standards using the same concentrations of oxidants and aqueous phase as the samples were used to address any matrix effects associated with the presence of PM and/or PS. A random calibration standard was measured every five samples, and the change from the value initially recorded for that standard was recorded

to ensure the deviation remained under 5 %. Fluoride quantification was conducted within a few hours of sampling to avoid the use of additional quenching agents. Further details regarding the use of a FSE can be found in Chapter 2.

### 3.3.4   PFAS Analysis

Solid-phase extractions (SPE) were conducted within 1 day of sampling to prepare the samples for PFAS analysis. To improve the quantification of the lower concentration short-chain PFASs, two dilution factors (20x and 1000x) were applied for each sample containing PFOA or PFOS. Methanol-preserved samples were brought to room temperature and vortexed for 30 s prior to preparing for SPE dilutions. The samples were diluted with ultrapure water to a volume of 20 mL to ensure that the resulting concentrations were within the instrument calibration range. All dilutions were spiked with a mixed PFAS mass-labeled internal standard. Prior to use, each sorbent cartridge (Oasis HLB 3cc, Waters Corporation, Dublin, Ireland) was conditioned with 2 mL of methanol, followed by 2 mL of ultrapure water. The diluted sample was passed through a conditioned cartridge under gravity drainage. Ultrapure water (2 mL) was used to wash the cartridge, and the cartridge was vacuumed dry. Two (2) mL of methanol was then used to elute the PFASs from a cartridge and was collected in 5 mL Eppendorf tube (VWR, Radnor, PA, US). The SPE procedure has been adjusted from USEPA (2009) and Yamashita et al. (2004).

PFOA, PFOS and short-chain PFASs were analyzed within two weeks of SPE using liquid chromatography tandem mass spectrometry (LC-MS/MS) on a 6460 Triple Quad LC-MS/MS (Agilent Technologies). The SPE methanol eluate was brought to room temperature, prior to being vortexed and pipetted into new 1.5 mL PP vials (isoSPEC, Mississauga, Ontario, Canada). Injections (10 µL) of each sample were applied to a Pursuit XRs Ultra 2.8 µm C18 2 × 50 mm column (Agilent Technologies), held at 55 °C. The mobile phases were 2 mM ammonium acetate

in ultrapure water (mobile phase A) and 2 mM ammonium acetate in 99:1 methanol: ultrapure water (mobile phase B). The gradient (0.5 mL min$^{-1}$ flow rate) started at 10 % mobile phase B for the 0.5 min, increased to 70 % mobile phase B over the next 4.5 min, held at 70 % mobile phase B for 7 min, dropped back to 10 % for 0.1 min, and held at 10 % mobile phase B to re-equilibrate for 4.9 min. The quantified PFASs eluted between 2.3 and 8.6 min. The mass spectrometer used Agilent Jet Source electrospray ionization in negative mode. The capillary voltage was 3750 volts, and the nebulizer pressure was 414 kPa (60 psi). The gas temperature was kept at 350 °C and a flow of 4 L min$^{-1}$. Sheath gas was kept at 350 °C, with a flow rate of 12 L min$^{-1}$. Qualifier and quantifier transitions are summarized in Table 3.2.

The mixed PFAS mass-labeled internal standard was used in the 7 methanol-based calibration curve standards at the same concentration as the processed samples. The calibration curves for all nine PFASs included in the analytical method were linear over the range of 0.5 to 30 µg L$^{-1}$ (R$^2$ > 0.987). The method detection limit (excluding dilution) for the analyzed PFASs ranged from 0.11 to 1.43 µg L$^{-1}$ (Table 3.1) based on the analysis of seven different 0.5 µg L$^{-1}$ SPE standards. Both a quality control sample and a repeated, random calibration standard were included for every five samples to ensure instrument and sample preparation consistency, as well as to monitor matrix interference. Quality control samples included duplicates, matrix spikes, and SPE standards. The quality control samples were monitored simultaneously for all the PFAS analytes and were flagged if recoveries fell outside the range of 75 – 125 % of the theoretical value (matrix spikes, SPE standards), or were over ± 20% different (duplicates). Values quantified below the minimum reporting level (MRL, MDL × dilution factor) are presented graphically for data interpretation purposes.

## 3.4 Results and Discussion

### 3.4.1 PFOA Treatment in Ultrapure Water at Ambient and Elevated Temperature

Treatment experiments (Figure 3.1) were conducted for the removal of PFOA in ultrapure water using thermally-activated dual-oxidant (T-PS/PM/60°C), thermally-activated persulfate (T-PS/60°C), ambient dual-oxidant (T-PS/PM/20°C), and heated permanganate (T-PM/60°C). The average initial pH was $4.6 \pm 0.5$ for all treatment systems (Figure 3.2). In both the T-PS/PM/60°C and T-PS/60°C systems, the pH decreased to $< 2.0$ in 0.25 days, where it remained for the duration of the experimental period. At a pH $< 3.0$, acid-catalyzed PS degradation occurs where $SO_4^{\bullet-}$ is not formed (Sra et al. 2010).

$$S_2O_8^{2-} + H_2O \xrightarrow{H^+} H_2SO_5 + SO_4^{2-} \qquad \text{Equation 3.4}$$

Therefore, removal of PFOA through reactions with $SO_4^{\bullet-}$ could be limited after pH fell below 3.0 in these systems. At ambient temperature, the T-PS/PM/20°C system only fell to a pH of 3.5. The pH of the T-PM/60°C system increased to pH 7.6. Black-brown solid particles (assumed to be $MnO_{2(s)}$) were visible in the T-PS/PM/60°C and T-PS/PM/20°C system by Day 0.5 and remained until the Day 7. No such particles were visible in the T-PM/60°C system, and it retained the initial purple hue from the addition of PM. Control systems (Figure 3.1) were used to observe the behaviour of PFOA under heat (C-PFOA/60°C), identify any contamination from the oxidants (C-PS/PM/60°C), and determine if background contamination was present (C-BLANK/60°C). For the controls without oxidants (C-PFOA/60°C; C-BLANK/60°C), the pH remained constant at 4.7 – 5.7 through the 7-day experimental period. The oxidant control was similar to the T-PS/PM/60°C system with a terminal pH $< 2.0$.

The initial PFOA concentrations in the ultrapure water reactors (Figure 3.3) were within 81 and 105 % of the theoretical spike concentration of 15000 µg L$^{-1}$. PFOA concentrations

decreased significantly at 0.25 days in the T-PS/PM/60°C (removal of 69 %) and T-PS/60°C (removal of 74 %) systems. This rapid decrease in PFOA concentration using heat and PS is consistent with other studies (Park et al. 2016; Yin et al. 2016; Santos et al. 2016). After 7 days, PFOA removal was > 99 % in T-PS/PM/60°C and T-PS/60°C systems. The T-PS/PM/20°C system showed a slight decrease in PFOA concentration (removal of 12 %) after 7 days. PFOA concentrations increased for the T-PM/60°C system (increase of 29 %). A control (C-PFOA/60°C) was used to evaluate the stability of PFOA under heated experimental conditions; concentration of PFOA increased up to 24 % in the C-PFOA/60°C system after 7 days. PFOA values for each set of duplicate reactors were consistent; on average, values were within ± 10 %. Concentrations of PFOA were below the MRL in the controls used to investigate the reagents, ultrapure water, and reactor materials (C-PS/PM/60°C, C-BLANK/60°C), suggesting that no background PFOA was present in the experimental procedure.

At 0.25 days, short-chain PFCAs and $F^-$ were detected in the T-PS/PM/60°C and T-PS/60°C systems (Figure 3.4). In these systems, short-chain PFCAs were detected between 0.25 and 1 days, but not after 2 days. The release of $F^-$ was observed in the T-PS/PM/60°C and T-PS/60°C systems. At 7 days, the DF in the systems was over 90 %: T-PS/PM/60°C (90 %), and T-PS/60°C (91 %). The high DF observed for these systems indicates that defluorination of PFOA was almost fully complete within 7 days. The present study had a higher DF than other studies; thermally-activated persulfate experiments at 50 °C for the removal of PFOA report DF of 24 % after about 4 days (100 h) (Yin et al. 2016) and DF of 13 – 20 % after more than 1 day (31 h) (Park et al. 2016). A higher release of $F^-$ occurs with increased temperature and a longer experimental period. The measured DF was about 10 % lower than the removal of PFOA for T-PS/PM/60°C and T-PS/60°C. A recent study hypothesized that not all PFOA degradation can be measured

43

through a change in F- concentration, due to the inconsistency between these two values (Yin et al. 2016). In the absence of PS and elevated temperature (T-PS/PM/20°C, T-PM/60°C), no short-chain PFCAs were formed and no F- was released. This result is consistent with the absence of PFOA removal in the experiment (Figure 3.3).

The aqueous PFOA, PFCAs, and F- concentrations measured in each reactor could be used to account for 88 – 125 % of the initial PFOA mass across the experiment for the removal of PFOA in ultrapure water. Mass balances have been reported in several other studies for aqueous samples with quantification down to PFCAs with a carbon chain length of two (C2): 64 – 69 % (Park et al. 2016), 95 – 100 % (Lee et al. 2010), 93 – 96 % (Lee et al. 2012a), 95 – 101 % (Lee et al. 2012b), and 105 % (Yin et al. 2016). The present analysis only included the measurement of PFCAs down to a chain length of four carbons, omitting the inclusion of C2 and C3 PFCAs in the mass balance (up to 22 % of the total in the literature examples). More complete mass balances that included short-chain PFCAs quantified down to C2 PFCAs may have resulted in improved mass accounting for complete degradation pathways.

## 3.4.2 PFOA Treatment in Simulated Groundwater at Ambient and Elevated Temperatures

The complete set of treatment and control combinations was repeated with simulated groundwater as the matrix (Figure 3.1), to determine if a change from ultrapure water to simulated groundwater would modify the rate of removal of PFOA. The preparation of simulated groundwater using 0.8 mM $NaHCO_3$ in ultrapure water was selected to prevent the formation of calcium fluoride. When calcium ($Ca^{2+}$) and F- are present in an aqueous system, the formation of calcium fluorite ($CaF_2$) may occur, limiting aqueous F- concentrations (Edmunds and Smedley 2013) and subsequent analytical detection. The initial pH values in all simulated groundwater

treatment and control systems were higher (average pH $7.5 \pm 0.3$) than the pH in the corresponding ultrapure water systems (Figure 3.2). The pH of the thermally-activated dual-oxidant (T-PS/PM/60°C) and thermally-activated persulfate (T-PS/60°C) systems dropped < 2.0 within 1 day (*i.e.*, acid-catalyzed range for persulfate degradation). Again, at ambient temperature, the pH of the dual-oxidant system at ambient temperature (T-PS/PM/20°C) decreased less (pH of 6.6) than the T-PS/PM/60°C system. The solution pH in the treatment system without PS (T-PM/60°C) was elevated (pH > 8.0) for the entire experimental period. In the control systems, the pH in the C-PFOA/60°C and C-BLANK/60°C systems remained > 8.0, while the solution pH in the reagent control system (C-PS/PM/60°C) dropped < 2.0 after 7 days.

In the simulated groundwater systems, the PFOA removal in the T-PS/PM/60°C and T-PS/60°C systems ranged from 94 – 96 % at 0.5 days (Figure 3.3), which was greater than the removal observed for these systems in ultrapure water (90 % – 91 %). An increase in pH promotes PS degradation (Li et al. 2017), which occurred in the initial stages of these simulated groundwater experiments. For the degradation of another halogenated organic compound (TCE), PS treatment at ambient temperatures (20 °C) is higher in groundwater compared to ultrapure water (Liang et al. 2007). The increased degradation of TCE in groundwater was hypothesized to be a result of the buffering of the pH to neutral pH conditions by the groundwater constituents (Liang et al. 2007). The degradation of TCE was higher when both $^{\bullet}OH$ and $SO_4^{\bullet-}$ radicals were present (pH ~ 7) than when only $SO_4^{\bullet-}$ radicals were present (pH < 4) (Liang et al. 2007). However, removal and degradation of PFOA is enhanced under acidic conditions (Lee et al. 2009). The buffering behavior of the simulated groundwater in this experiment may have simply delayed the transition into acid-catalyzed conditions where $SO_4^{\bullet-}$ radicals would not be generated. After 7 days, the removal of PFOA was > 99 % in both the T-PS/PM/60°C and T-PS/60°C systems, consistent with the

ultrapure water experiment. The PFOA concentration in the T-PS/PM/20°C, T-PM/60°C, and C-PFOA/60°C systems remained relatively constant over the 7-day experimental period. PFOA concentrations were < MRL in the C-PS/PM/60°C and C-BLANK/60°C systems.

The formation of short-chain PFCAs and F$^-$ in the simulated groundwater T-PS/PM/60°C and T-PS/60°C systems was similar to the corresponding ultrapure water experiment (Figure 3.5). Short-chain PFCAs were observed at 0.5 days, but not after 2 days in the T-PS/PM/60°C and T-PS/60°C reactors. Defluorination in these simulated groundwater treatment systems was 4 – 7 % lower than the DF measured in ultrapure water: 86 % (T-PS/PM/60°C) and 84 % (T-PS/60°C) after 7 days. No degradation products were detected in the other systems (T-PS/PM/20°C, T-PM/60°C, and C-PFOA/60°C), consistent with the stable PFOA concentrations. Using the short-chain PFCAs and F$^-$, 81 – 142 % of the initial PFOA could be accounted for in the simulated groundwater systems.

### 3.4.3 PFOS Treatment in Ultrapure Water at Ambient and Elevated Temperatures

The same treatment and control system conditions used in the experiments for PFOA treatment were repeated for the removal of PFOS in ultrapure water (Figure 3.1). The PFOS experiment was run for a longer experimental period of 21 days, as preliminary results did not show any removal of PFOS after 7 days. Consistent with the PFOA ultrapure water experiment, the pH decreased < 2.0 in the thermally-activated T-PS/PM/60°C and T-PS/60°C systems. The T-PS/PM/20°C system had a pH of 3.5 after 21 days, while the T-PM/60°C system rose slightly to 6.3 by Day 21. The pH in the control systems (C-PFOS/60°C, C-PS/PM/60°C, C-BLANK/60°C) were consistent with the control systems used in the ultrapure PFOA removal experiment; the average initial pH was for the ultrapure water PFOS reactors 5.4 ± 1.3. The PFOS concentration data was normalized using the data from the C-PFOS/60 system (Figure 3.6) to account for

46

oscillation of the PFOS concentration around the calculated initial concentration. The concentration of PFOS did not decrease by the end of the 21-day experimental period for any of the treatment systems (T-PS/PM/60°C, T-PS/60°C, T-PS/PM/20°C, T-PM/60°C). The variability of PFOS unadjusted control system concentrations (C-PFOS/60°C) suggests that the 15000 µg L$^{-1}$ aqueous PFOS stock solution was not stable or homogenous while creating the reactors for the various systems (2 days between preparation of stock and reactors). Since the degradation mechanism of PFOS may include the formation of PFCAs (Yamamoto et al. 2007), short-chain PFSAs and PFCAs were both included in the analysis. Other potential degradation products, such as $C_nHF_{2n+1}$ (Yamamoto et al. 2007), were not included in the PFAS analysis. Concentrations of the short-chain PFCAs and PFSAs were very low and consistent throughout the experimental period, and no fluoride was observed in any of the treatment systems (Figure 3.7). Whereas the thermally-activated PS results for PFOS were consistent with those reported in Park et al. (2016), no removal of PFOS in the either of the dual-oxidant (persulfate and permanganate) systems was observed, inconsistent with the results reported by Pancras et al. (2013). Unreported experimental details, such as the ratio of PS: PM, could be one of the reasons for the discrepancy.

## 3.5 Implications

No removal of PFOA or PFOS was evident in the dual-oxidant experiment at ambient temperature (T-PS/PM/20°C), contrary to what was reported by Pancras et al. (2013). The lack of PFAS removal suggests that persulfate was not activated by the presence of permanganate and/ or $MnO_{2(s)}$. The ratio of PS: PM, as well as the form of manganese present in the reactors may have resulted in this lack of activation. Jin (2017) determined that a minimum molar ratio of PS: PM of 1:13 is required for activation of persulfate to occur in experiments for the removal of TCE in aqueous systems. The ratio of 100:1 PS: PM used in this experiment would not have produced

47

sufficient mass of $MnO_{2(s)}$, but was used in this experiment to mimic the conditions from Pancras et al. (2013). Furthermore, not all of the $MnO_{2(s)}$ produced by reactions with target contaminants is able to activate PS (Jin 2017). Since black-brown particles were observed in all of the T-PS/PM/60°C, T-PS/PM/20°C, and C-PS/PM/60°C systems, it can be assumed that $MnO_{2(s)}$ was formed in these experiments. However, the reaction of PM with PFOA or PFOS may have not produced $MnO_{2(s)}$ that would be able to activate PS. The conditions in the ambient dual-oxidant experiment were not observed to activate persulfate to form radical products that were able to degrade PFOA or PFOS.

The addition of permanganate did not increase the removal of PFOA or PFOS in the thermally-activated dual-oxidant (T-PS/PM/60°C) system compared to thermally-activated persulfate alone (T-PS/60°C). An analogy to the combination of permanganate with thermally-activated persulfate can be drawn to the treatment of PFOA by thermally-activated PS with added iron. The removal of PFOA is reduced by the addition of $Fe^{2+}$ at a molar ratio of 1:20000:2000 for PFOA: PS: $Fe^{2+}$ in aqueous experiments with thermal (85 °C) activation (Liu et al. 2012a). Ferrous iron can both activate persulfate to form sulfate radicals (Equation 3.2), and scavenge the produced radicals (Liu et al. 2012a; Lee et al. 2010). A study by Lee et al. (2010) investigated the removal of PFOA with thermally-activated (90 °C) PS, heated zero-valent iron (ZVI), and combined thermally-activated PS and ZVI (PFOA: PS: ZVI, 1:21:15). The combined PS and ZVI system removed more PFOA (59 %) than the persulfate only (39 %) and ZVI only (9 %) systems after 1 hour (Lee et al. 2010). Removal of PFOA can occur from direct reaction with ZVI (Lee et al. 2010). Furthermore, ZVI is oxidized to produce $Fe^{2+}$ slowly, and avoids the build-up of excess $Fe^{2+}$ that can act as a scavenger (Lee et al. 2010). Therefore, enhanced removal of PFOA in the PS + ZVI system would be expected, compared to the PS + $Fe^{2+}$ system. Between the two studies,

higher removal of PFOA by thermally-activated persulfate occurred in the study by Liu et al. (2012a), likely as a result of the much greater molar ratio of PS: PFOA. At lower temperatures (*i.e*., 20, 50 °C compared to 90 °C), enhancement of radical production from PS activated by $Fe^{2+}$ is noted (Zhang et al. 2015). All reactions, including scavenging reactions, occur at increased rates at higher temperatures; therefore, at elevated temperatures, scavenging of radicals by $Fe^{2+}$ may be enhanced (Petri et al. 2011). If these trends could be extended to PS systems with heat and permanganate, the similarity of the T-PS/60°C and T-PS/PM/60°C results in the present study could be attributed to the use of a high persulfate dosage (PS: PFOA, 1380:1), elevated temperature (60 °C), and PS-dominant dosage ratio of PS:PM (~ 99:1). As a result, thermally-activated PS may have become the dominant reaction producing radicals to remove PFOA, limiting any activation of persulfate by PM or $MnO_{2(s)}$ to produce other radicals.

## 3.6 Conclusions

PFOA concentrations decreased rapidly (> 99 % removal in 7 days) in the ultrapure water and simulated groundwater for thermally-activated dual-oxidant (T-PS/PM/60°C) and thermally-activated persulfate (T-PS/60°C) systems. The initial removal of PFOA in the simulated groundwater T-PS/PM/60°C and T-PS/60°C systems was higher than for the ultrapure water systems. Short-chain PFCAs were observed between 0.25 and 2 days. Defluorination of PFOA was 90 – 91 % (in ultrapure water) and 85 – 86 % (in simulated groundwater) in the T-PS/PM/60°C and T-PS/60°C systems. For the PFOA experiments in ultrapure water and simulated groundwater, no PFOA was removed in the ambient dual-oxidant (T-PS/PM/20°C) and heated permanganate (T-PM/60°C) systems after 7 days. PFOS concentration was not observed to decrease, and no formation of degradation by-products was identified after 21 days for all the systems explored. At

the ratio tested (100:1 PS: PM), the removal of PFOA or PFOS did not increase with the addition

of permanganate to a thermally-activated persulfate system.

Table 3.1. PFAS internal and external standards.

| Full Standard Name | Acronym | Chemical Formula | Purity | Internal Standard |
|---|---|---|---|---|
| Perfluoro-n-butanoic acid | PFBA | $C_3F_7COOH$ | - | M3PFBA |
| Sodium perfluoro-1-butanesulfonate | PFBS | $C_4F_9SO_3\text{-}Na$ | - | MPFHxS |
| Perfluoro-n-pentanoic acid | PFPeA | $C_4F_9COOH$ | - | MPFHxA |
| Perfluoro-n-hexanoic acid | PFHxA | $C_5F_{11}COOH$ | - | MPFHxA |
| Sodium perfluoro-1-hexanesulfonate | PFHxS | $C_6F_{13}SO_3\text{-}Na$ | - | MPFHxS |
| Perfluoro-n-heptanoic acid | PFHpA | $C_6F_{13}COOH$ | - | MPFHxA |
| Sodium perfluoro-1-heptanesulfonate | PFHpS | $C_7F_{15}SO_3\text{-}Na$ | - | MPFHxS |
| Perfluoro-n-[2,3,4-$^{13}C_3$] butanoic acid | M3PFBA | $C_3F_7COOH$ | >99% | - |
| Perfluoro-n-[1,2-$^{13}C_2$] hexanoic acid | MPFHxA | $C_5F_{11}COOH$ | >99% | - |
| Sodium perfluoro-1-hexane[$^{18}O_2$] sulfonate | MPFHxS | $C_6F_{13}SO_3\text{-}Na$ | 94% | - |
| Perfluoro-n-[1,2,3,4-$^{13}C_4$] octanoic acid | MPFOA | $C_7F_{15}COOH$ | >99% | - |
| Sodium perfluoro-1-[1,2,3,4-$^{13}C_4$]-octanesulfonate | MPFOS | $C_8F_{17}SO_3\text{-}Na$ | >99% | - |

Table 3.2. Precursor ions (m/z), quantifier product ions (m/z), qualifier product ions (m/z), retention time (min), and method detection limit (MDL, µg L$^{-1}$) for PFASs measured by LC-MS/MS.

| Compound | Precursor Ion (m/z) | Quantifier Product Ion (m/z) | Qualifier Product Ion (m/z) | Retention Time (min) | MDL (µg L$^{-1}$) |
|---|---|---|---|---|---|
| PFBA | 213.0 | 168.9 | N/A | 2.2 | 1.43 |
| PFPeA | 263.0 | 218.9 | N/A | 5.9 | 0.20 |
| PFHxA | 313.0 | 268.9 | 118.9 | 7.0 | 0.14 |
| PFHpA | 363.0 | 318.9 | 168.9 | 7.5 | 0.11 |
| PFOA | 413.0 | 368.9 | 168.9 | 7.9 | 0.11 |
| PFBS | 298.9 | 80.0 | 98.9 | 6.3 | 0.24 |
| PFHxS | 398.9 | 79.9 | 98.9 | 7.6 | 0.19 |
| PFHpS | 448.9 | 79.9 | 98.9 | 8.0 | 0.39 |
| PFOS | 498.9 | 79.9 | 98.9 | 8.5 | 0.20 |
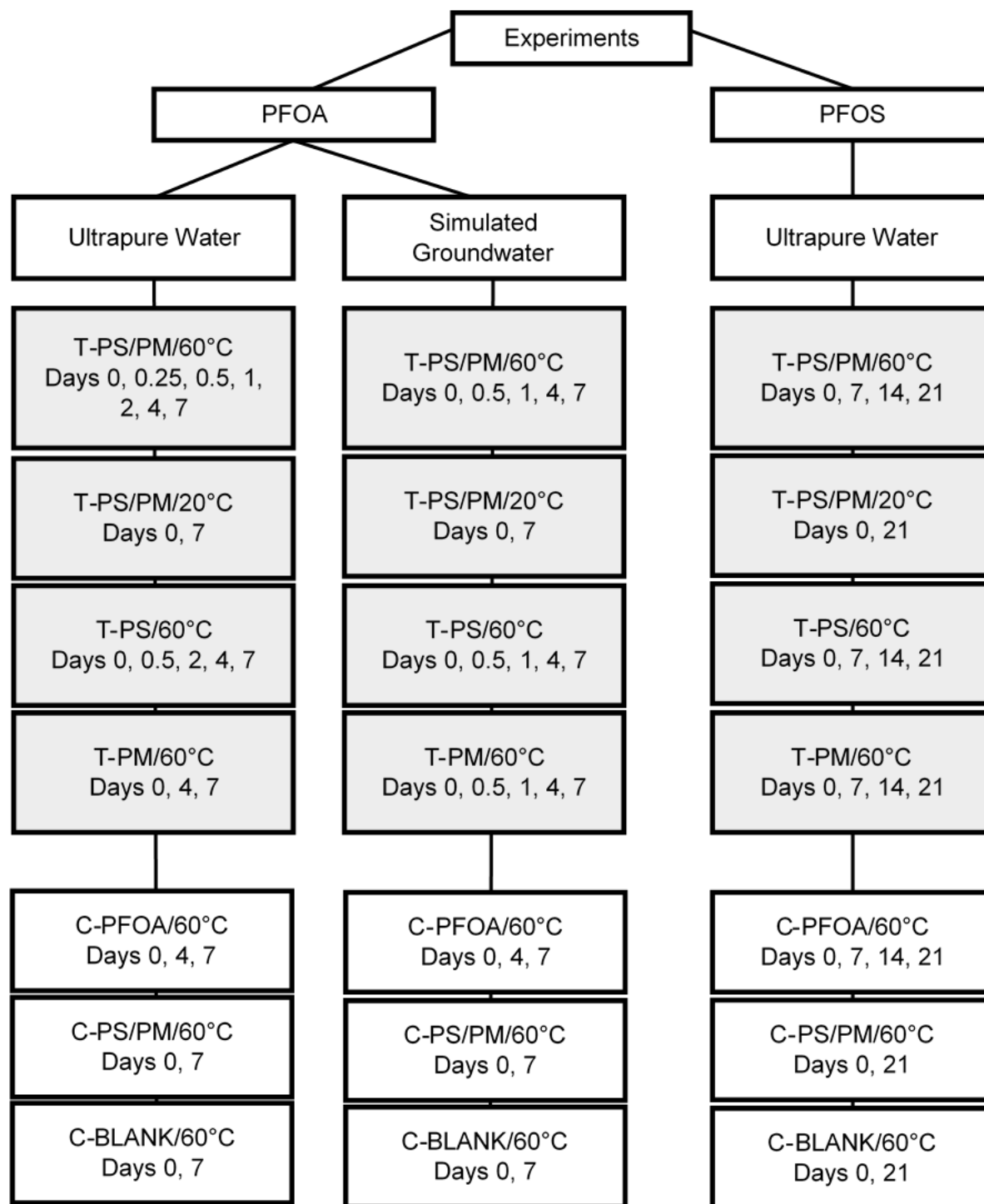
Figure 3.1. Summary of experiments used to investigate treatment (grey-shaded) of PFOA (15000 µg L$^{-1}$) and PFOS (15000 µg L$^{-1}$) using thermally-activated or heated oxidant mixtures (persulfate (PS), 50 mM, and permanganate (PM), 500 µM) in ultrapure water or NaHCO$_3$ simulated groundwater. The control systems (no shading) are also shown. Time points listed represent days when duplicate sacrificial reactors were sampled.
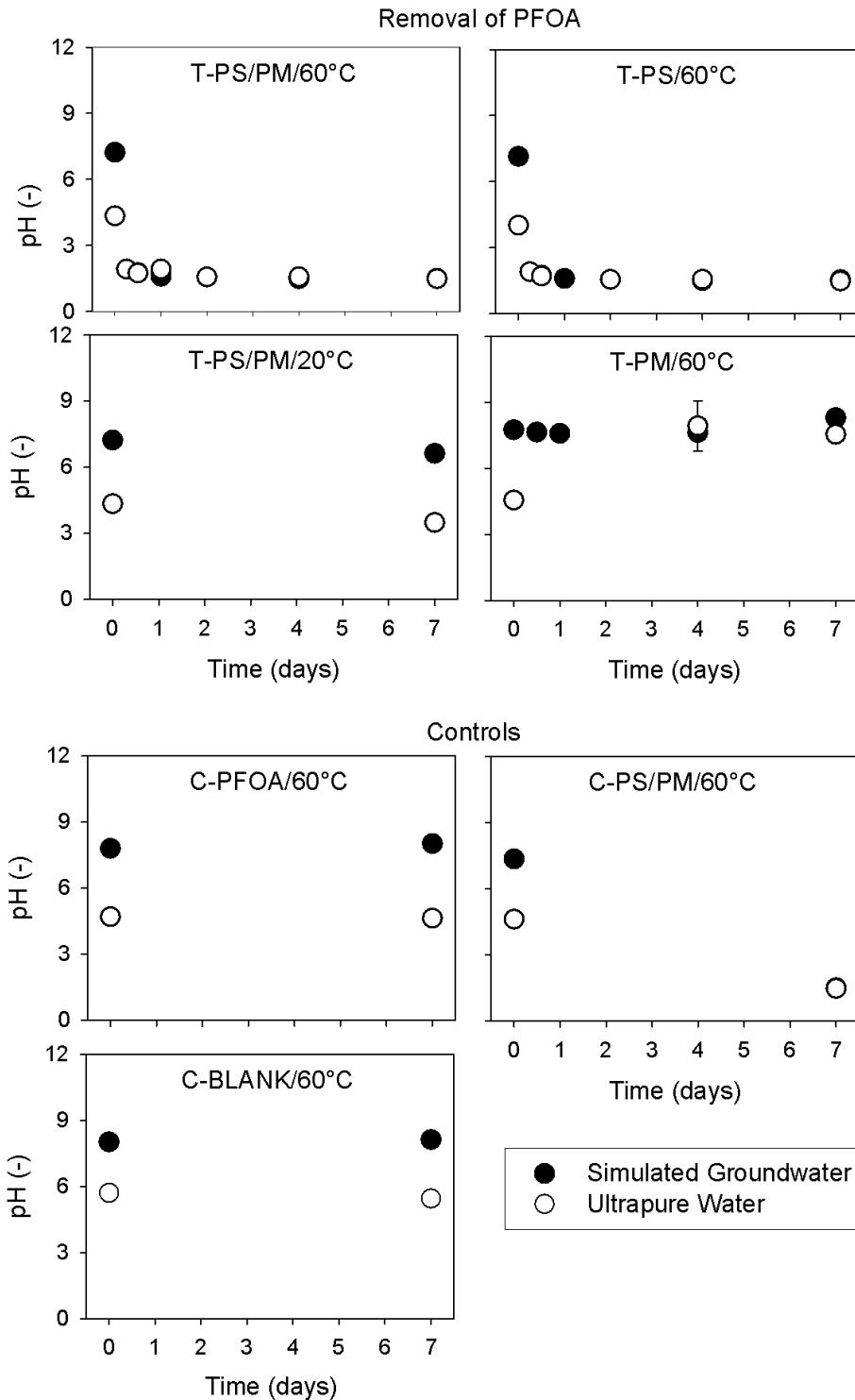
Figure 3.2. pH for all PFOA treatment (top) and control (bottom) systems in both ultrapure water (empty circles) and NaHCO₃ simulated groundwater (filled circles) over the experimental period (7 days). Treatment combinations using persulfate (PS, 50 mM), permanganate (PM, 500 µM), and/ or heat (60 °C) are presented. Each data point is the average of duplicate sacrificial reactors. Error bar indicate maximum and minimum values.
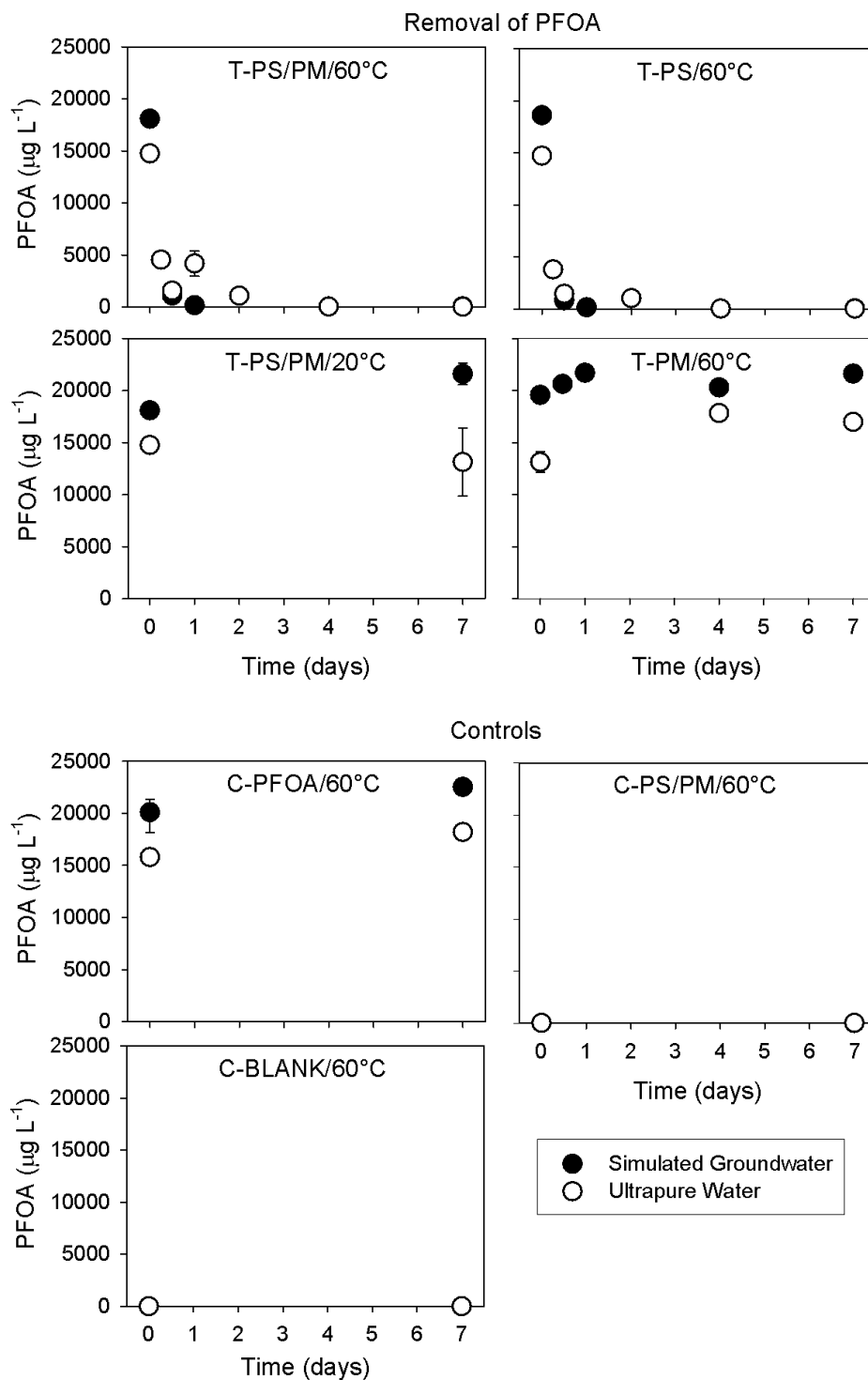
Figure 3.3. Aqueous PFOA concentration (µg L$^{-1}$) over the 7-day experimental period for all treatment (top) and control (bottom) systems in ultrapure water (open circles) and simulated groundwater (filled circles) using persulfate (PS, 50 mM), permanganate (PM, 500 µM), and/or heat (60 °C). The theoretical initial PFOA spike was 15000 µg L$^{-1}$. Each data point represents the average of duplicate reactors. Error bars indicate maximum and minimum values. The MRL for PFOA is 111 µg L$^{-1}$, data below the MRL are shown here for completeness.

55
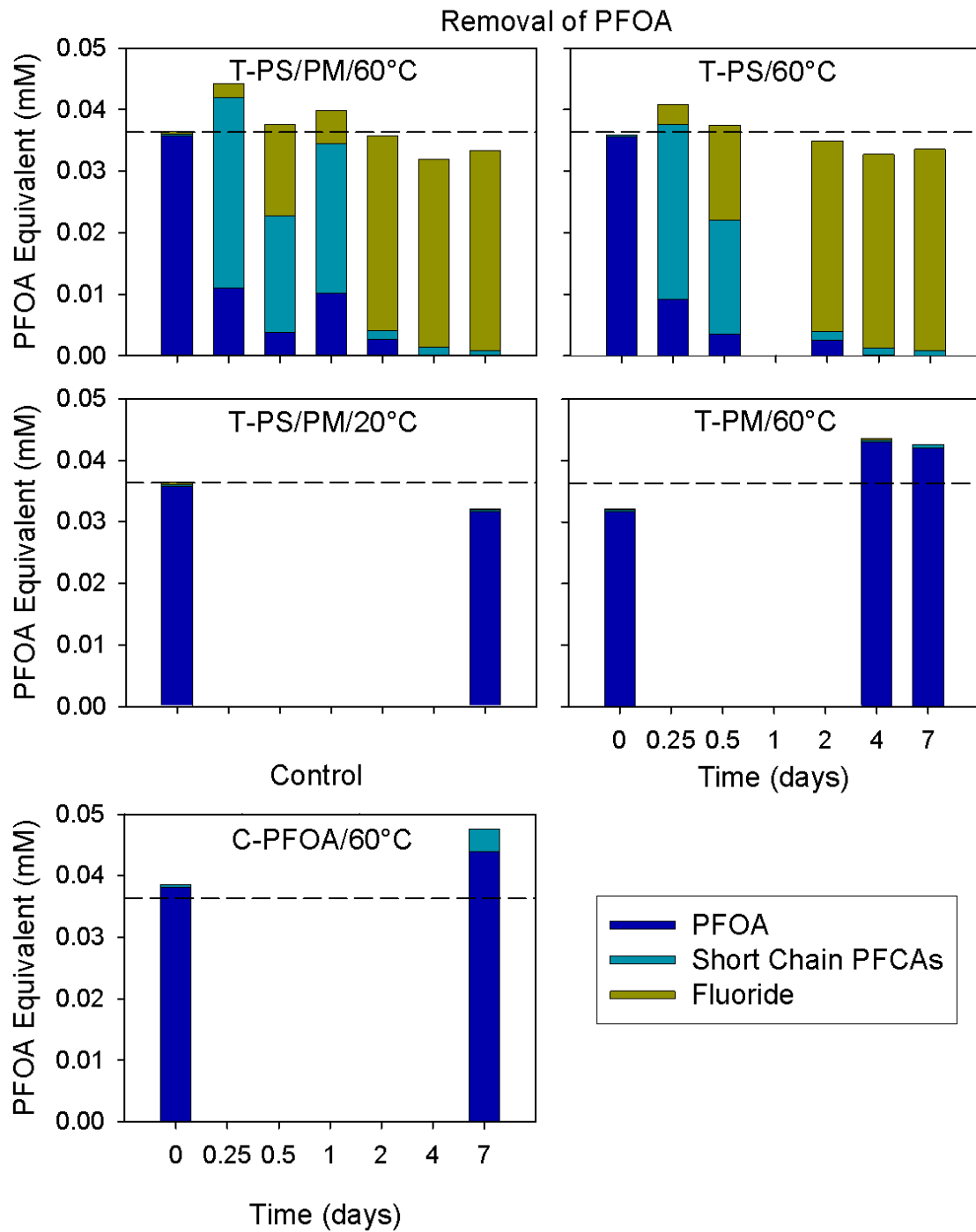
Figure 3.4. Equivalent PFOA concentration (mM) contributed by aqueous PFOA, aqueous short-chain PFCAs, and aqueous F⁻. All treatment systems (top) and the PFOA control system (bottom) in ultrapure water using persulfate (PS, 50 mM), permanganate (PM, 500 µM), and/ or heat (60 °C) are presented. The horizontal dashed line indicates the theoretical initial PFOA concentration of 0.036 mM. The data presented is the average from duplicate reactors.
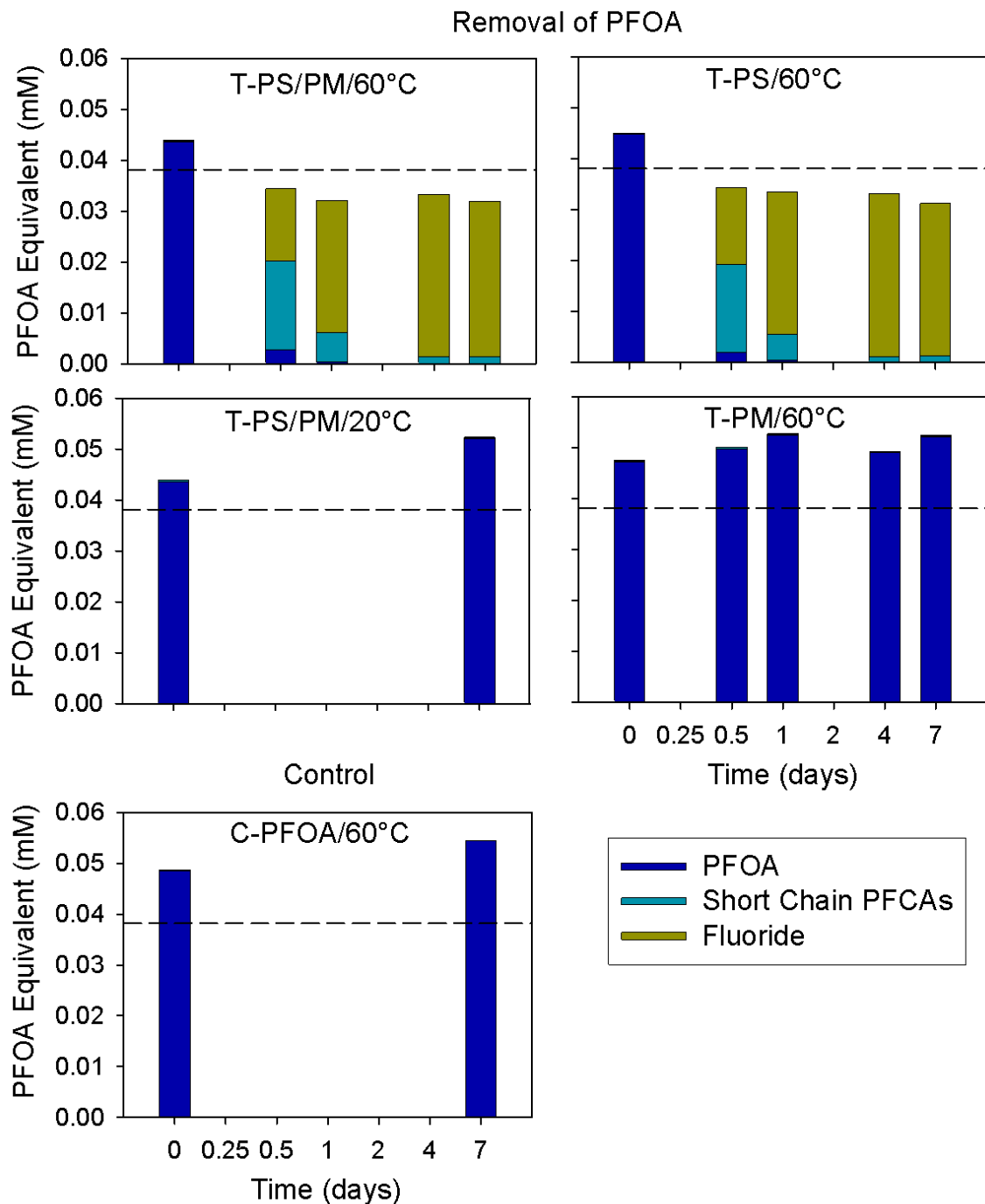
Figure 3.5. Estimate for the mass balance in equivalent PFOA concentration (mM) contributed by aqueous PFOA, aqueous short-chain PFCAs, and aqueous F⁻. The PFOA treatment systems (top) and PFOA control system (bottom) were prepared using simulated groundwater (0.8 mM NaHCO$_3$ in ultrapure water) with treatment from persulfate (PS, 50 mM), permanganate (PM, 500 µM), and/ or heat (60 °C). The horizontal dashed line indicates the initial PFOA concentration of 0.038 mM in these systems. The data shown is the average of duplicate reactors.
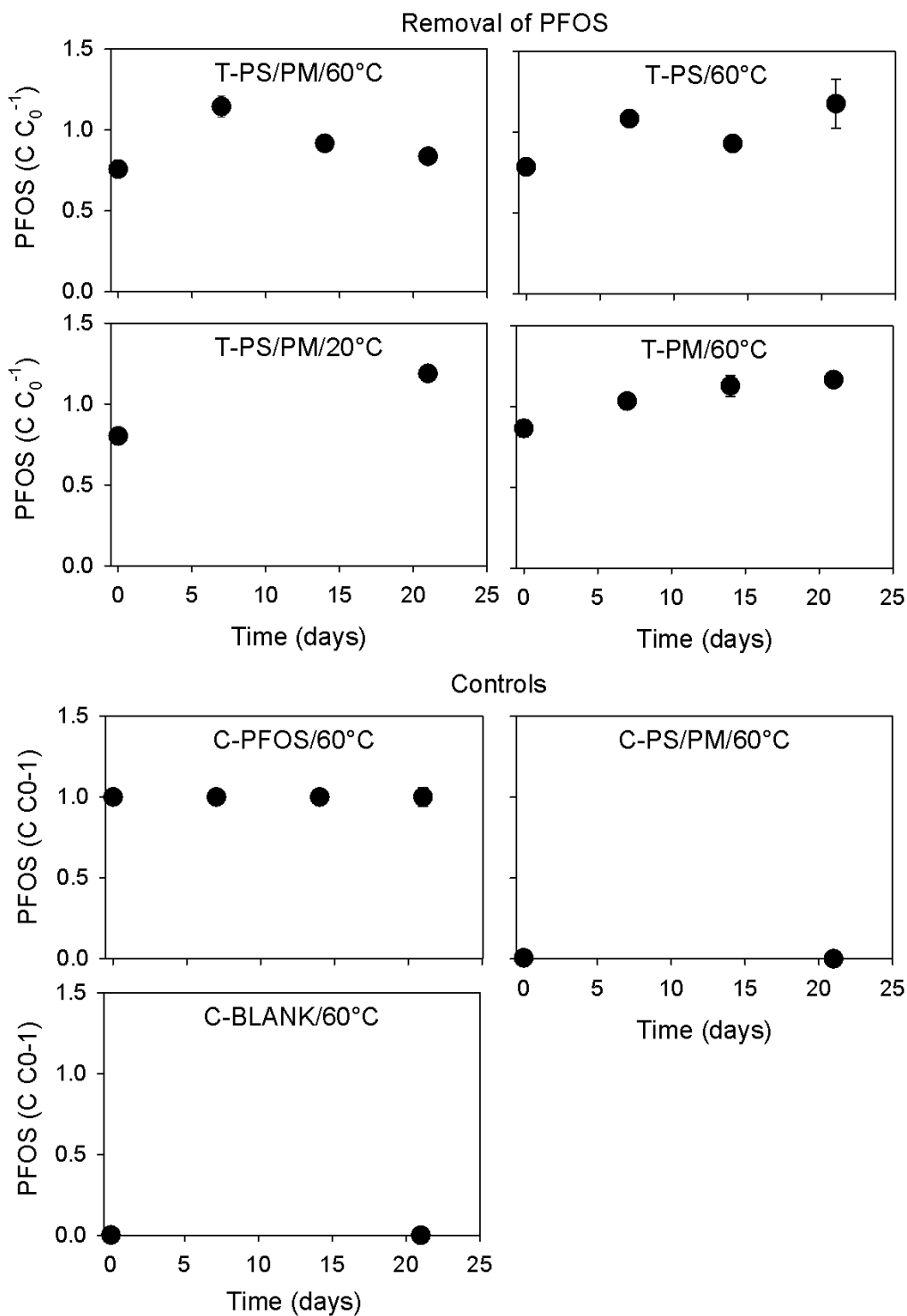
Figure 3.6. Normalized PFOS concentration over a lengthened experiment time (21 days) for all treatment (top) and control (bottom) systems in ultrapure water. Reactors containing an initial theoretical concentration of 15000 µg L$^{-1}$ PFOS were treated with persulfate (PS, 50 mM), permanganate (PM, 500 µM), and/ or heat (60 °C). Each data point represents the average of duplicate reactors, with error bars indicating the maximum and minimum values.
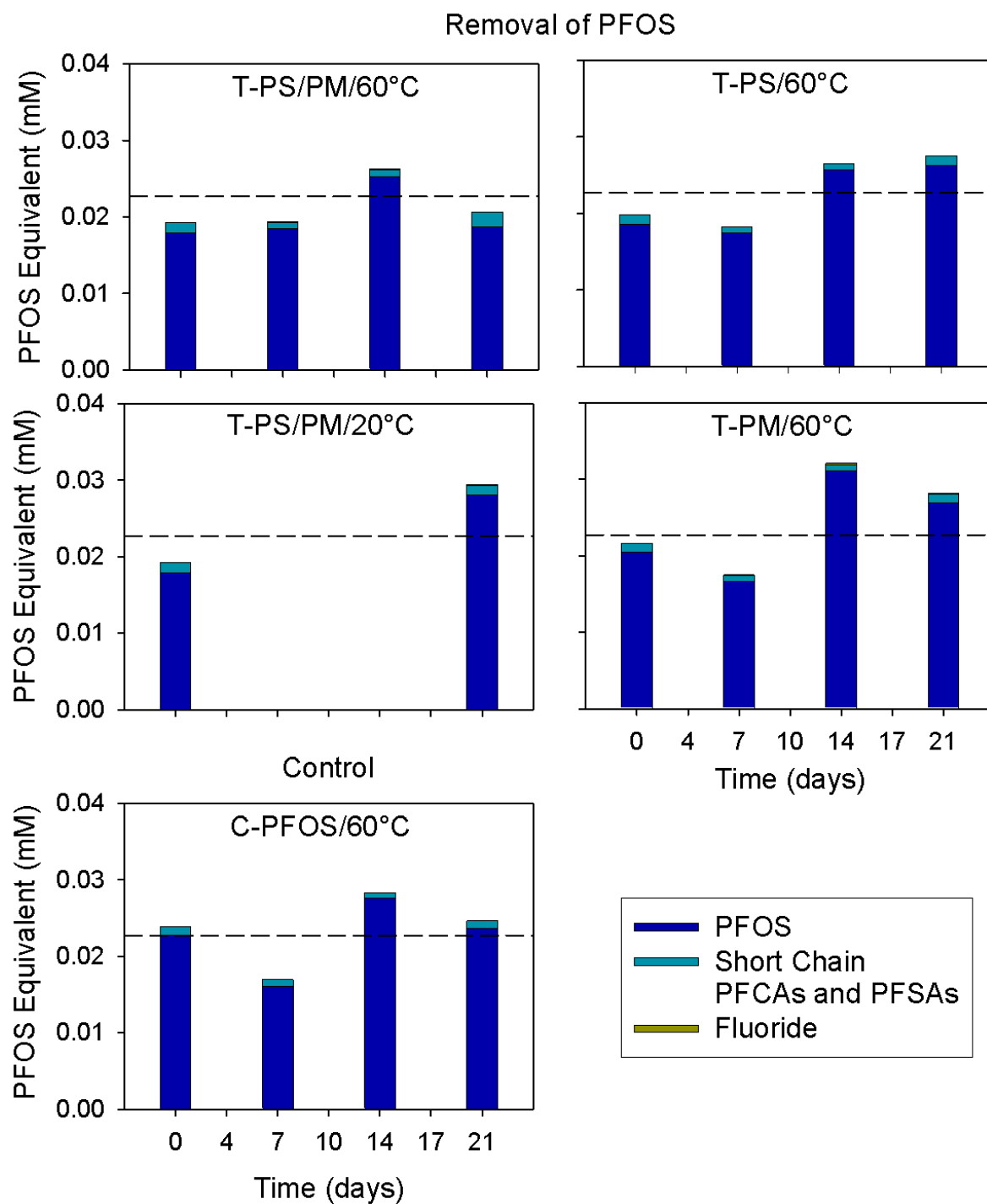
Figure 3.7. Mass balance estimate in equivalent PFOS concentration (mM) contributed by aqueous PFOS, aqueous short-chain PFCAs and PFSAs, and aqueous F⁻. The PFOS treatment systems (top) and PFOS control (bottom) system were prepared using ultrapure water and treated by persulfate (PS, 50 mM), permanganate (PM, 500 uM), and/ or heat (60 °C). The horizontal dashed line indicates the average PFOS concentration in the C-PFOS/60°C system (0.030 mM). The data shown for each sampling time is the average from duplicate reactors.

# Chapter 4: Treatment of Perfluorooctanoic Acid (PFOA) by Thermally-Activated Persulfate in Different Types of Aquifer Materials

## 4.1 Executive Summary

Perfluorooctanoic acid (PFOA) is an emerging contaminant that can be found in groundwater at potentially harmful concentrations. Thermally-activated persulfate has been reported to effectively remove aqueous PFOA, but further information is required to evaluate its potential applicability for *in situ* use. PFOA treatment efficiency in three different sediment-slurries were compared, using silica sand, calcareous sand, and organic-rich river floodplain sediment. Fifty mM persulfate (9.6 g $L^{-1}$) and moderate temperature (60 °C) were used to remove PFOA (15000 µg $L^{-1}$). Over 60 % of the initial PFOA was removed after 7 days by thermally-activated persulfate in all sediments, with the majority of the removal occurring in the first day. In the sediment slurries, there was less removal of PFOA, increased retention of short-chain PFCAs, and lower measured fluoride ($F^-$) concentration than in a corresponding aqueous control. No degradation products (PFCAs or $F^-$) were released from PFOA in the ambient temperature persulfate treatment system. PFOA extracted from the sediments using liquid-solid extraction indicated that the sediment with organic carbon had 4 – 40 times more extractable PFOA than the other sediments, based on extractions from the top 5 cm. However, the extracted PFOA may not be representative of the PFOA sorbed to the bulk sediment mass. Quantification of aqueous $F^-$ in sediments containing carbonate and high organic carbon was likely hindered by the formation of calcium fluoride and sorption. Although the different sediments had varying impacts on treatment

efficiency, removal of PFOA by thermally-activated persulfate did occur in each of the tested sediment-slurries

## 4.2 Introduction

Per- and polyfluoroalkyl substances (PFASs) are used for a variety of industrial and manufacturing processes, including fire-fighting foams, lubricants, and surface treatments (Pancras et al. 2016). Perfluorooctanoic acid (PFOA) is one of the most widely detected PFASs in the natural environment (USEPA 2014a). PFOA is classified as a potential carcinogen (Health Canada 2016b; Pancras et al. 2016; USEPA 2009) and has been linked through epidemiological studies to adverse effects to the thyroid, gastrointestinal system, and liver (Pancras et al. 2016). As such, the recommended environmental quality standard for PFOA in North America is 0.2 – 0.4 µg L$^{-1}$ (Health Canada 2016b; US Department of Health and Human Services 2015). The health concerns associated with human PFAS intake has led to an increase in research concerning the treatment of PFOA. PFOA contamination can often be found in groundwater, resulting in an interest in developing *in situ* remedial technologies (Park et al. 2016).

Many recent studies investigate the possibility of degrading PFASs using activated persulfate (PS). While alkaline (Houtz and Sedlak 2012), iron (Lee et al. 2010), and ultraviolet (Chen and Zhang 2006; Hori et al. 2005) activation methods for PS are used for the removal of PFASs, thermal activation of PS is the most commonly reported method showing effective treatment (Park et al. 2016; Yin et al. 2016; Santos et al. 2016; Lee et al. 2012a; Lee et al. 2012b; Liu et al. 2012a; Lee et al. 2009; Hori et al. 2008).

$$S_2O_8^{2-} \xrightarrow{heat} 2SO_4^{\cdot-} \hspace{4cm} \text{Equation 4.1}$$

Initial aqueous system studies used high temperatures (> 80 °C) and PS dosage (> 50 mM, or > 9.6 g L$^{-1}$) to remove high concentrations of PFOA (> 100000 µg L$^{-1}$) (Hori et al. 2008; Lee et al.

2009). A high degree of defluorination (DF; > 75 %) was measured after 6 hours (Hori et al. 2008; Lee et al. 2009). A wide range of PS dosages (10 – 200 mM, 1.9 – 38.4 g L$^{-1}$) and temperatures (40 – 90 °C) have since been tested, with PFOA removal greater than 80 % for all studies (Santos et al. 2016; Lee et al. 2012a; Lee et al. 2012b; Liu et al. 2012a). At lower reaction temperatures, the length of the experiments increase, and higher concentrations of PS tend to be used for experiments at lower temperatures (Santos et al. 2016; Lee et al. 2012a; Lee et al. 2012b; Liu et al. 2012a). Most recently, the focus has been on milder treatment conditions, such as low PS dosage (down to 2 mM, or 0.4 g L$^{-1}$), lower temperature (50 °C), and lower initial concentrations of PFOA (500 – 8282 µg L$^{-1}$; Yin et al. 2016; Park et al. 2016). Under these conditions, 75 – 100 hours are required to reach > 90 % removal of PFOA, with DF up to 25 % (Yin et al. 2016; Park et al. 2016). Concentrations of short-chain perfluorocarboxylic acids (PFCAs) and fluoride (F$^-$) are measured as indicators of PFOA degradation (Park et al. 2016; Yin et al. 2016; Santos et al. 2016; Lee et al. 2012a; Lee et al. 2012b; Lee et al. 2009; Hori et al. 2008). It is hypothesized that PFOA degrades in a stepwise process, forming shorter PFCAs each cycle and releasing F$^-$ (Tang et al. 2012; Hori et al. 2008). A recent study included a mixed soil and water slurry test in the evaluation of thermally-activated PS treatment of PFOA (Park et al. 2016). Less PFOA is removed in a sediment-slurry than in aqueous conditions (Park et al. 2016). Research concerning the removal of PFOA by thermally-activated PS has progressed over the past few years, and is starting to address the challenges that will be faced during *in situ* application.

When PS is applied as an *in situ* groundwater remediation technique, treatment efficiency can either be increased by the presence of reductants that activate PS to release radicals, or decreased through unproductive interactions with scavengers (Oliveira et al. 2016). Reduced

minerals in aquifer sediments, such as iron or manganese sulfides or oxides, can react with PS (Liu et al. 2014; Sra et al. 2010), causing the formation of sulfate radicals ($SO_4^{\cdot-}$) (Oliveira et al. 2016).

$$S_2O_8^{2-} + Fe^{2+} \rightarrow Fe^{3+} + SO_4^{\cdot-} + SO_4^{2-}$$                     Equation 4.2

Conversely, interactions between PS and natural organic matter (NOM) may inhibit the release of radicals. In a simple sandy sediment, a decrease of 52 % in the amount of organic carbon occurred with the addition of PS to the system (Oliveira et al. 2016). However, organic carbon in sediments with hematite, goethite, and aluminum formed stable complexes that limited PS degradation (Oliveira et al. 2016). The hydroxide ion ($H^+$) can also act as a scavenger. The acid-catalyzed reaction for the degradation of PS (pH < 3) does not release $SO_4^{\cdot-}$, yet increases the rate of decomposition of PS (Sra et al. 2010).

$$S_2O_8^{2-} + H_2O \xrightarrow{H^+} H_2SO_5 + SO_4^{2-}$$                     Equation 4.3
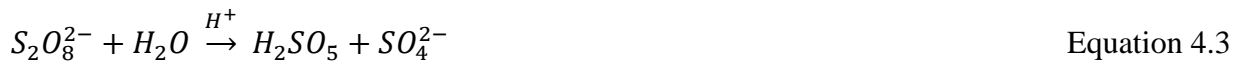
Therefore, aquifer sediment and groundwater geochemistry have an impact on the behaviour of activated PS in full-scale field applications of thermally-activated PS.

Aqueous PFASs may be removed by sorption if solid materials are present. PFASs have two sorption mechanisms: hydrophobic sorption to organic matter, and sorption to charged surfaces (Pancras et al. 2016). Longer chain length PFASs generally have greater hydrophobic sorption (Higgins and Luthy 2006; Milinovic et al. 2015, Pancras et al. 2016), similar to other organic compounds. Sorption of PFASs to organic carbon is a more dominant mechanism than sorption to the mineral fraction of sediments (Du et al. 2014). Sorption of anionic organic chemicals (*e.g.*, PFASs) is enhanced in the presence of divalent cations, such as calcium (Higgins and Luthy 2006). Divalent cations can create a bridge between negatively-charged groups and PFASs, or form complexes between two PFASs (Du et al. 2014). The effects of increasing polyvalent cations on sorption of PFASs are reported to be greater than the effects associated with

decreasing pH (McKenzie et al. 2015a). The solution pH changes the surface charge of the organic matter or other phases; low pH leads to increased positive soil charge (Higgins and Luthy 2006). PFASs are mostly anionic at environmental pH, (*e.g.*, pKa of PFOA = 0 – 3.8) (Burns et al. 2008; Goss 2008), leading to electrostatic attraction between PFASs and positively charged surfaces (Johnson et al. 2007). Therefore, in treatment studies that include solid materials, PFOA should be measured in the aqueous and solid phases to determine true removal of PFOA.

The goal of this study was to determine the impact of aquifer sediments on the removal of PFOA by thermally-activated PS. Three sediments, each with distinctive properties, were used to represent a range of environmental conditions. Extraction of PFCAs from the sediments was conducted to determine the effects of sorption on compound removal. A high initial PFOA concentration ($15000 \, \mu g \, L^{-1}$) was used in these experiments to ensure quantification of short-chain PFCAs and F$^-$ in the corresponding treatment systems; concentrations of short-chain PFCAs and F$^-$ were tracked to indicate the extent of degradation. All analyses were combined to calculate mass balances based on the initial addition of PFOA.

## 4.3  Materials and Methods

### 4.3.1  Reagents

Methanol based standards were purchased from Wellington Laboratories (Guelph, ON, CA) and are listed in Table 4.1. PFOA salt ($C_7F_{15}COOH$, 96 %), potassium hydroxide (KOH, > 85 %) and methanol (HPLC grade, > 99.9 %) were obtained from Sigma-Aldrich (St. Louis, MO, US). Ammonium acetate ($C_2H_7NO_2$, 99.999 %) was purchased from Sigma Aldrich (Tokyo, Japan). Sodium persulfate ($Na_2S_2O_8$), sodium fluoride (NaF, 99 %), and 1,2 cyclohexane diamine tetra acetic acid (98 %) were purchased from Anachemia (Montreal, QC, CA). Glacial acetic acid was obtained from Fisher Scientific (Nepean, ON, CA). Sodium chloride (NaCl) was purchased

from Merck (Darmstadt, Germany). Sodium bicarbonate (> 99.7 %) was obtained from BDH, VWR Analytical (Radnor, PA, US). Reagents were not altered prior to use. Ultrapure water was produced using a Milli-Q® direct water purification system (EMD Millipore, 18.2 MΩ·cm at 25 °C).

### 4.3.2   Sediment Characterization

Three different sediments were selected: Ottawa silica sand (OSS), Borden sand (BS), and South River sediment (SRS). A summary of the soil characterization conducted is presented in Table 4.2. The OSS was 20 – 30 standard sand from Ottawa (IL, US) and prepared according to the ASTM C 778-02; OSS is homogenous, silica sand, composed predominantly of quartz, with a negligible  organic carbon fraction (ASTM C 778-02 2002). The BS (Borden, ON, CA) was from the bulk homogenized sample prepared by Ball et al. (1990). BS is also a relatively homogenous silica sand, including low concentrations of amphibole, feldspar, and calcium carbonate (Xu and Thomson 2009; Ptacek and Gillham 1992; Ball et al. 1990). BS also has a low organic carbon fraction (Ptacek and Gillham 1992). SRS was collected from floodplain sediments of the South River (VA, US), homogenized with mechanical mixing (Paulson 2014), and air-dried. SRS is a sandy silt with some clay, and has a much higher fraction of organic carbon ($f_{oc}$ = 0.0137) than the other sands (Paulson, personal communication).

### 4.3.3   Batch Experiments

All experiments were conducted using duplicated sacrificial 50 mL polypropylene (PP) batch reactors (VWR, Radnor, PA, US). Polypropylene was used over other materials (*e.g.*, glass) due to negligible PFAS sorption (Guelfo and Higgins 2013). Following the addition of 20 g of sediment, 30 mL of simulated groundwater was massed into each reactor. The sediment: solution ratio for this experiment is within the range (1 g: 1 mL – 2 g: 3 mL) of other studies investigating

the interaction of PS with sediments (Sra et al. 2010; Oliveira et al. 2016). Sodium bicarbonate ($NaHCO_3$, 0.8 mM) was used as the only component of the synthetic groundwater. An aqueous PFOA stock solution (100000 $\mu$g $L^{-1}$) was used to spike each reactor to an initial PFOA concentration of 15000 $\mu$g $L^{-1}$. Following spiking, the reactors were placed on a rotator (Glas-Col) for 1 week at room temperature (~ 20 °C) to allow PFOA to reach sorption equilibrium between the solid and aqueous phases. Solid sodium persulfate was then massed and transferred into the reactor to an initial target concentration of 50 mM PS (9.6 g $L^{-1}$) and the reactors were vortexed (945404, Fisher Scientific) for 30 s. The reactors in the thermally-activated PS treatment system (T-PS/60°C) were then placed on a microcontrolled (Arduino) hot water bath set to 60 °C on an orbital shaker (Lab Line) for mixing at 10 rpm during the experimental period. The reactors for the ambient PS treatment system (T-PS/20°C) were placed on a separate orbital shaker (Lab Line) for mixing (10 rpm) at room temperature (~ 20 °C). The treatment systems were allowed to react for 7 days (Figure 4.1), consistent with Park et al. (2016).

Alongside the sediment-slurry treatment systems, a series of experimental controls were also prepared: sediment controls, aqueous controls, and $F^-$ controls. The sediment controls included PFOA in a heated reactor without any PS (C-PFOA/60°C), PS in a heated reactor with no PFOA (C-PS/60°C), and a heated reactor without added PFOA or PS (C-BLANK/60°C). The aqueous controls (AQ) included the thermally-activated persulfate (T-PS/60°C), heated PFOA (C-PFOA/60°C), and heated blank (C-BLANK/60°C) systems. Finally, fluoride controls with each of the sediments were prepared with a $F^-$ spike (2000 $\mu$g $L^{-1}$) instead of a PFOA spike in reactors with thermally-activated PS conditions (F-PS/60°C). The $F^-$-spiked controls were compared to the determination of $F^-$ concentration from the thermally-activated PS sediment control, without a $F^-$ spike (C-PS/60°C). The controls used the same materials, sediments, simulated groundwater, and

appropriate reagent concentrations as the treatment systems; the controls were also run for 7 days (Figure 4.1).

At the pre-determined sampling intervals (Figure 4.1), the reactors were taken out of the hot water bath and cooled to room temperature using an ice bath. The containers were then placed on a Z300 centrifuge (Hermle Labnet) for 30 mins at 3000 rpm. The supernatant was pipetted off into a 50 mL PP centrifuge tube. Following 30 s of vortexing, aliquots for pH (5 mL) and $F^-$ quantification (up to 10 mL) were removed from the supernatant sample. Readings for pH were taken immediately using an Orion 3 Star pH probe (Thermo Scientific). The remaining aqueous sample was preserved with an equal volume of methanol to ensure $SO_4^{\bullet-}$ were quenched (Park et al. 2016; McKenzie et al. 2015a). Both aqueous and solid phase samples were preserved at 4 °C following preparation for $F^-$ and PFCA analysis.

### 4.3.4 Fluoride Analysis

Determination of aqueous $F^-$ concentration was conducted using a fluoride-selective electrode (FSE, RK-27502-19, Cole Parmer) connected to a pH meter (Orion Star A321, Thermo Scientific) within a few hours of sampling. Concentrations of $F^-$ can be reliably determined in the presence of PS (Chapter 2), providing an alternative for ion chromatography. The large concentrations of sulfate released from the decomposition of PS resulted in skewed peaks with the ion chromatograph configuration used in this study. An equal amount of the total ionic strength adjustment buffer (TISAB II) was added immediately after the $F^-$ aliquot was removed from the aqueous phase sample. TISAB II is used to adjust the solution pH to an appropriate range for measurement of $F^-$, and break down any fluoride complexes (Nicholson and Duff 1981; Kauranen 1977). Samples were left for 1 hour after adding the buffer before recording any FSE readings. Analytical and quality control procedures followed those provided in Chapter 2. Fluoride

concentrations measured below the lower limit of the calibration curve ($0.2 – 2.0$ mg L$^{-1}$) are shown on figures for visual purposes only.

### 4.3.5 PFCA Analysis

Samples were prepared for PFCA analysis using solid-phase extraction (SPE) within 1 day of sampling. Methanol-preserved samples were diluted to 20 mL using ultrapure water to an appropriate range for the calibration curve, and a mixed PFAS internal standard was added to each sample dilution. Two dilution factors (1000x, 20x) were applied for each sample containing PFCAs to ensure that the low concentrations of short-chain PFCAs (compared to PFOA) could be measured in the calibration range. Clean 50 mL PP centrifuge tubes were used for the SPE dilution process. Oasis HLB 3cc cartridges (Waters Corporation, Dublin, Ireland) were used for PFCA extraction, and were conditioned prior to use with 2 mL of methanol, followed by 2 mL of ultrapure water. The diluted samples were vortexed for 30 s prior to being passed through the conditioned cartridges under gravity drainage. A post-wash of 2 mL ultrapure water followed the diluted sample, and then the cartridge was vacuumed dry. PFASs were eluted with 2 mL of methanol and the eluates were collected in new 5 mL PP Eppendorf tubes (VWR, Radnor, PA, US). The methanol SPE eluates were stored at 4 °C until analysis. Methods reported by USEPA (2009) and Yamashita et al. (2004) were used to develop the SPE procedure.

Analysis for PFOA and short-chain PFCAs was conducted using liquid chromatography tandem mass spectrometry (LC-MS/MS) on a 6460 Triple Quad LC-MS/MS (Agilent Technologies). Samples were analyzed within two weeks of the SPE procedure. The methanol SPE eluate was brought to room temperature, vortexed for 30 s, and then 400 µL was pipetted into a new 1.5 mL PP vial (isoSPEC, Mississauga, ON, CA). Injections (10 µL) for each sample were pumped through a Pursuit XRs Ultra 2.8 µm C18 2 × 50 mm column (Agilent Technologies) held

at 55 °C. The mobile phases were 2 mM ammonium acetate in ultrapure water, and 2 mM ammonium acetate in 99:1 methanol: ultrapure water. The gradient program started at 10 % of the methanol phase, increased to 70 % of the methanol phase from 0.5 to 5.0 mins, remained at 70 % of the methanol phase for 7.0 mins, and then decreased back to 10 % of the methanol phase in 0.1 min. A column re-equilibration period of 4.9 min was used at the end of each gradient run. Compounds of interest eluted between 2.3 and 8.3 mins. The mass spectrometer was operated in negative electrospray ionization mode, with a capillary voltage of 3750 V and a nebulizer pressure of 414 kPa (60 psi). The nebulizer gas was kept at 350 °C and a 4 L min$^{-1}$ flow rate, while the sheath gas was at 350 °C and a flow rate of 12 L min$^{-1}$.

The calibration curve for the reported PFCAs used the internal standard method to calculate concentrations of PFCAs from 0.5 to 30 µg L$^{-1}$. A set of 7 methanol-based standards was used for the calibration curve; the curves for all five PFCAs were linear over the defined range ($R^2 > 0.987$). The method detection limit (MDL) for each reported PFCA was determined through the analysis of 7 separate 0.5 µg L$^{-1}$ SPE standards: 0.11 µg L$^{-1}$ (PFOA, PFHpA), 0.14 µg L$^{-1}$ (PFHxA), 0.20 µg L$^{-1}$ (PFPeA), and 1.43 µg L$^{-1}$ (PFBA). Methanol blanks were inserted between each standard and sample to ensure no sample carryover or contamination occurred. One quality control (blank, duplicate, matrix spike, or SPE standard) and one random calibration standard was measured after the analysis of five samples. The quality controls were used to ensure that the processing procedure in the laboratory was reliable, and that any matrix effects could be identified. The repeated calibration standards were used to monitor instrument performance. Samples with values below the minimum reporting level (MRL, MDL × dilution factor) are presented on the figures for visualization only; the MRL is included in each figure caption, as appropriate.

### 4.3.6   Liquid-Solid Extraction

Liquid-solid extraction (LSE) was used to quantify PFCAs sorbed on the reserved sediment phase. In this procedure, compounds of interest are transferred from the solid phase to a liquid phase through a triplicate extraction procedure, adapted from Arvaniti et al. (2014b). A small amount of the wet sediment (~ 0.1 g) taken from the top 5 cm of the reserved sediment was measured into a clean 15 mL PP centrifuge tube (VWR, Radnor, PA, US) and allowed to air-dry overnight. In the first extraction, 1.5 mL methanol and 7.5 mL 1 % acetic acid in ultrapure water were pipetted into the centrifuge tube containing the air-dried sediment. The centrifuge tube was then vortexed for 1 min, sonicated for 15 mins in an ultrasonic bath (M3800, Branson), and centrifuged for 15 mins at 3500 rpm. Five mL of the supernatant was removed and placed in a separate 15 mL PP centrifuge tube. Two more sequential extractions using 7.5 mL each of 1 % acetic acid, and the vortex/ sonicator/ centrifuge process was repeated. The mixed supernatant from each extraction was vortexed for 30 s before processing for PFCA analysis, using the SPE procedure described above.

For OSS and BS, the air-dried mass was about 76 – 85 % of the initial wet mass; however, for the SRS, the air-dried mass was 40 – 45 % of the initial wet mass. The entrapment of pore water containing PFCAs in the sediment sample, and subsequent extraction of these PFCAs into the liquid phase, would lead to an overestimation of sorbed PFCAs. Therefore, a correction for the soil pore water was applied, similar to McKenzie et al. (2015)

$$C_s = \frac{m_{extracted} - C_w V_{water}}{m_{sed}}$$
Equation 4.4

where $C_s$ is the concentration of PFCAs corresponding to the solids ($\mu g \ g^{-1}$), $C_w$ is the aqueous concentration of PFCAs ($\mu g \ L^{-1}$), $m_{extracted}$ is the mass of PFCA extracted through the LSE

procedure (µg), $m_{sed}$ is the mass of wet sediment used for the extraction (g), and $V_{water}$ is the calculated volume of water lost after air drying (L).

## 4.4 Results and Discussion

### 4.4.1 Behaviour of Control Systems

Two controls without PFOA, were used to determine the behaviour of the sediments while heated (C-BLANK/60°C) and the impacts of thermally-activated PS on the sediments (C-PS/60°C) (Figure 4.1). After 7 days of reaction with the sediments alone, the aqueous pH for the Borden sand (BS) and Ottawa sand (OSS) sediment controls (C-BLANK/60°C) remained close to the initial pH of the simulated groundwater (within ± 0.3), measured at 8.0 in the aqueous system (AQ). However, the solution pH in South River sediment (SRS) C-BLANK/60°C had decreased to 5.0 – 5.5 after the 7-day mixing period (Figure 4.2). The decreased pH in the SRS sediment-slurries suggests that the SRS was acid-generating as a result of the decomposition of organic material in the sediment (Bickelhaupt 2017). The pH in the C-BLANK/60°C system was constant or increased slightly over the experimental period for all three sediments and AQ. With the addition of thermally-activated persulfate, the solution pH in C-PS/60°C was highly acidic after 7 days in the SRS and OS sediment-slurries (pH 2.5 and 1.6, respectively). The solution pH in the BS C-PS/60°C system was 7.5 after 7 days. The dissolution of calcium carbonate buffers excess $H^+$ through the formation of bicarbonate (Langmuir 1968).

Background PFAS contamination from the reagents, sediments or reactor materials could be identified using the C-BLANK/60°C and C-PS/60°C systems. The PFOA concentrations in the C-PS/60°C and C-BLANK/60°C control systems were < MRL of 111 µg $L^{-1}$ (Figure 4.3). Negligible extractable PFOA (< 2 % of $C_0$) was measured in the sediments in the C-PS/60°C and C-BLANK/60°C control batches (Figure 4.4). Low concentrations of short-chain PFCAs were

detected in the control batches (Appendix C). The low concentrations measured in the C-BLANK/60°C and C-PS/60°C systems indicate that there was no source of PFCA contamination in the PS, sediments, or sample containers.

The C-PFOA/60°C system was used to determine the behaviour of PFOA in the heated sediment slurries. In the C-PFOA/60°C system, the solution pH was consistent with the C-BLANK/60°C system (Figure 4.2). Aqueous PFOA concentrations in duplicated reactors were within 10 % of each other over the experimental period (Figure 4.3). Variability between the duplicated reactors was anticipated because of the potential for heterogeneity in the aqueous PFOA stock solution. Concentrations of PFOA in the C-PFOA/60°C system remained constant over the experimental period of 7 days.

Extractable PFOA concentrations were < 20 % $C_0$ or < 5 µg g$^{-1}$ (*i.e.*, µg PFOA per g sediment) (Figure 4.4) for the C-PFOA/60°C system. Concentrations in the OSS and BSS sediment-slurries were constant over 7 days (< 10 % $C_0$), while the SRS sediment-slurry had a slightly increased concentration of extracted PFOA at Day 1 only (17 % $C_0$). Park et al. (2016) used a soil organic carbon-water partitioning coefficient (log $K_{oc}$) value of 2.23 for PFOA to calculate the percentage of PFOA sorbed to the solid phase in batch reactors. Using the same log $K_{oc}$ value, and the $f_{oc}$ value for the OSS (~ 0), BS (0.00021), and SRS (0.0137) sediment-slurries, sorption of PFOA can be estimated using the same assumptions for this experiment: 0 µg g$^{-1}$ (OSS), 0.011 µg g$^{-1}$ (BS), and 0.687 µg g$^{-1}$ (SRS). At a ratio of 4 g soil to 20 mL aqueous phase, sorption of PFOA to the solid phase ($f_{oc}$ ~ 0.002, similar to tested sediments) is estimated to be 0.2 µg g$^{-1}$, or 4 % of the initial PFOA (Park et al. 2016). At a lower sediment: aqueous radio (3 g: 30 mL) and higher $f_{oc}$ values, sorption of PFOA ranges from 7 – 46 % of the initial aqueous PFOA ($f_{oc}$ = 0.1), and 70 – 81 % ($f_{oc}$ ~ 0.4) (Milinovic et al. 2015). Therefore, the amount of PFOA sorption

measured in the C-PFOA/60°C sediment systems are higher than the respective estimated calculations and literature values.

### 4.4.2 Removal of PFOA by Thermally-Activated Persulfate

Thermally-activated (60 °C) PS (50 mM) was used in reactors containing 15000 µg L$^{-1}$ PFOA for the T-PS/60°C system (Figure 4.1). In the T-PS/60°C system, the pH dropped to 2.2 ± 0.6 at 0.5 days in all experiments (Figure 4.2), generating 18.0 mM (Ottawa sand, OSS), 1.5 mM (Borden sand, BS), 12.0 mM (South River sediment, SRS), and 17.6 mM (aqueous, AQ) of H$^+$. After 7 days, the solution pH in the T-PS/60°C treatment system for the AQ, OSS, and SRS experiments remained low (1.6 to 2.3). By Day 4, the pH in the BS T-PS/60°C system increased to 6.7 and by Day 7 was 7.4; the increasing trend of pH is consistent with the high carbonate content and buffering provided by this sediment, as observed in C-PS/60°C. The OSS sediment-slurry consumed less H$^+$ than the SRS and BS sediment-slurries, behaving similar to the AQ experiment. The similarity between the AQ and OSS experiments is indicative of the low reactivity properties of silica sand. All pH data was consistent (± 0.5) between the two duplicate reactors at each time point.

PFOA concentrations decreased in all sediment-slurries by Day 7 for T-PS/60°C. A set of extended samples (14 days) was added for the T-PS/60°C system, but measured values remained relatively consistent between 7 and 14 days (Appendix C). The removal of PFOA in the T-PS/60°C systems is characterized by a rapid decrease in aqueous PFOA mass up to 1 day (average of 353 µg d$^{-1}$), followed by a negligible decrease (average of 0.4 µg d$^{-1}$) from 1 – 7 days. Previous studies have hypothesized that pseudo-first-order kinetics can be used to describe the removal of PFOA under thermally-activated PS conditions (Yin et al. 2016; Liu et al. 2012a; Lee et al. 2012a). For the sediment and aqueous T-PS/60°C systems, pseudo-first-order kinetics can be fit to the data, if

it is split into rapid and slow rate stages (Appendix C). The fitted kinetic constant ($k$) for the rapid stage of the system without sediment (AQ T-PS/60°C: -0.20 h$^{-1}$) was 4 times greater than the average of the rapid stage with sediment (-0.05 h$^{-1}$, SD = 0.008 h$^{-1}$). The slow stage had a $k < $ -0.0005 h$^{-1}$ for all the AQ and sediment T-PS/60°C systems. At 0.5 days, the solution pH in the T-PS/60°C systems was < 3, so the shift to acid-catalysis of PS may have contributed to the switch from rapid to slow degradation. The slow rate stage could also be an indicator of the consumption of persulfate in all systems.

The resulting molar ratio of PS: PFOA for the presented experiments is 1380:1. In a study by Lee et al. (2012a), a molar ratio of 39:1 (PS: PFOA) for thermally-activated PS in an aqueous experiment at 60 °C resulted in 95 % decomposition of PS after 8 hours. Based on the higher molar ratio of PS: PFOA used in this study, it is suggested that the aqueous (AQ) batch had excess PS. Excess PS is required at high temperatures due to self-scavenging of the $SO_4^{\cdot-}$ by PS (Liu et al. 2012a, Lee et al. 2012a, Park et al. 2016). However, the presence of sediments impacts the consumption of PS. Unactivated PS (104 mM) consumption in Borden sand is low (~ 25 %) after 300 days at 0.1 mmol PS per g sediment (Sra et al. 2010). The consumption of PS would be higher in the present experiments, as the dosage of PS (0.075 mmol PS per g sediment) was lower, and heat was added to activate PS. Therefore, PS may not be in excess for the tested sediment-slurries, and could have been fully consumed.

The removal of PFOA reached 80 %, 65 %, and 64 % of $C_0$ for OSS, BS, and SRS sediment-slurries by Day 7. In the AQ T-PS/60°C system, over 99 % of the initial PFOA was removed under the same temperature and PS dosage. Therefore, for all sediment-slurries, the presence of sediment led to a significant reduction on removal of PFOA. Removal of PFOA in the BS sediment-slurry was about 15% lower than OSS, which could be attributed to the additional

presence of carbonates in the BS. The removal of PFOA in the more organic-rich sediment (SRS) was also about 15 % lower than the quartz sand (OSS) over the same experimental period. The organic carbon present in the SRS may have reacted with PS, which would decrease the amount available to react with PFOA. At a lower temperature (50 °C), dosage of PS (42 mM), and ratio of sediment: aqueous phase (4 g: 20 mL), PFOA removal of 25 % occurs after 7 days (Park et al. 2016). Removal of PFOA increases with higher temperatures or persulfate concentration over a constant time period (Santos et al. 2016; Lee et al. 2012a; Lee et al. 2012b; Liu et al. 2012a), which explains the increased removal of PFOA observed in the present study.

The extractable PFOA (21 – 81 % of $C_0$) from SRS was 4 – 40 times more than OSS (up to 9 % of $C_0$) and BS (up to 10 % of $C_0$) in T-PS/60°C. SRS had more organic carbon, which can sorb aqueous PFOA through hydrophobic interactions (Du et al. 2014). However, compared to the estimated sorption of PFOA based on hydrophobic sorption alone from the literature and controls, the extracted PFOA measured in the SRS T-PS/60°C was much higher. The solution pH in the SRS reactors was < 7 for the entire experimental period, which may have contributed positively charged surfaces for electrostatic attraction of PFOA and enhanced sorption of PFOA (Pancras et al. 2016). Extractable PFOA in the OSS and BS T-PS/60°C systems were under 10 % of $C_0$, similar to the respective C-PFOA/60°C systems. The acidic solution pH (< 3) in the OSS experiment did not increase the amount of extractable PFOA detected in the T-PS/60°C system compared to C-PFOA/60°C (pH 7.7 ± 0.1). The carbonate pH buffering in the BS T-PS/60°C system is expected to minimize the impact of electrostatic attraction of PFOA to positively charged surfaces. Differences between the extractable PFOA measured in duplicate reactors were < 20 % when extracted PFOA exceeded 3.5 µg g$^{-1}$.

### 4.4.3 Removal of PFOA by Persulfate under Ambient Conditions

For the persulfate treatment system run at 20 °C (T-PS/20°C) (Figure 4.1), the pH decreased to 2.4 – 3.5 after 7 days in the Ottawa sand (OSS) and South River sediment (SRS) slurries, while the pH was buffered at 7.7 in the Borden sand (BS) slurry (Figure 4.2). For T-PS/20°C in the OSS and BS sediment-slurries, PFOA concentration remained close to the theoretical input concentration after 7 days (Figure 4.3). A decrease in PFOA concentration of 44% was observed in SRS. The presence of $F^-$ and/ or short-chain PFCAs helps to tie the decreases in concentration to degradation. The duplicated reactors for T-PS/20°C had consistent concentrations for aqueous PFOA (within 11 %). Minimal PFOA was extracted ($< 10$ % of $C_0$) from the sediments in the OSS and BS T-PS/20°C systems, but the amount of PFOA extracted from the sediments in the SRS T-PS/20°C system increased over 7 days (Figure 4.4) up to 63 % of $C_0$. The pH in the SRS T-PS/20°C system decreased over the same period, which could have contributed more positively-charged organic surfaces to attract PFOA.

### 4.4.4 Fluoride Spike Recovery in Sediment Slurries

To track degradation of PFASs, the determination of aqueous $F^-$ production is desired. However, the presence of sediments can impact aqueous $F^-$ concentrations. From previous experiments investigating the FSE, it was determined that $F^-$ matrix spike recovery is low in samples containing Borden sediment (Chapter 2). There are many ways that aqueous $F^-$ can be removed by sediment (Edmunds and Smedley 2013). Fluoride can be adsorbed by iron and aluminum oxides, clay minerals, and soil organic matter. Acidic conditions enhance the adsorption of $F^-$ by inducing positive charges on surfaces. Aqueous calcium and calcite concentrations can also control aqueous $F^-$ through the formation of calcium fluoride ($CaF_2$). The sediment and geochemical characteristics of a slurry can impact the accuracy of $F^-$ determinations.

The simulated groundwater in these experiments used $NaHCO_3$ to minimize the introduction of $Ca^{2+}$ from the aqueous phase and removal of $F^-$ through formation of $CaF_2$. However, interactions between the fluoride and sediments were still expected. For the OSS F-PS/60°C control, the measured concentrations of $F^-$ were all within 25 % of the theoretical $F^-$ spike (Figure 4.5). In the BS slurry, $F^-$ concentration for F-PS/60°C dropped below 45 % of the theoretical $F^-$ spike after 1 day, rising slightly to 55 % after 7 days. The formation of $CaF_2$ may have occurred in BS as a result of high carbonate content (Xu and Thomson 2009) present from $CaCO_3$. Finally, with SRS, the $F^-$ concentration immediately (Day 0) fell to 15 % of the theoretical $F^-$ spike. Measured aqueous $F^-$ rose from 15 % to 56 % by Day 1, but returned to 11 % of the $F^-$ theoretical spike after 7 days. The solution pH in the SRS reactors decreased from 5.0 to 1.9 over the experimental period, which would lead to increased positively charged organic matter, known to sorb $F^-$ (Edmunds and Smedley 2013). The control sediment and persulfate reactors (C-PS/60°C) showed that no $F^-$ was released from any of the sediments under thermally-activated PS. Therefore, while the $F^-$ spike was recovered in the OSS sediment-slurry, decreased recovery of the $F^-$ spike in the BS and SRS sediment-slurries indicates that the production of $F^-$ by the degradation of PFOA could not be accurately measured in these sediment-slurries.

## 4.4.5   Mass Balance and Degradation Products

Using a mass balance approach, the mass contributions from aqueous PFOA, aqueous short-chain PFCAs, extractable PFCAs, and aqueous $F^-$ were compared to the calculated mass of PFOA added to each reactor (Figure 4.6). The sum of extractable PFCAs was dominated by PFOA (> 89 % of total) in reactors with total PFCAs > 3.5 µg g$^{-1}$ (Appendix C). The enhanced sorption of PFOA compared to shorter-chain PFCAs is consistent with the higher hydrophobic sorption of PFOA compared to short-chain PFCAs (Higgins and Luthy 2006; Milinovic et al. 2015, Pancras

et al. 2016). Degradation products (*i.e.*, short-chain PFCAs and F$^-$) were measured in the T-PS/60°C system. Short-chain PFCAs were detected in the T-PS/60°C system for the three sediments on Day 0.5 and were present until Day 7. The concentration of these short-chain PFCAs remained relatively constant in each batch over the experimental period (Figure 4.7). However, in the AQ T-PS/60°C system, short-chain PFCAs were detected between 0.5 and 2 days, after which they were no longer detected above the respective MRLs. The retention of short-chain PFCAs in the sediment-slurries suggests that persulfate may have been consumed by scavenging reactions with sediments. The consumption of persulfate would lead to incomplete progression through the stepwise degradation of PFOA. Furthermore, the detection of F$^-$ was much lower in the sediment-slurries compared to AQ. Part of the decreased F$^-$ detection is due to the reactions between F$^-$ and the BS and SRS sediments, as discussed in Section 4.4.4. However, with decreased removal of PFOA in the presence of sediments, less F$^-$ would be generated.

Neither short-chain PFCAs, nor F$^-$ were present in most of the T-PS/20°C or control systems, further supporting the conclusion that PFOA was not removed in these experiments. However, fluoride was detected in the batch reactors for the SRS T-PS/20°C slurry at days 4 and 7. However, no short-chain PFCAs were detected on these days. It is possible that an unknown compound was released in these reactors that caused a response similar to F$^-$ to be measured using the FSE. However, if the presence of F$^-$ was truly measured without short-chain PFCAs, it suggests that an alternative activation mechanism for PS or a different degradation pathway was present in these reactors. Iron or manganese oxides can increase PS decomposition (Sra et al. 2007), but aquifer minerals containing these oxides would need to be present at a high mass (> 2 % aquifer solids) to impact PS reactivity (Liu et al. 2014; Ahmad et al. 2010). The SRS only had < 0.8 % (by mass) of Fe or Mn, making these aquifer minerals an unlikely source of activation. Therefore, it is

unclear whether the detected fluoride is an analytical artefact or evidence of any degradation of PFOA.

The calculated mass balance in the T-PS/60°C, T-PS/20°C, and C-PFOA/60°C systems is summarized for each experiment: OSS (75 – 115 %), BS (68 – 126 %), SRS (88 – 136 %), and AQ (61 – 107 %). In recent studies of aqueous phase thermally-activated PS reactors, mass balances range from 64 % (Park et al. 2016) to 105 % (Yin et al. 2016) of the initial PFOA mass with the analysis of PFCAs down to a two-carbon (C2) chain length. However, the presence of sediments and use of the LSE process adds complexity to the mass balance. Mass recovery of PFCA spikes in sediment batch tests in the presence of activated PS ranged from 83 – 130 % (McKenzie et al. 2015b), closer to the range of reported mass balances presented in this study. Therefore, the calculated mass balances from the study can be considered to adequately account for the initial mass of PFOA in each system.

The overall calculated mass in the T-PS/60°C system decreased for all sediment-slurries, with a 31 % (OSS), 24 % (BS), and 20 % (SRS) decrease in PFOA mass from the initial conditions after 7 days. Sorption of $F^-$ or formation of $CaF_2$ could have contributed to the loss of mass that could be included in the calculations. Another contributor could be irreversible sorption of PFOA or short-chain PFCAs to the sediment. Furthermore, the presence of degradation products not measured in the current analytical method (such as C2, C3 PFCAs) could also be the reason for this discrepancy. There is no expected impact to the determination of aqueous $F^-$ or aqueous PFCAs from the ice bath cooling procedure (Appendix C).

## 4.5 Implications

In the presence of sediments, removal of PFOA by thermally-activated PS was less effective than in a purely aqueous experiment. To be used for *in situ* remediation, sufficient

degradation must be attained using thermally-activated PS, regardless of the scavenging effects of sediments. Therefore, repeated PS injections are suggested for full scale *in situ* treatment (Park et al. 2016). In soil slurry batch tests, repeated thermally-activated persulfate dosages remove an additional 30 % of the initial PFOA (Park et al. 2016).

The extractable PFOA in the SRS sediment-slurry may be over-estimated, as up to 81 % of the initial aqueous PFOA was calculated to be sorbed to the sediments. The small sample of sediment (0.5 %) used for the LSE procedure was taken from the top 5 cm of the reserved bulk sediment. This sediment sample may have had higher extractable PFOA than for the bulk sediment, since it is expected that the fine sediments would have remained near the top of the bulk sediment after settling. The fine sediment material may be where most of the organic carbon is concentrated, leading to increased sorption of PFOA. Further refinement of the liquid-solid extraction procedure is advised, especially for sediments with fine fractions.

## 4.6 Conclusions

The concentration of aqueous PFOA decreased significantly after 0.5 days of treatment with thermally-activated PS, and slowly continued to a final removal of 64 – 80 % of the initial PFOA added to the systems after 7 days. In all sediment slurries, the removal of PFOA by thermally-activated PS was less than the removal in the aqueous experiment (99 %). Greater removal was observed in the silica sand (OSS) and calcareous sand (BS), compared to the sandy silt with organic carbon (SRS). Short-chain PFCAs and $F^-$ were detected in the T-PS/60°C sediment-slurry systems, but were not fully converted to $F^-$. Sediments containing calcium or organic carbon also resulted in large decrease in recovery of an aqueous $F^-$ spike. PFOA concentration decreased slightly in the unheated persulfate tests, but without any corresponding detection of degradation products. The sediment with a high fraction of organic carbon (SRS)

adsorbed more PFCAs (mostly PFOA, > 89 %) than the sediments with low organic carbon, although the extraction procedure may have over-estimated sorbed PFCAs.

Table 4.1. PFAS internal and external standards.

| Full Standard Name | Acronym | Chemical Formula | Purity | Internal Standard |
|---|---|---|---|---|
| Perfluoro-n-butanoic acid | PFBA | $C_3F_7COOH$ | - | M3PFBA |
| Perfluoro-n-pentanoic acid | PFPeA | $C_4F_9COOH$ | - | MPFHxA |
| Perfluoro-n-hexanoic acid | PFHxA | $C_5F_{11}COOH$ | - | MPFHxA |
| Perfluoro-n-heptanoic acid | PFHpA | $C_6F_{13}COOH$ | - | MPFHxA |
| Perfluoro-n-[2,3,4-$^{13}C_3$] butanoic acid | M3PFBA | $C_3F_7COOH$ | >99% | - |
| Perfluoro-n-[1,2-$^{13}C_2$] hexanoic acid | MPFHxA | $C_5F_{11}COOH$ | >99% | - |
| Perfluoro-n-[1,2,3,4-$^{13}C_4$] octanoic acid | MPFOA | $C_7F_{15}COOH$ | >99% | - |

Table 4.2. Relevant characteristics of the sediments used in the sediment-slurry experiments.

| Name | | Ottawa Silica Sand (OSS) | Borden Sand (BS) | South River Sediment (SRS) |
|---|---|---|---|---|
| **Location** | | Ottawa, IL, US | CFB Borden, ON, CA | South River, VA, US |
| **Description** | | Silica sand | Calcareous sand | Riverbank sediment |
| **Bulk Mineralogy** | | Quartz (99.7 %) | Quartz (~45 %), amphibole (~15 %), feldspar (~10 %), carbonates (~10 – 15 %, mostly calcium carbonate) | Quartz, aluminum/ iron-silicates, feldspar |
| **Mass Distribution by Size Range (mm)** | 4.75 – 1.7 | 0 | 0.0058 | 0.017 |
| | 1.7 – 0.85 | 0.0003 | 0.0091 | 0.012 |
| | 0.85 – 0.42 | 0.9962 | 0.0524 | 0.049 |
| | 0.42 – 0.25 | 0.0031 | 0.163 | 0.102 |
| | 0.25 – 0.18 | | 0.257 | |
| | 0.18 – 0.125 | 0.004 | 0.315 | 0.086 |
| | 0.125 – 0.075 | | 0.165 | 0.105 |
| | < 0.075 | 0 | 0.0341 | 0.634 |
| **Pertinent Concentrations (µg/g)** | | $f_{oc} \sim 0$ | C: 15800<br>Fe: 17500<br>$Fe_{Am}$: 300<br>Mn: 421<br>$Mn_{Am}$: 4<br>TOC: 240<br>$f_{oc}$: 0.00021 | Al: 7200<br>C: 13922<br>Ca: 840<br>Fe: 7600<br>Mn: 370<br>TOC: 13700<br>$f_{oc}$: 0.0137 |
| **References** | | (ASTM C 778-02 2002) | Xu and Thomson (2009); Ptacek and Gillham (1992); Ball et al. (1990) | (Paulson 2014) |
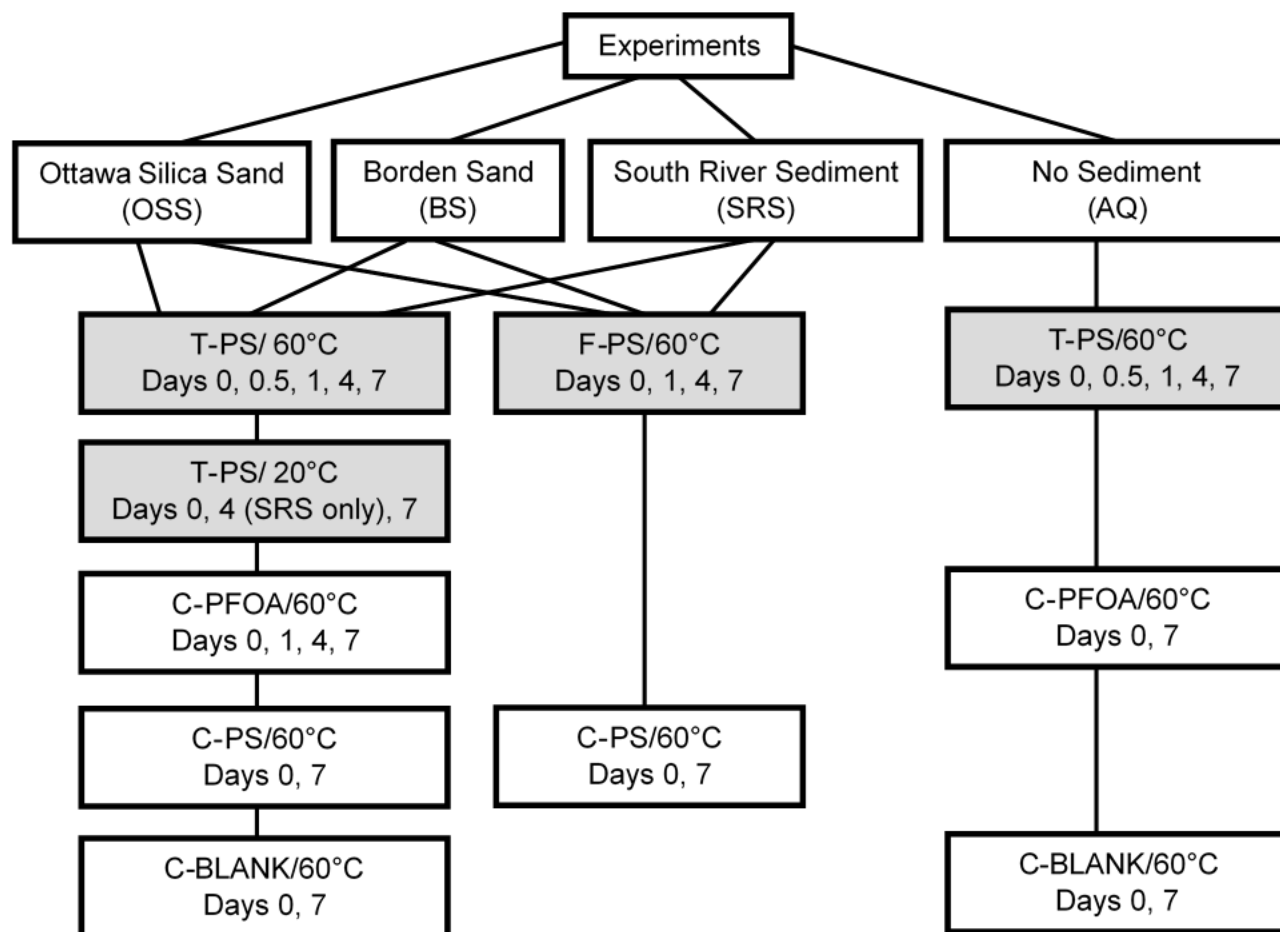
Figure 4.1. Experimental structure for thermally-activated (T-PS/60°C) and ambient PS (T-PS/20°C) treatment systems (grey shading), along with the associated control systems (C-PFOA/60°C, PS/60°C, C-BLANK/60°C). The behaviour of PFOA, spiked to an initial concentration of 15000 µg L$^{-1}$, in reactors containing 20 g sediment (OSS, BS, or SRS) to 30 mL NaHCO$_3$ simulated groundwater was investigated. Sorption of fluoride (F$^-$, 2000 µg L$^{-1}$) in the same conditions was evaluated using F-PS/60°C and C-PS/60°C. Comparisons can also be made with sediment-free reactors (AQ), specifically for the thermally-activated PS treatment system (T-PS/60°C), and PFOA (C-PFOA/60°C)/ blank (BLANK/60°C) controls. The days listed represent duplicated sacrificial batch reactors.
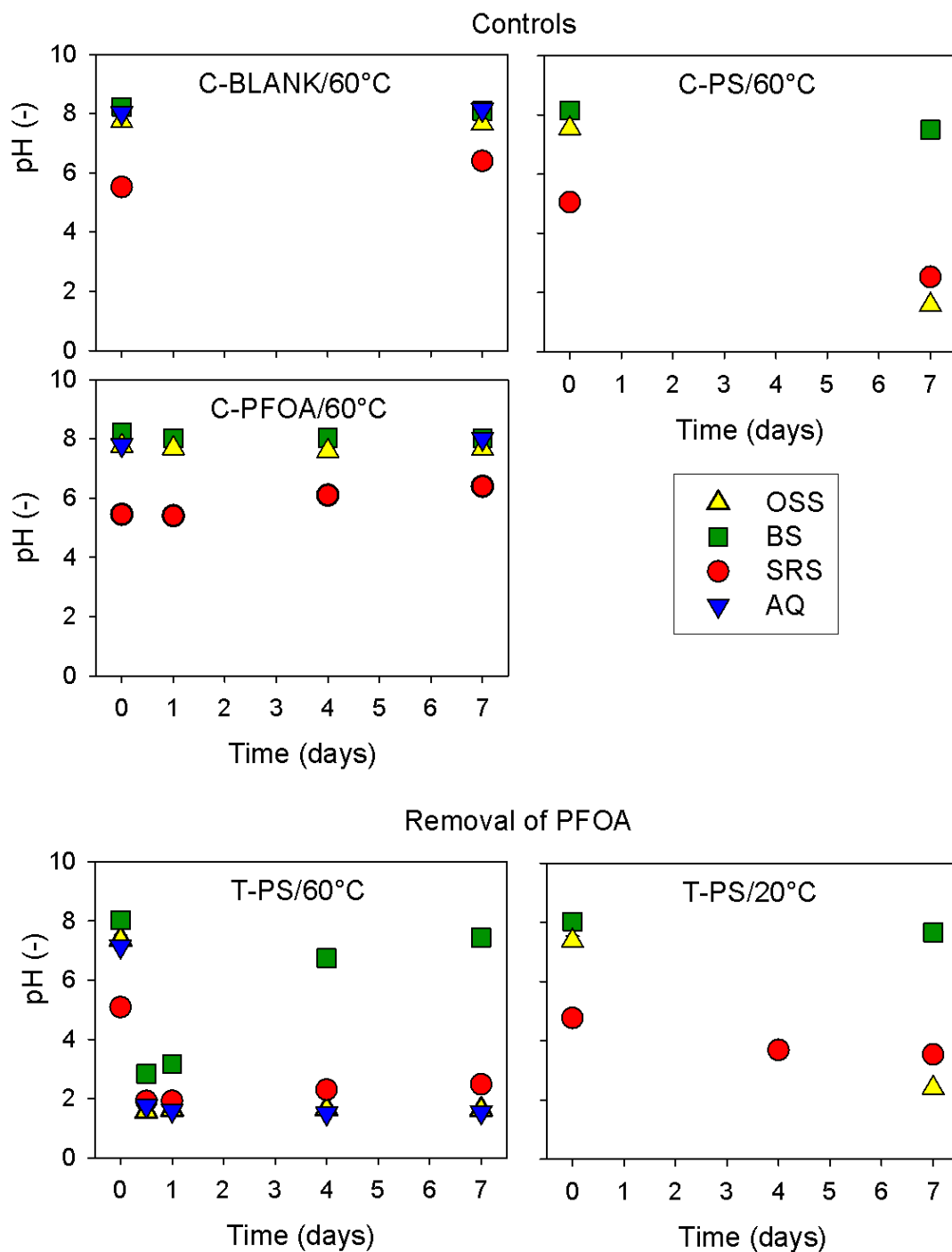
Figure 4.2. pH measured in the OSS, BS, SRS, and AQ experiments over the experimental period (7 days) for all PFOA control (C-PFOA/60°C, C-PS/60°C, C-BLANK/60°C) and treatment (T-PS/60°C, T-PS/20°C) systems. 50 mM persulfate (PS) was used in thermally-activated or ambient conditions for the removal of PFOA in $NaHCO_3$ simulated groundwater and sediment slurries (20 g: 30 mL). Each data point is the average from duplicate reactors, and the maximum/ minimum error bars are not visible, as they are contained within the plotted symbols.
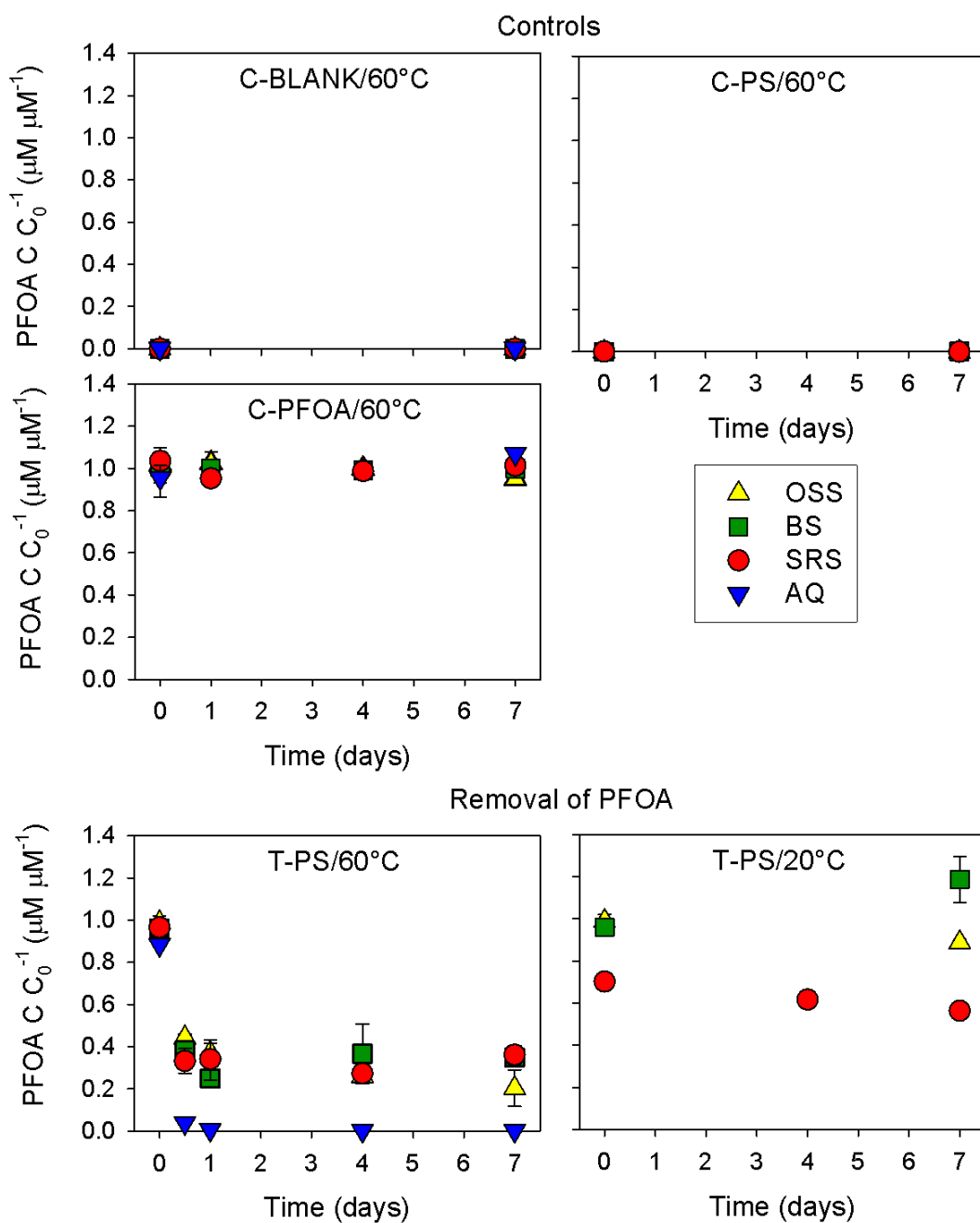
Figure 4.3. Aqueous PFOA concentration ($C\ C_0^{-1}$) for the sediment-slurries (OSS, BS, and SRS) and aqueous (AQ) experiments over the experimental period (7 days) for all control (C-PFOA/60°C, C-PS/60°C, C-BLANK/60°C) and treatment (T-PS/60°C, T-PS/20°C) systems for the removal of PFOA ($PFOA_i$= 15000 µg $L^{-1}$) using thermally-activated persulfate (PS, 50 mM). The data shows average values, with error bars indicating maximum and minimum values. The MRL for PFOA is 111 µg $L^{-1}$; data below this concentration are still included for visual clarity.
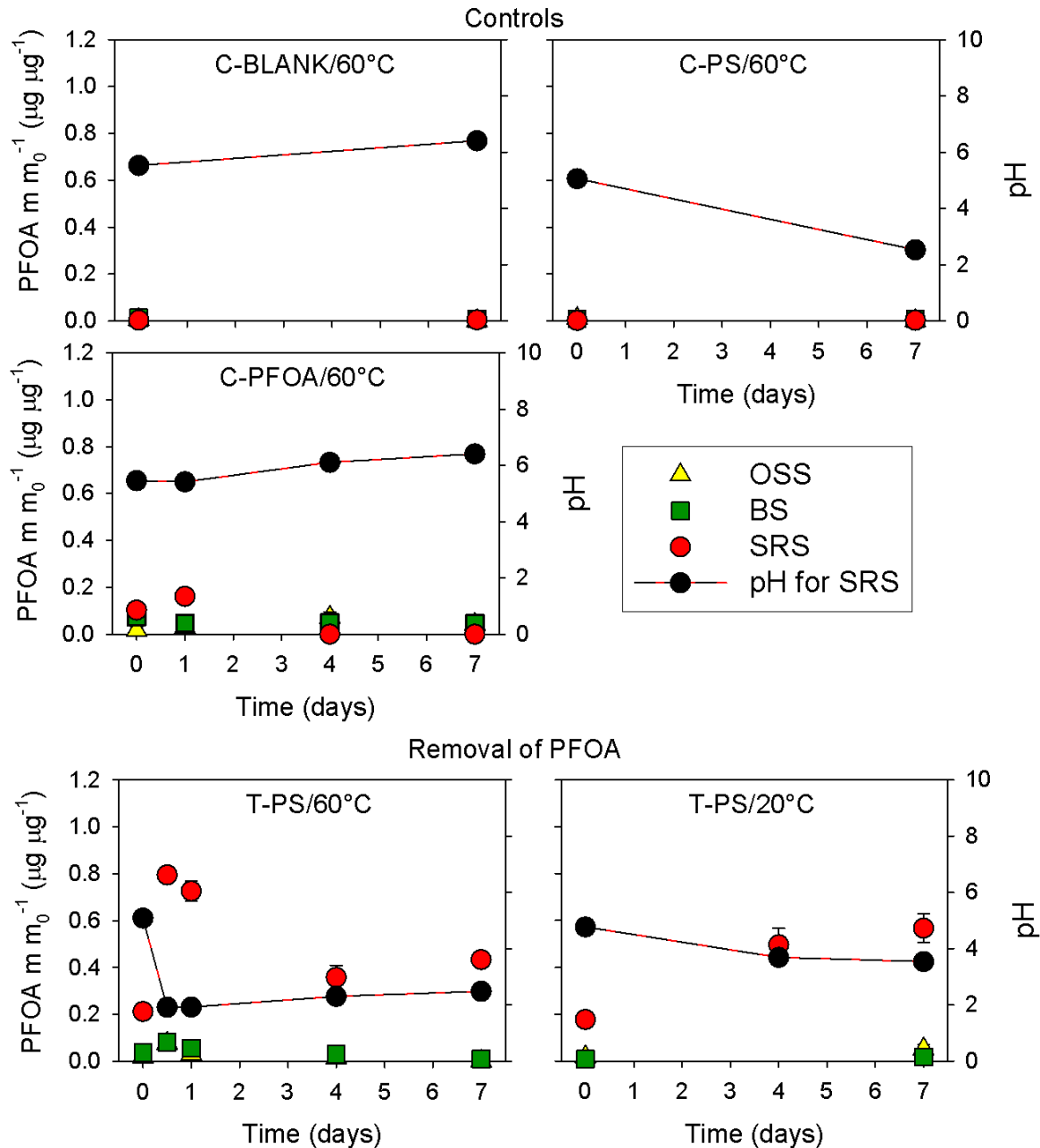
Figure 4.4. PFOA (m $m_0^{-1}$) extracted from reserved sediments in the sediment-slurries (OSS, BS, SRS). All control (C-PFOA/60°C, C-PS/60°C, C-BLANK/60°C) and treatment (T-PS/60°C, T-PS/20°C) systems are presented from the experiments that used thermally-activated or ambient persulfate (PS, 50 mM). Time points have been averaged, with error bars to show the maximum and minimum values. The pH values for the SRS control and treatment systems is also shown.
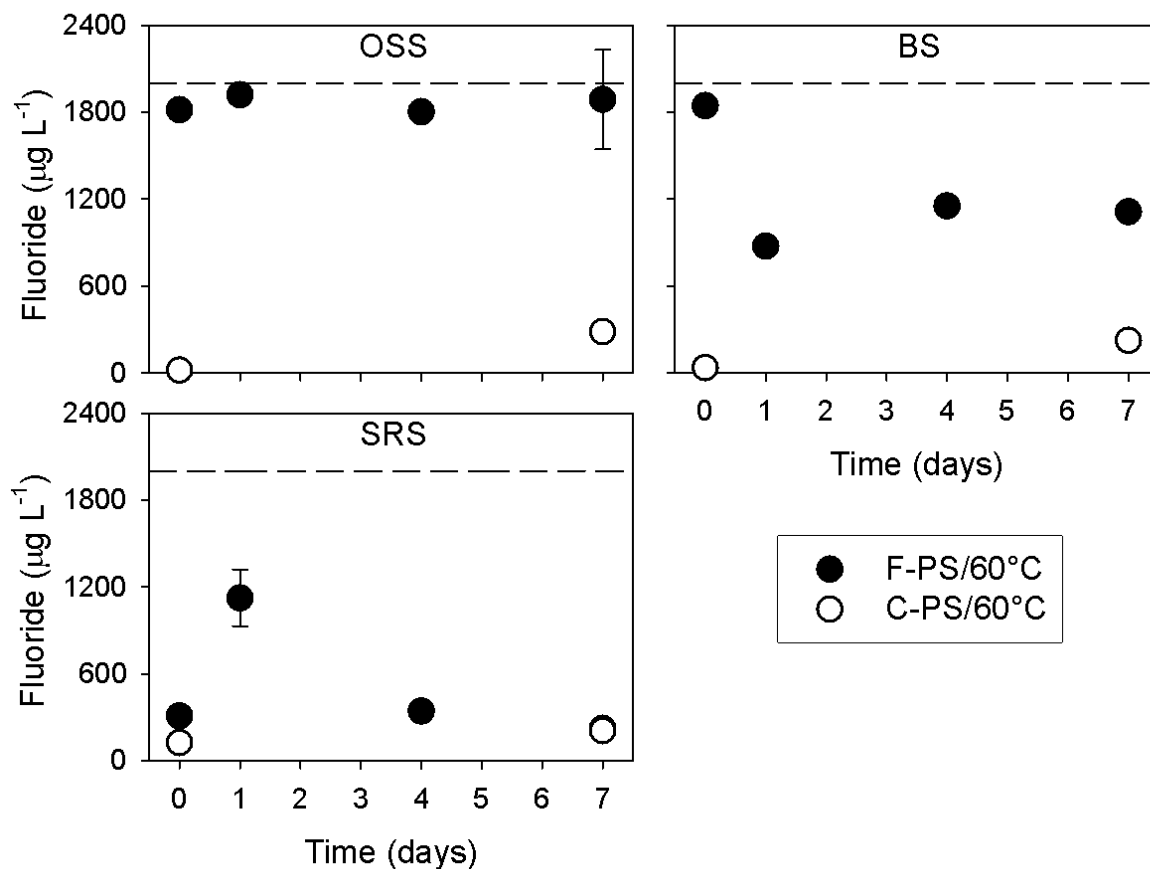
Figure 4.5. Aqueous F⁻ concentration (µg L⁻¹) in presence of the three different sediments (OSS, BS, and SRS) in NaHCO₃ simulated groundwater are shown over 7 days, for both the F-PS/60°C spiked system and C-PS/60°C control. Each F-PS/60°C system reactor had an initial theoretical concentration of 2000 µg L⁻¹ F⁻¹, shown on the graphs as a horizontal dashed line. Time points for Days 1, 4, and 7 (F-PS/60°C) were duplicated for each sediment, and the corresponding minimum/ maximum error bars are shown.
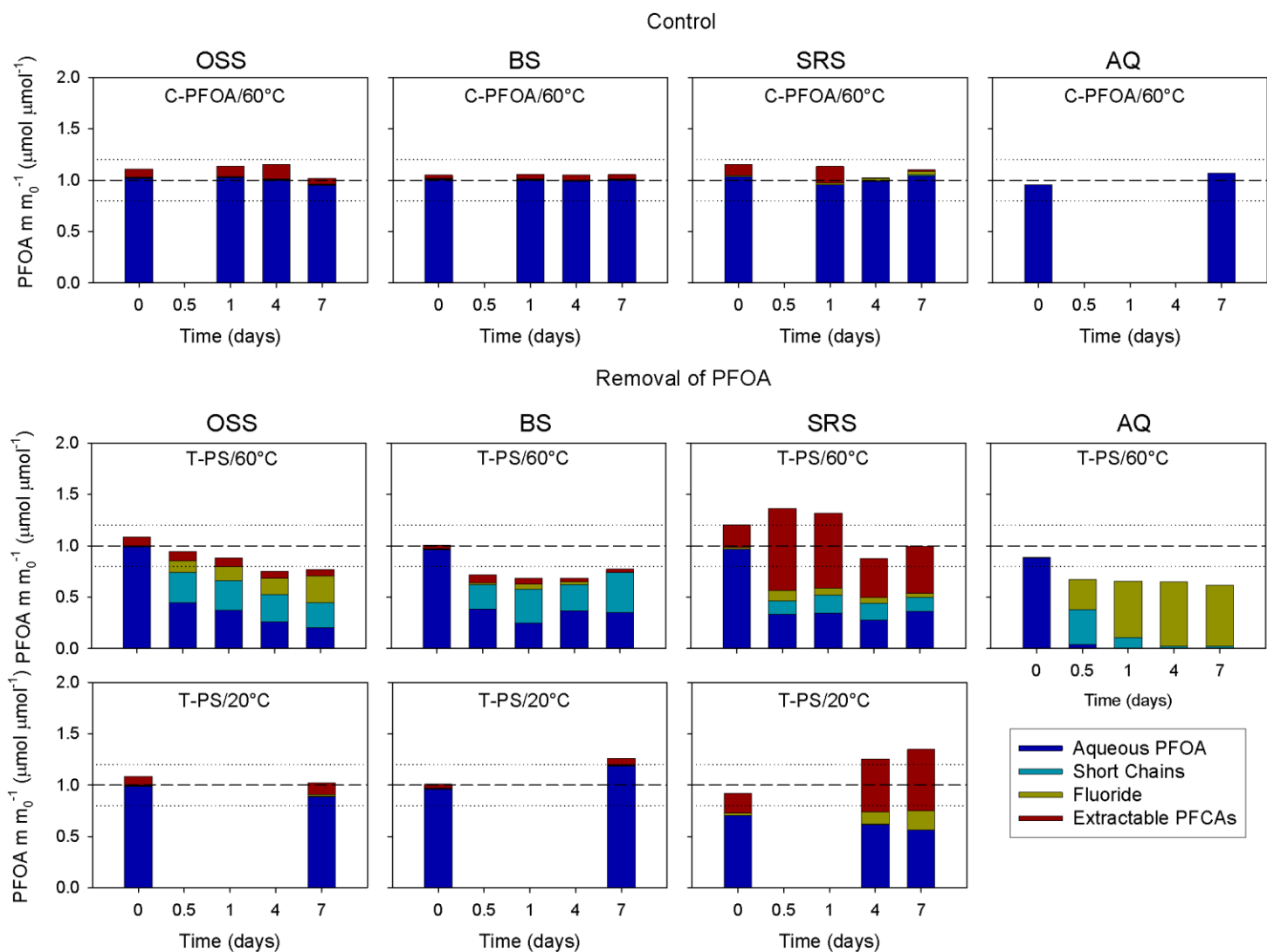
Figure 4.6. PFOA equivalent mass balances (m $m_0^{-1}$) from contributions by aqueous PFOA, aqueous short-chain PFCAs, aqueous F$^-$, and extractable PFCAs. Reactors contained 20 g of the respective sediments (OSS, BS, SRS) and 30 mL NaHCO$_3$ simulated groundwater. The aqueous experiment (AQ) is presented as a comparison. The treatment systems (T-PS/60°C, T-PS/20°C) used 50 mM of persulfate (PS). The PFOA control system (C-PFOA/60°C) is also presented. The horizontal dashed line shows full mass recovery (m $m_0^{-1}$ = 1), while the horizontal dotted lines are one standard deviation ($\sigma$ = 0.20) above and below, based on the overall mass balance sum statistics. The data shown is the average of duplicate measurements for each time point.
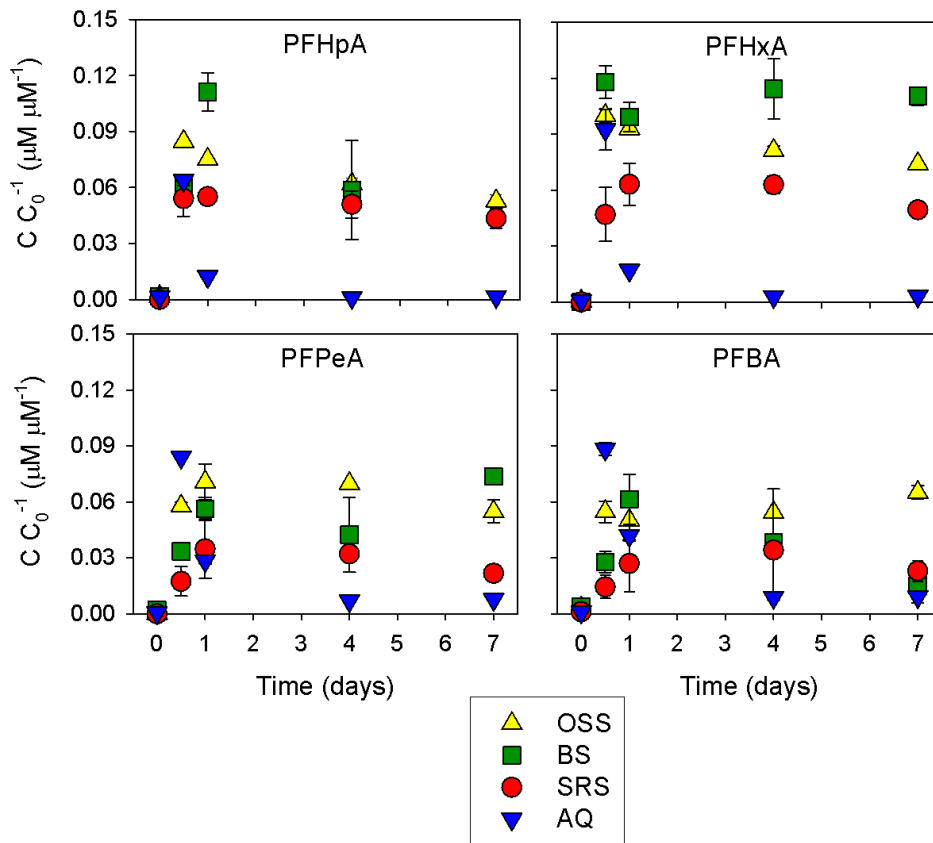
Figure 4.7. Aqueous PFHpA (MRL 2 µg L$^{-1}$), PFHxA (MRL 3 µg L$^{-1}$), PFPeA (MRL 4 µg L$^{-1}$), and PFBA (MRL 29 µg L$^{-1}$) concentrations (C C$_{0, \text{PFOA}}^{-1}$) for the T-PS/60°C system over the experimental period (7 days) are shown. Each of the sediments (OSS, BS, SRS) and aqueous control (AQ) are presented. Each data point shows the average of duplicated reactors, with maximum and minimum error bars. Data below the MRL is still included in the graph for visualization purposes.

# Chapter 5: Conclusions, Implications, and Future Work

## 5.1 Summary of Findings

PFOA and PFOS are classified as emerging contaminants and linked to potential human health impacts. Many researchers are refining remediation methods to be used for *in situ* removal of PFOA and PFOS. Previous research has focused on thermally-activated persulfate treatment for the removal of aqueous PFOA; however, thermally-activated persulfate has not been shown to consistently remove PFOS. There have also been limited studies that include the presence of sediments in thermally-activated persulfate experiments for the removal of PFOA. Results from this thesis contribute to the understanding of the impact of sample constituents on measurement of $F^-$ by a FSE, potential benefits from the addition of permanganate to thermally-activated and ambient persulfate systems for the removal of PFOA and PFOS, and the impact that different sediment types can have on the removal of PFOA in thermally-activated persulfate slurries.

The main findings from Chapter 2, *Evaluation of Direct Measurement of Fluoride Concentration with a Fluoride-Selective Electrode for Applications in Advanced Oxidation Remediation of Sites Contaminated by Per- and Polyfluoroalkyl Substances*, describe the impact that geochemical composition, oxidant-based reagents, and sediments can have on the measurement of aqueous $F^-$ by a FSE. Matrix spike recovery of $F^-$ and electrode slope were used as indicators of electrode performance. Recovery of the $F^-$ matrix spike was high (> 90 %) and consistent (within 5 %) for ultrapure water, ultrapure water with NaCl, and simulated groundwater; the electrode slopes measured were also within the desired range (-54 mV – -60 mV). Matrix spike recovery was also high in the presence of persulfate and/ or permanganate (> 87 %), however the electrode slope was < 50 mV in samples containing permanganate. The presence of ascorbic acid resulted in unacceptable matrix spike recovery (< 74 %). When the sediment and $F^-$ spike had time

to interact, matrix spike recovery was very low (< 38 %) as a result of sorption of F⁻ to the sediment. The recovery of the F⁻ matrix spike was high (> 96 %) when the sediments were filtered prior to the addition of the F⁻ spike.

The main findings from Chapter 3, *Evaluation of a Thermally-Activated Persulfate System with Added Permanganate for the Treatment of Perfluorooctanoic Acid (PFOA) and Perfluorooctane Sulfonic Acid (PFOS) in Different Aqueous Phases*, are focused on the potential for the addition of permanganate to improve the removal of PFOA or PFOS in thermally-activated or ambient persulfate systems. The thermally-activated persulfate and permanganate (dual-oxidant) and persulfate treatment series resulted in the same removal of PFOA (> 99 %) in both the simulated groundwater and ultrapure water systems after 7 days. Short-chain PFCAs were produced between 0.25 and 2 days, after which the mass balance was almost completely composed of F⁻. PFOA was not removed in the ambient persulfate and heated permanganate systems. Mass balances for the PFOA experiments resulted in recoveries ranging from 81 – 142 % of the initial PFOA concentration. PFOS was not removed in the thermally-activated dual-oxidant, thermally-activated persulfate, heated permanganate, or ambient dual-oxidant series, and no degradation products (short-chain PFCAs/ PFSAs or F⁻) were produced in any of these experiments.

The main findings from Chapter 4, *Treatment of Perfluorooctanoic Acid (PFOA) by Thermally-Activated Persulfate in Different Types of Aquifer Materials*, highlight the impacts that the presence of sediments can have on the removal of PFOA by thermally-activated or ambient persulfate. The presence of aquifer sediments resulted in PFOA sorption that increased with high organic carbon content and lower pH (< 5). The removal of PFOA by thermally-activated persulfate was lower in the presence of sediments (62 – 79 %) relative to without sediments (99 %) after 7 days. Conversion of the initial PFOA to F⁻ did not occur to the same extent in the soil

slurries as the aqueous system. Accurate measurements of aqueous $F^-$ could not be obtained for systems containing carbonate or organic-rich sediments. Mass balances for the soil slurry experiments ranged from 74 to 140 %.

## 5.2 Implications

The implications of this research include:

- Direct measurement of aqueous $F^-$ concentrations in samples containing persulfate and simple geochemical composition can be conducted using a FSE and an ultrapure water calibration curve

- Matrix-matched calibration curves or the method of standard addition(s) should be used to measure $F^-$ in samples containing permanganate with the FSE

- Alternate quenching methods, such as an ice bath, should be used to avoid the addition of ascorbic acid to samples for the FSE

- Sediments can sorb aqueous $F^-$, and prevent the measurement of these $F^-$ concentrations by the FSE

- Persulfate was not activated by permanganate and/ or $MnO_{2(s)}$ at the ratio of 100:1 PS:PM to produce radicals that would be able to degrade PFOA or PFOS under ambient conditions

- At the ratio tested, the addition of permanganate did not change the radicals produced by the thermal-activation of persulfate for the removal of PFOA or PFOS

- Repeated injections of persulfate may be required in thermally-activated persulfate systems in the presence of sediments to attain similar rates of removal of PFOA as in aqueous systems

- The use of a very small sediment sample taken from the top of the reserved solids in the liquid-solid extraction procedure may over-estimate sorbed PFAS for the bulk sediment

## 5.3 Direction of Future Work

There are a few directions to extend the research relating to the topics contained within this thesis. The recovery of $F^-$ matrix spikes could be measured in other sample matrices for different treatment methods (*e.g.*, reductive treatment systems) to determine if the FSE would be a reliable tool for those studies as well. To determine if the addition of permanganate can improve the removal of PFOA or PFOS by thermally-activated or ambient persulfate, a wider range of permanganate to persulfate ratios and temperatures should be investigated. The addition of a lag period to allow the formation of $MnO_{2(s)}$ from permanganate is another factor that should be investigated in the dual-oxidant (persulfate and permanganate) system for removal of PFOA or PFOS. Finally, the refinement of heating methods that can maintain temperatures in the subsurface around 60°C will be required to support the field-application of thermally-activated persulfate.

# References

Ahmad, M., A. L. Teel, and R. J. Watts. 2010. Persulfate activation by subsurface minerals. *J. Contam. Hydrol.* 115 (1–4). Elsevier B.V.: 34–45. DOI: 10.1016/j.jconhyd.2010.04.002.

Ahrens, L., and M. Bundschuh. 2014. Fate and effects of poly- and perfluoroalkyl substances in the aquatic environment: A review. *Environ. Toxicol. Chem.* 33 (9): 1921–29. DOI: 10.1002/etc.2663.

Arvaniti, O. S., H. R. Andersen, N. S. Thomaidis, and A. S. Stasinakis. 2014a. Sorption of perfluorinated compounds onto different types of sewage sludge and assessment of its importance during wastewater treatment. *Chemosphere* 111. Elsevier Ltd: 405–11. DOI: 10.1016/j.chemosphere.2014.03.087.

Arvaniti, O. S., A. G. Asimakopoulos, M. E. Dasenaki, E. I. Ventouri, A. S. Stasinakis, and N. S. Thomaidis. 2014b. Simultaneous determination of eighteen perfluorinated compounds in dissolved and particulate phases of wastewater, and in sewage sludge by liquid chromatography-tandem mass spectrometry. *Anal. Methods* 6 (5): 1341. DOI: 10.1039/c3ay42015a.

Arvaniti, O. S., Y. Hwang, H. R. Andersen, A. S. Stasinakis, N. S. Thomaidis, and M. Aloupi. 2015. Reductive degradation of perfluorinated compounds in water using mg-aminoclay coated nanoscale zero valent iron. *Chem. Eng. J.* 262. Elsevier B.V.: 133–39. DOI: 10.1016/j.cej.2014.09.079.

ASTM C 778-02. 2002. Standard Specification for Standard Sand.

Atkinson, C., S. Blake, T. Hall, R. Kanda, and P. Rumsby. 2008. Survey of the Prevalence of Perfluorooctane Sulphonate (PFOS), Perfluorooctanoic Acid (PFOA) and Related Compounds in Drinking Water and Their Sources.

Awad, E., X. Zhang, S. P. Bhavsar, S. Petro, P. W. Crozier, E. J. Reiner, R. Fletcher, S. A. Tittlemier, and E. Braekevelt. 2011. Long-term environmental fate of perfluorinated compounds after accidental release at toronto airport. *Environ. Sci. Technol.* 45 (19): 8081–89. DOI: 10.1021/es2001985.

Babatunde, O. A. 2008. A Study of the kinetics and mechanism of oxidation of L -ascorbic acid by permanganate ion in acidic medium. *World J. Chem.* 3 (1): 27–31.

Ball, W. P., C. H. Buehler, T. C. Harmon, D. M. Mackay, and P. V. Roberts. 1990. Characterization of a sandy aquifer material at the grain scale. *J. Contam. Hydrol.* 5: 253–95.

Barnard, W. R, and D. K. Nordstrom. 1982. Fluoride in precipitation—I. Methodology with the fluoride-selective electrode. *Atmos. Environ.* 16 (1): 99–103. DOI: 10.1016/0004-6981(82)90316-X.

Bhhatarai, B., and P. Gramatica. 2011. Prediction of aqueous solubility, vapor pressure and critical micelle concentration for aquatic partitioning of perfluorinated chemicals. *Environ. Sci. Technol.* 45 (19): 8120–28. DOI: 10.1021/es101181g.

Burns, D. C., D. A. Ellis, H. Li, C. J. McMurdo, and E. Webster. 2008. Experimental pKa determination for perfluorooctanoic acid (PFOA) and the potential impact of pKa concentration dependence on laboratory-measured partitioning phenomena and environmental modeling. *Environ. Sci. Technol.* 42: 9283–88.

Cha, K. Y., M. Crimi, M. A. Urynowicz, and R. C. Borden. 2012. Kinetics of permanganate consumption by natural oxidant demand in aquifer solids. *Environ. Eng. Sci.* 29 (7): 646–53. DOI: 10.1089/ees.2011.0211.

Chen, J., and P. Zhang. 2006. Photodegradation of perfluorooctanoic acid in water under irradiation of 254 nm and 185 nm light by use of persulfate. *Water Sci. Technol*. 54 (11–12): 317–25. DOI: 10.2166/wst.2006.731.

Chen, J., P. Zhang, and J. Liu. 2007. Photodegradation of perfluorooctanoic acid by 185 nm vacuum ultraviolet light. *J. Environ. Sci.* 19 (4): 387–90. DOI: 10.1016/S1001-0742(07)60064-3.

Chen, Y.-C., S.-L. Lo, and Y. Lee. 2012. Distribution and fate of perfluorinated compounds (PFCs) in a pilot constructed wetland. *Desal. Water Treat.* 37 (1–3): 178–84. DOI: 10.1080/19443994.2012.661270.

Cheng, J., E. Psillakis, M. R. Hoffmann, and A. J. Colussi. 2009. Acid dissociation versus molecular association of perfluoroalkyl oxoacids: Environmental implications. *J. Phys. Chem. A*. 113: 8152–56. DOI: 10.1021/jp9051352.

Cheng, J., C. D. Vecitis, H. Park, B. T. Mader, and M. R. Hoffmann. 2008. Sonochemical degradation of perfluorooctane sulfonate (PFOS) and perfluorooctanoate (PFOA) in landfill groundwater: environmental matrix effects. *Environ. Sci. Technol.* 42 (21): 8057–63. DOI: 10.1021/es8013858.

Chromatography Today. 2014. *How to Avoid HPLC Column Overload.* Accessed November 14, 2017. https://www.chromatographytoday.com/news/hplc-uhplc/31/breaking-news/how-to-avoid-hplc-column-overload/31536.

Cole-Parmer Company. 2008. Fluoride Ion Electrodes Instruction Manual.

Crosby, N. T., A. L. Dennis, and J. G. Stevens. 1968. An evaluation of some methods for the determination of fluoride in potable waters and other aqueous solutions. *Analyst* 93: 643–52.

Cummings, L., N. Nelson, F. Sickels, and C. T. Storms. 2015. Recommendation on Perfluorinated Compound Treatment Options for Drinking Water New Jersey Drinking Water Quality Institute.

da Silva-Rackov, C. K. O., W. A. Lawal, P. A. Nfodzo, M. M. G. R. Vianna, C. A. O. do Nascimento, and H. Choi. 2016. Degradation of PFOA by hydrogen peroxide and persulfate activated by iron-modified diatomite. *Appl. Catal., B* 192. Elsevier B.V.: 253–59. DOI: 10.1016/j.apcatb.2016.03.067.

Deng, S., Q. Yu, J. Huang, and G. Yu. 2010. Removal of perfluorooctane sulfonate from wastewater by anion exchange resins: Effects of resin properties and solution chemistry. *Water Res.* 44 (18). Elsevier Ltd: 5188–95. DOI: 10.1016/j.watres.2010.06.038.

Du, Z., S. Deng, Y. Bei, Q. Huang, B. Wang, J. Huang, and Ga. Yu. 2014. Adsorption behavior and mechanism of perfluorinated compounds on various adsorbents - A review. *J. Hazard. Mater.* 274. Elsevier B.V.: 443–54. DOI: 10.1016/j.jhazmat.2014.04.038.

Du, Z., S. Deng, S. Zhang, W. Wang, B. Wang, J. Huang, Y. Wang, G. Yu, and B. Xing. 2017. Selective and fast adsorption of perfluorooctane sulfonate from wastewater by magnetic fluorinated vermiculite. *Environ. Sci. Technol.* DOI: 10.1021/acs.est.6b06540.

Edmunds, W. M., and P. L. Smedley. 2013. Fluoride in Natural Waters. In *Essentials of Medical Geology*, 279–304. DOI: 10.1007/978-94-007-4375-5.

Ellison, Stephen L. R., and Michael Thompson. 2008. Standard additions: Myth and reality. *The Analyst* 133 (8): 992. DOI: 10.1039/b717660k.

European Union. 2006. Directive 2006/122/EC of the European Parliament and of the Council.

Falkenberg, J., A. M. Lindof, M. M. Mygind, J. K. Olsen, J. Dengsø, and A. G. Christensen. 2015. Screening for fluorinated compounds (PFAS) around potential sources of pollution at Danish defence establishments. In *AquaConSoil 2015*.

Fazlul Hoque, A. K. M., M. Khaliquzzaman, M. D. Hossain, and A. Khan. 2002. Determination of fluoride in water residues by proton induced gamma emission measurements. *Fluoride* 35 (3): 176–84.

Frant, M. S., and J. W. Ross. 1968. Determination of fluoride in water supplies. *Orion Research Inc* 40 (7): 1169–71.

Geo-Cleanse International Inc. 2017. Potential In-Situ Chemical Treatment Strategy for Remediation of PFAS Compounds.

Goss, K. -U. 2008. The pKa values of PFOA and other highly fluorinated carboxylic acids. *Environ. Sci. Technol.* 42: 456–58. DOI: 10.1021/es702192c.

Guan, B., J. Zhi, X. Zhang, T. Murakami, and A. Fujishima. 2007. Electrochemical route for fluorinated modification of boron-doped diamond surface with perfluorooctanoic acid. *Electrochem. Commun.* 9 (12): 2817–21. DOI: 10.1016/j.elecom.2007.10.003.

Guelfo, J. L., and C. P. Higgins. 2013. subsurface transport potential of perfluoroalkyl acids at aqueous film-forming foam (AFFF)-impacted sites. *Environ. Sci. Technol.* 47 (9): 4164–71. DOI: 10.1021/es3048043.

Hanna Instruments. n.d. Instruction Manual: Fluoride Ion Selective Electrode.

Hansen, M. C., M. H. Børresen, M. Schlabach, and G. Cornelissen. 2010. Sorption of perfluorinated compounds from contaminated water to activated carbon. *J. Soils Sediments* 10 (2): 179–85. DOI: 10.1007/s11368-009-0172-z.

Harwood, J. E. 1969. The use of an ion-selective electrode for routine fluoride analyses on water samples. *Water Res.* 3 (4): 273–80. DOI: 10.1016/0043-1354(69)90024-4.

Health Canada. 2016a. Perfluorooctane Sulfonate (PFOS) in Drinking Water.

———. 2016b. Perfluorooctanoic Acid (PFOA) in Drinking Water.

Higgins, C. P., and R. G. Luthy. 2006. Sorption of perfluorinated surfactants on sediments. *Environ. Sci. Technol.* 40 (23): 7251–56. DOI: 10.1021/es061000n.

Hori, H., E. Hayakawa, H. Einaga, S. Kutsuna, K. Koike, T. Ibusuki, H. Kiatagawa, and R. Arakawa. 2004. Decomposition of environmentally persistent perfluorooctanoic acid in water by photochemical approaches. *Environ. Sci. Technol.* 38 (22): 6118–24. DOI: 10.1021/es049719n.

Hori, H., Y. Nagaoka, M. Murayama, and S. Kutsuna. 2008. Efficient decomposition of perfluorocarboxylic acids and alternative fluorochemical surfactants in hot water. *Environ. Sci. Technol.* 42 (19): 7438–43. DOI: 10.1021/es800832p.

Hori, H., Y. Nagaoka, A. Yamamoto, T. Sano, N. Yamashita, S. Taniyasu, S. Kutsuna, I. Osaka, and R. Arakawa. 2006. Efficient decomposition of environmentally persistent perfluorooctanesulfonate and related fluorochemicals using zerovalent iron in subcritical water. *Environ. Sci. Technol.* 40 (3): 1049–54. DOI: 10.1021/es0517419.

Hori, H., A. Yamamoto, E. Hayakawa, S. Taniyasu, N. Yamashita, S. Kutsuna, H. Kiatagawa, and R. Arakawa. 2005. Efficient decomposition of environmentally persistent perfluorocarboxylic acids by use of persulfate as a photochemical oxidant. *Environ. Sci. Technol.* 39 (7): 2383–88. DOI: 10.1021/es0484754.

Houtz, E. F., and D. L. Sedlak. 2012. Oxidative conversion as a means of detecting precursors to perfluoroalkyl acids in urban runoff. *Environ. Sci. Technol.* 46 (17): 9342–49. DOI: 10.1021/es302274g.

Huang, Q. 2013. Remediation of Perfluoroalkyl Contaminated Aquifers Using an In-Situ Two-Layer Barrier: Laboratory Batch and Column Study.

Huling, S. G., S. Ko, and B. Pivetz. 2011. Groundwater sampling at ISCO sites: Binary mixtures of volatile organic compounds and persulfate. *Ground Water Monit. Rem.* 31 (2): 72–79. DOI: 10.1111/j1745.

Jin, L., P. Zhang, T. Shao, and S. L. Zhao. 2014. Ferric ion mediated photodecomposition of aqueous perfluorooctane sulfonate (PFOS) under UV irradiation and its mechanism. *J. Hazard. Mater.* 271. Elsevier B.V.: 9–15. DOI: 10.1016/j.jhazmat.2014.01.061.

Jin, Y. 2017. Dual Oxidant System for In Situ Treatment of Organic Contaminants. University of Waterloo

Johnson, R. L., A. J. Anschutz, J. M. Smolen, M. F. Simcik, and R. Lee Penn. 2007. The adsorption of perfluorooctane sulfonate onto sand, clay, and iron oxide surfaces. *J. Chem. Eng. Data* 52 (4): 1165–70. DOI: 10.1021/je060285g.

Kaiser, M.A., Barton, C.A., Botelho, M., Buck, R.C., Buxton, L.W., Gannon, J., Kao, C.C., Larsen, B.S., Russel, M.H., Wang, N., Waterland, R.L., 2006. Understanding the transport of anthropogenic fluorinated compounds in the environment. *Organohalogen Compounds* 68: 675-678.

Kauranen, P. 1977. The use of buffers in the determination of fluoride by an ion-selective electrode at low concentrations and in the presence of aluminum. *Anal. Lett.* 10 (6): 451–65. DOI: 10.1080/00032717708079390.

Kingston, J. L. T. 2008. A Critical Evaluation of *In-Situ* Thermal Technologies. Arizona State University.

Kissa, E. 1983. Determination of fluoride at low concentrations with the ion-selective electrode. *Anal. Chem.* 55: 1445–48.

Kupryianchyk, D., S. E. Hale, G. D. Breedveld, and G. Cornelissen. 2015. Treatment of sites contaminated with perfluorinated compounds using biochar amendment. *Chemosphere* 142. Elsevier Ltd: 35–40. DOI: 10.1016/j.chemosphere.2015.04.085.

Kuroda, K., M. Murakami, K. Oguma, H. Takada, and S. Takizawa. 2014. Investigating sources and pathways of perfluoroalkyl acids (PFAAs) in aquifers in Tokyo using multiple tracers. *Sci. Total Environ.* 488–489. Elsevier B.V.: 51–60. DOI: 10.1016/j.scitotenv.2014.04.066.

Langmuir, D. 1968. Stability of calcite based on aqueous solubility measurements. *Geochimica et Cosmochimica Acta* 32 (67): 835–51. DOI: 10.1016/0016-7037(68)90099-9.

Lee, L. S. 2009. Quantification of In Situ Chemical Reductive Defluorination (ISCRD) of Perfluoroalkyl Acids in Groundwater Impacted by AFFFs.

Lee, Y.-C., Y.-P. Chen, M. J. Chen, J. Kuo, and S.-L. Lo. 2017. Reductive defluorination of perfluorooctanoic acid by titanium(III) citrate with vitamin B12 and copper nanoparticles. *J. Hazard. Mater.* Elsevier B.V. DOI: 10.1016/j.jhazmat.2017.06.020.

Lee, Y.-C., S. L. Lo, J. Kuo, and C. P. Huang. 2013. Promoted degradation of perfluorooctanic acid by persulfate when adding activated carbon. *J. Hazard. Mater.* 261. Elsevier B.V.: 463–69. DOI: 10.1016/j.jhazmat.2013.07.054.

Lee, Y., S.-L. Lo, P.-T. Chiueh, and D.-G. Chang. 2009. Efficient decomposition of perfluorocarboxylic acids in aqueous solution using microwave-induced persulfate. *Water Res.* 43 (11). Elsevier Ltd: 2811–16. DOI: 10.1016/j.watres.2009.03.052.

Lee, Y., S.-L. Lo, P.-T. Chiueh, Y.-H. Liou, and M.-L. Chen. 2010. Microwave-hydrothermal decomposition of perfluorooctanoic acid in water by iron-activated persulfate oxidation. *Water Res.* 44 (3). Elsevier Ltd: 886–92. DOI: 10.1016/j.watres.2009.09.055.

Lee, Y., S.-L. Lo, J. Kuo, and C. Hsieh. 2012a. Decomposition of perfluorooctanoic acid by microwave activated persulfate: Effects of temperature, pH, and chloride ions. *Front. Environ. Sci. Eng. China* 6 (1): 17–25. DOI: 10.1007/s11783-011-0371-x.

Lee, Y., S.-L. Lo, J. Kuo, and Y.-L. Lin. 2012b. Persulfate oxidation of perfluorooctanoic acid under the temperatures of 20 - 40 C. *Chem. Eng. J.* 198–199. Elsevier B.V.: 27–32. DOI: 10.1016/j.cej.2012.05.073.

Li, W., R. Orozco, N. Camargos, and H. Liu. 2017. Mechanisms on the impacts of alkalinity, pH and chloride on persulfate-based groundwater remediation. *Environ. Sci. Technol.* DOI: 10.1021/acs.est.6b04849.

Li, X., S. Chen, X. Quan, and Y. Zhang. 2011. Enhanced adsorption of PFOA and PFOS on multiwalled carbon nanotubes under electrochemical assistance. *Environ. Sci. Technol.* 45 (19): 8498–8505. DOI: 10.1021/es202026v.

Liang, C., and H. W. Su. 2009. Identification of sulfate and hydroxyl radicals in thermally activated persulfate. *Ind. Eng. Chem. Res.* 48 (11): 5558–62. DOI: 10.1021/ie9002848.

Liang, C., Z. S. Wang, and C. J. Bruell. 2007. Influence of pH on persulfate oxidation of TCE at ambient temperatures. *Chemosphere* 66 (1): 106–13. DOI: 10.1016/j.chemosphere.2006.05.026.

Lin, A. Y.-C., S. C. Panchangam, C.-Y. Chang, P. K. A. Hong, and H.-F. Hsueh. 2012. Removal of perfluorooctanoic acid and perfluorooctane sulfonate via ozonation under alkaline condition. *J. Hazard. Mater.* 243. Elsevier B.V.: 272–77. DOI: 10.1016/j.jhazmat.2012.10.029.

Liu, C. S., C. P. Higgins, F. Wang, and K. Shih. 2012a. Effect of temperature on oxidative transformation of perfluorooctanoic acid (PFOA) by persulfate activation in water. *Sep. Purif. Technol.* 91. Elsevier B.V.: 46–51. DOI: 10.1016/j.seppur.2011.09.047.

Liu, C. S., K. Shih, and F. Wang. 2012b. Oxidative decomposition of perfluorooctanesulfonate in water by permanganate. *Sep. Purif. Technol.* 87. Elsevier B.V.: 95–100. DOI: 10.1016/j.seppur.2011.11.027.

Liu, D., Z. Xiu, F. Liu, G. Wu, D. Adamson, C. Newell, P. Vikesland, A.-L. Tsai, and P. J. Alvarez. 2013. Perfluorooctanoic acid degradation in the presence of Fe(III) under natural sunlight. *J. Hazard. Mater.* 262. Elsevier B.V.: 456–63. DOI: 10.1016/j.jhazmat.2013.09.001.

Liu, H., T. A. Bruton, F. M. Doyle, and D. L. Sedlak. 2014. In situ chemical oxidation of contaminated groundwater by persulfate: Decomposition by Fe(III)- and Mn(IV)-containing oxides and aquifer materials. *Environ. Sci. Technol.* 48 (17): 10330–36. DOI: 10.1021/es502056d.

Luo, Q., and R. S. Sidhu. 2013. Remediation of perfluorooctanoic acid contaminated aquifer using an in situ permeable reactive barrier. In *Battelle Bioremediation and Sustainable Environmental Technologies*.

McGuire, M. E. 2013. An In-Depth Site Characterization of Poly-and Perfluoroalkyl Substances at an Abandoned Fire Protection Training Area. Colorado State University.

McKenzie, E. R., R. L. Siegrist, J. E. McCray, and C. P. Higgins. 2015a. Effects of chemical oxidants on perfluoroalkyl acid transport in one-dimensional porous media columns. *Environ. Sci. Technol.* 49 (3): 1681–89. DOI: 10.1021/es503676p.

———. 2015b. SI: Effects of chemical oxidants on perfluoroalkyl acid transport in one-dimensional porous media columns. *Environ. Sci. Technol.* 49 (3): 1681–89. DOI: 10.1021/es503676p.

Merino, N., Y. Qu, R. A. Deeb, E. L. Hawley, M. R. Hoffmann, and S. Mahendra. 2016. Degradation and removal methods for perfluoroalkyl and polyfluoroalkyl substances in water. *Environ. Eng. Sci.* 33 (9). DOI: 10.1089/ees.2016.0233.

Mikhelson, K. N. 2013. Chapter 2: The Basics of the ISEs. In *Ion-Selective Electrodes*, 81:11–32. DOI: 10.1007/978-3-642-36886-8.

Milinovic, J., S. Lacorte, M. Vidal, and A. Rigol. 2015. Sorption behaviour of perfluoroalkyl substances in soils. *Sci. Total Environ.* 511: 63–71. DOI: 10.1016/j.scitotenv.2014.12.017.

Mitchell, S. M., M. Ahmad, A. L. Teel, and R. J. Watts. 2014. Degradation of perfluorooctanoic acid by reactive species generated through catalyzed H2O2 propagation reactions. *Environ. Sci. Technol. Lett.* 1 (1): 117–21. DOI: 10.1021/ez4000862.

Moody, C. A., and J. A. Field. 1999. Determination of perfluorocarboxylates in groundwater impacted by fire-fighting activity. *Environ. Sci. Technol.* 33 (16): 2800–2806. DOI: 10.1021/es981355.

———. 2000. Perfluorinated surfactants and the environmental implications of their use in fire-fighting foams. *Environ. Sci. Technol.* 34 (18): 3864–70. DOI: 10.1021/es991359u.

Moody, C. A., G. Hebert, S. Strauss, and J. A. Field. 2003. Occurrence and persistence of perfluorooctanesulfonate and other perfluorinated surfactants in groundwater at a fire-training area at Wurtsmith Air Force Base, Michigan, USA. *J. Environ. Monit.* 5 (2): 341–45. DOI: 10.1039/b212497a.

Moriwaki, H., Y. Takagi, M. Tanaka, K. Tsuruho, K. Okitsu, and Y. Maeda. 2005. Sonochemical decomposition of perfluorooctane sulfonate and perfluorooctanoic acid. *Environ. Sci. Technol.* 39 (9): 3388–92. DOI: 10.1021/es040342v.

Nicholson, K., and E. J. Duff. 1981. Fluoride determination in water: an optimum buffer system for use with the flouride-selective electrode. *Anal. Lett.* 14 (A12): 887–912. DOI: 10.1080/00032718108081423.

O'Hagan, D. 2008. Understanding organofluorine chemistry. An introduction to the C-F bond. *Chem. Soc. Rev.* 37 (2): 308–19. DOI: 10.1039/b711844a.

Ochoa-Herrera, V., R. Sierra-Alvarez, A. Somogyi, N. E. Jacobsen, V. H. Wysocki, and J. A. Field. 2008. Reductive defluorination of perfluorooctane sulfonate. *Environ. Sci. Technol.* 42 (9): 3260–64. DOI: 10.1021/es702842q.

Oliaei, F., D. Kriens, R. Weber, and A. Watson. 2013. PFOS and PFC releases and associated pollution from a pfc production plant in Minnesota (USA). *Environ. Sci. Pollut. Res.* 20 (4): 1977–92. DOI: 10.1007/s11356-012-1275-4.

Oliveira, F. C., J. G. Freitas, S. A.C. Furquim, R. M. Rollo, N. R. Thomson, L. R. F. Alleoni, and C. A. O. Nascimento. 2016. Persulfate interaction with tropical soils. *Water Air Soil Pollut.* 227 (9). DOI: 10.1007/s11270-016-3000-2.

Pancras, T. A., W. Plaisier, P. J. A. Dols, and J. A. Barbier. 2013. Degrading non-volatile halogenated organic compounds, patent issued 2013.

Pancras, T. A., G. Schrauwen, T. Held, K. Baker, I. Ross, and H. Slenders. 2016. Environmental fate and effects of poly- and perfluoroalkyl substances (PFAS).

Park, H., C. D. Vecitis, J. Cheng, W. Choi, B. T. Mader, and M. R. Hoffmann. 2009. Reductive defluorination of aqueous perfluorinated alkyl surfactants: Effects of ionic headgroup and chain length. *J. Phys. Chem. A* 113 (4): 690–96. DOI: 10.1021/jp807116q.

Park, S., L. S. Lee, V. F. Medina, A. Zull, and S. Waisner. 2016. Heat-activated persulfate oxidation of PFOA, 6:2 fluorotelomer sulfonate, and PFOS under conditions suitable for in-situ groundwater remediation. *Chemosphere* 145. Elsevier Ltd: 376–83. DOI: 10.1016/j.chemosphere.2015.11.097.

Park, S., J. E. Zenobio, and L. S. Lee. 2017. Perfluorooctane sulfonate (PFOS) removal with Pd 0 /nFe 0 nanoparticles: Adsorption or aqueous Fe-complexation, not transformation? *J. Hazard. Mater.* Elsevier B.V., 0–30. DOI: 10.1016/j.jhazmat.2017.08.001.

Paulson, K. 2014. Methylmercury Production in Riverbank Sediments of the South River, Virginia (USA) and Assessment of Biochar as a Mercury Treatment Option. University of Waterloo.

Petri, B. G., R. J. Watts, A. Tsitonaki, M. Crimi, N. R. Thomson, and A. L. Teel. 2011. Chapter 4: Fundamentals of ISCO Using Persulfate. In *In Situ Chemical Oxidation for Groundwater Remediation*, edited by R. L. Siegrist, M. Crimi, T. L. Simpkin, and R. C. Borden, 3:147–91. doi:10.1007/978-1-4419-7826-4.

Plumlee, M. H., J. Larabee, and M. Reinhard. 2008. Perfluorochemicals in water reuse. *Chemosphere* 72 (10): 1541–47. DOI: 10.1016/j.chemosphere.2008.04.057.

Post, G. B., P. D. Cohn, and K. R. Cooper. 2012. Perfluorooctanoic acid (PFOA), an emerging drinking water contaminant: A critical review of recent literature. *Environ. Res.* 116. Elsevier: 93–117. DOI: 10.1016/j.envres.2012.03.007.

Ptacek, C. J., and R. W. Gillham. 1992. Laboratory and field measurements of non-equilibrium transport in the Borden aquifer, Ontario, Canada. *J. Contam. Hydrol.* 10 (2): 119–58. DOI: 10.1016/0169-7722(92)90026-B.

Quinnan, J., A. Malcolm, A. Bodour, S. Brock, J. Hess-Wilson, and C. Long. 2013. Fungal degradation of perfluorooctane sulfonate (PFOS) and perfluorooctanoic acid (PFOA). In *Battelle Bioremediation and Sustainable Environmental Technologies*.

Quinones, O., and S. A. Snyder. 2009. Occurrence of perfluoroalkyl carboxylates and sulfonates in drinking water utilities and related waters from the United States. *Environ. Sci. Technol.* 43 (24): 9089–95. DOI: 10.1021/es9024707.

Rahman, M. F. 2014. Removal of Perfluorinated Compounds from Ultrapure and Surface Waters by Adsorption and Ion Exchange. University of Waterloo.

Rahman, M. F., S. Peldszus, and W. B. Anderson. 2014. Behaviour and fate of perfluoroalkyl and polyfluoroalkyl substances (PFASs) in drinking water treatment: A review. *Water Res.* 50. Elsevier Ltd: 318–40. DOI: 10.1016/j.watres.2013.10.045.

Saha, J. K., and S. Kundu. 2003. Determination of fluoride in soil water extract through ion chromatography. *Commun. Soil Sci. Plant Anal.* 34: 181–88. DOI: 10.1081/CSS-120017424.

Santos, A., S. Rodriguez, F. Pardo, and A. Romero. 2016. Use of Fenton reagent combined with humic acids for the removal of PFOA from contaminated water. *Sci. Total Environ.* 563–564. Elsevier B.V.: 657–63. DOI: 10.1016/j.scitotenv.2015.09.044.

Schaefer, C. E., C. Andaya, A. Urtiaga, E. R. McKenzie, and C. P. Higgins. 2015. Electrochemical treatment of perfluorooctanoic acid (PFOA) and perfluorooctane sulfonic acid (PFOS) in groundwater impacted by aqueous film forming foams (AFFFs). *J. Hazard. Mater.* 295. Elsevier B.V.: 170–75. DOI: 10.1016/j.jhazmat.2015.04.024.

Schaider, L. A., R. A. Rudel, J. M. Ackerman, S. C. Dunagan, and J. G. Brody. 2014. Pharmaceuticals, perfluorosurfactants, and other organic wastewater compounds in public drinking water wells in a shallow sand and gravel aquifer. *Sci. Total Environ.* 468–469. DOI: 10.1016/j.scitotenv.2013.08.067.

Schimadzu. 2015. pKa and Dissociation Equilibrium. http://www.shimadzu.com/an/hplc/support/lib/lctalk/29/29intro.html

Schultz, M. M., D. F. Barofsky, and J. A. Field. 2003. Fluorinated alkyl surfactants. *Environ. Eng. Sci.* 20 (5): 487–501. DOI: 10.1089/109287503768335959.

———. 2004. Quantitative determination of fluorotelomer sulfonates in groundwater by LC MS/MS. *Environ. Sci. Technol.* 38 (6): 1828–35. DOI: 10.1021/es035031j.

Skoog, D. A., D. M. West, F. J. Holler, and S. R. Crouch. 2014. Fundamentals of Analytic Chemistry. 9th ed.

Song, B., G. Zeng, J. Gong, J. Liang, P. Xu, Z. Liu, Y. Zhang, et al. 2017. Evaluation methods for assessing effectiveness of in situ remediation of soil and sediment contaminated with organic pollutants and heavy metals. *Environ. Int.* 105. Elsevier: 43–55. DOI: 10.1016/j.envint.2017.05.001.

Song, Z., H. Tang, N. Wang, and L. Zhu. 2013. Reductive defluorination of perfluorooctanoic acid by hydrated electrons in a sulfite-mediated UV photochemical system. *J. Hazard. Mater.* 262. Elsevier B.V.: 332–38. DOI: 10.1016/j.jhazmat.2013.08.059.

Sousa, A. R., and M. A. Trancoso. 2005. Uncertainty of measurement for the determination of fluoride in water and wastewater by direct selective electrode potentiometry. *Accred. Qual. Assur.* 10 (8): 430–38. DOI: 10.1007/s00769-005-0009-4.

Sra, K. S., N. R. Thomson, and J. F. Barker. 2010. Persistence of persulfate in uncontaminated aquifer materials. *Environ. Sci. Technol.* 44 (8): 3098–3104. DOI: 10.1021/es903480k.

Sra, K. S., J. J. Whitney, N. R. Thomson, and J. F. Barker. 2007. Persulfate decomposition kinetics in the presence of aquifer materials. In *Proceedings of the Annual International Conference on Soils, Sediments, Water and Energy*, 12:1–10.

Stock, N. L., V. I. Furdui, D. C. G. Muir, and S. A. Mabury. 2007. Perfluoroalkyl contaminants in the Canadian arctic: Evidence of atmospheric transport and local contamination. *Environ. Sci. Technol.* 41 (10): 3529–36. DOI: 10.1021/es062709x.

Strajin, D., and W. B. Kerfoot. 2012. Perfluorocompound treatment by peroxide-coated nanobubble AOP. In *The Annual International Conference on Soils, Sediments, Water and Energy*, 1–25.

Stratton, G. R., F. Dai, C. L. Bellona, T. M. Holsen, E. R. V. Dickenson, and S. Mededovic Thagard. 2017. Plasma-based water treatment: Efficient transformation of perfluoroalkyl substances (PFASs) in prepared solutions and contaminated groundwater. *Environ. Sci. Technol.* DOI: 10.1021/acs.est.6b04215.

Stüber, M., and T. Reemtsma. 2004. Evaluation of three calibration methods to compensate matrix effects in environmental analysis with LC-ESI-MS. *Anal. Bioanal. Chem.* 378 (4): 910–16. DOI: 10.1007/s00216-003-2442-8.

Sun, B., J. Ma, and D. L. Sedlak. 2016. Chemisorption of perfluorooctanoic acid on powdered activated carbon initiated by persulfate in aqueous solution. *Environ. Sci. Technol.* DOI: 10.1021/acs.est.6b00411.

Tang, C. Y., Q. S. Fu, C. S. Criddle, and J. O. Leckie. 2007. Effect of flux (transmembrane pressure) and membrane properties on fouling and rejection of reverse osmosis and nanofiltration membranes treating perfluorooctane sulfonate containing wastewater. *Environ. Sci. Technol.* 41 (6): 2008–14. DOI: 10.1021/es062052f.

Tang, H., Q. Xiang, M. Lei, J. Yan, L. Zhu, and J. Zou. 2012. Efficient degradation of perfluorooctanoic acid by UV–Fenton orocess. *Chem. Eng. J.* 184. Elsevier B.V.: 156–62. DOI: 10.1016/j.cej.2012.01.020.

Tang, Y. C., Q. S. Fu, A. P. Robertson, C. S. Criddle, and J. O. Leckie. 2006. Use of reverse osmosis membranes to remove perfluorooctane sulfonate (PFOS) from semiconductor wastewater. *Environ. Sci. Technol.* 40 (23): 7343–49. DOI: 10.1021/es060831q.

Thermo Scientific. 2011. User Guide: Fluoride Ion Selective Electrode.

Thompson, J., G. Eaglesham, J. Reungoat, Y. Poussade, M. Bartkow, M. Lawrence, and J. F. Mueller. 2011. Removal of PFOS, PFOA and other perfluoroalkyl acids at water reclamation plants in South East Queensland Australia. *Chemosphere* 82 (1). Elsevier Ltd: 9–17. DOI: 10.1016/j.chemosphere.2010.10.040.

Tsai, Y.-T., A. Y.-C. Lin, Y.-H. Weng, and K.-C. Li. 2010. Treatment of perfluorinated chemicals by electro-microfiltration. *Environ. Sci. Technol.* 44 (20): 7914–20. DOI: 10.1021/es101964y.

Tsitonaki, A., B. Petri, M. Crimi, H. Mosbæk, R. L. Siegrist, and P. L. Bjerg. 2010. In situ chemical oxidation of contaminated soil and groundwater using persulfate: A review. *Crit. Rev. Env. Sci. Technol.* 40 (1): 55–91. DOI: 10.1080/10643380802039303.

United Nations Environmental Program. 2009. SC-4/17: Listing of perfluorooctane sulfonic acid, its salts and perfluorooctane sulfonyl fluoride. In *Stockholm Convention on Persistent Organic Pollutants*, 15–18.

US Department of Health and Human Services. 2015. Draft Toxicological Profile for Perfluoroalkyls.

USEPA. 1974. Method 340.2: Fluoride (Potentiometric, Ion Selective Electrode). EPA Methods.

———. 1996. Method 9214: Potentiometric Determination of Fluoride in Aqueous Samples with Ion-Selective Electrode. EPA Methods, 1–8.

———. 1997. Method 300.1: Determination of Inorganic Anions in Drinking Water by Ion Chromatography. DOI: 10.1016/S0165-9936(01)00070-X.

———. 2009. Method 537: Determination of Selected Perfluorinated Alkyl Acids in Drinking Water by Solid Phase Extraction and Liquid Chromatography/ Tandem Mass Spectrometry (LC/MS/MS). EPA Methods, 1–50.

———. 2014a. Emerging Contaminants – Perfluorooctane Sulfonate (PFOS) and Perfluorooctanoic Acid (PFOA) At a Glance.

———. 2014b. Project Quality Assurance and Quality Control. In Test Methods for Evaluating Solid Waste, Physical/ Chemical Methods.

Vecitis, C. D., H. Park, J. Cheng, B. T. Mader, and M. R. Hoffmann. 2008. Kinetics and mechanism of the sonolytic conversion of the aqueous perfluorinated surfactants,

perfluorooctanoate (PFOA), and perfluorooctane sulfonate (PFOS) into inorganic products. *J. Phys. Chem. A* 112 (18): 4261–70. DOI: 10.1021/jp801081y.

———. 2009. Treatment technologies for aqueous perfluorooctanesulfonate (PFOS) and perfluorooctanoate (PFOA). *Front. Environ. Sci. Eng. China* 3 (2): 129–51. DOI: 10.1007/s11783-009-0022-7.

Wang, F., X. Lu, X.-Y. Li, and K. Shih. 2015. Effectiveness and mechanisms of defluorination of perfluorinated alkyl substances by calcium compounds during waste thermal treatment. *Environ. Sci. Technol.* 49 (9): 5672–80. DOI: 10.1021/es506234b.

Wang, L., L. Peng, L. Xie, P. Deng, and D. Deng. 2017a. Compatibility of surfactants and thermally activated persulfate for enhanced subsurface remediation. *Environ. Sci. Technol.* DOI: 10.1021/acs.est.6b05477.

Wang, Z., J. C. DeWitt, C. P. Higgins, and I. T. Cousins. 2017b. A never-ending story of per- and polyfluoroalkyl substances (PFASs)? *Environ. Sci. Technol.* DOI: 10.1021/acs.est.6b04806.

Watts, R. J., and A. L. Teel. 2006. Treatment of contaminated soils and groundwater using ISCO. *Pract. Period. Hazard. Toxic Radioact. Waste Manage.* 10 (January): 2–9. DOI: 10.1061/(ASCE)1090-025X(2006)10:1(2).

Weiß, O., G. A. Wiesmüller, A. Bunte, T. Göen, C. K. Schmidt, M. Wilhelm, and J. Hölzer. 2012. Perfluorinated compounds in the vicinity of a fire training area - Human biomonitoring among 10 persons drinking water from contaminated private wells in Cologne, Germany. *Int. J. Hyg. Environ. Health* 215 (2). Elsevier GmbH.: 212–15. DOI: 10.1016/j.ijheh.2011.08.016.

Xiao, F., M. F. Simcik, T. R. Halbach, and J. S. Gulliver. 2015. Perfluorooctane sulfonate (PFOS) and perfluorooctanoate (PFOA) in soils and groundwater of a U.S. metropolitan area: Migration and implications for human exposure. *Water Res.* 72. Elsevier Ltd: 64–74. DOI: 10.1016/j.watres.2014.09.052.

Xu, X., and N. R. Thomson. 2009. A long-term bench-scale investigation of permanganate consumption by aquifer materials. *J. Contam. Hydrol.* 110 (3–4). Elsevier B.V.: 73–86. DOI: 10.1016/j.jconhyd.2009.09.001.

Yamamoto, T., Y. Noma, S. I. Sakai, and Y. Shibata. 2007. Photodegradation of perfluorooctane sulfonate by UV irradiation in water and alkaline 2-propanol. *Environ. Sci. Technol.* 41 (16): 5660–65. DOI: 10.1021/es0706504.

Yamashita, N., K. Kannan, S. Taniyasu, Y. Horii, T. Okazawa, G. Petrick, and T. Gamo. 2004. Analysis of perfluorinated acids at parts-per-quadrillion levels in seawater using liquid chromatography-tandem mass spectrometry. *Environ. Sci. Technol.* 38 (21): 5522–28. DOI: 10.1021/es0492541.

Yan, T., H. Chen, F. Jiang, and X. Wang. 2014. Adsorption of perfluorooctane sulfonate and perfluorooctanoic acid on magnetic mesoporous carbon nitride. *J. Chem. Eng. Data* 59: 508–15.

Yang, S., J. Cheng, J. Sun, Y. Hu, and X. Liang. 2013. Defluorination of aqueous perfluorooctanesulfonate by activated persulfate oxidation. *PLoS ONE* 8 (10): 1–10. DOI: 10.1371/journal.pone.0074877.

Yates, B. J., R. Darlington, R. Zboril, and V. K. Sharma. 2014. High-valent iron-based oxidants to treat perfluorooctanesulfonate and perfluorooctanoic acid in water. *Environ. Chem. Lett.* 12: 413–17. DOI: 10.1007/s10311-014-0463-5.

Yin, P., Z. Hu, X. Song, J. Liu, and N. Lin. 2016. Activated persulfate oxidation of perfluorooctanoic acid (PFOA) in groundwater under acidic conditions. *Int. J. Env. Res. Pub. Health* 13 (6): 602. DOI: 10.3390/ijerph13060602.

Yu, Q., S. Deng, and G. Yu. 2008. Selective removal of perfluorooctane sulfonate from aqueous solution using chitosan-based molecularly imprinted polymer adsorbents. *Water Res.* 42 (12): 3089–97. DOI: 10.1016/j.watres.2008.02.024.

Zareitalabad, P., J. Siemens, M. Hamer, and W. Amelung. 2013. Perfluorooctanoic acid (PFOA) and perfluorooctanesulfonic acid (PFOS) in surface waters, sediments, soils and wastewater - A review on concentrations and distribution coefficients. *Chemosphere* 91 (6). Elsevier Ltd: 725–32. DOI: 10.1016/j.chemosphere.2013.02.024.

Zhang, M., X. Chen, H. Zhou, M. Murugananthan, and Y. Zhang. 2015. Degradation of P-nitrophenol by heat and metal ions co-activated persulfate. *Chem. Eng. J.* 264. Elsevier B.V.: 39–47. DOI: 10.1016/j.cej.2014.11.060.

Zhou, Q., S. Deng, Q. Yu, Q. Zhang, G. Yu, J. Huang, and H. He. 2010. Sorption of perfluorooctane sulfonate on organo-montmorillonites. *Chemosphere* 78. Elsevier Ltd: 688–94. DOI: 10.1016/j.chemosphere.2009.12.005.

Zhou, Q., S. Deng, Q. Zhang, F. Qing, J. Huang, and G. Yu. 2010. Sorption of perfluorooctane sulfonate and perfluorooctanoate on activated sludge. *Chemosphere* 81. Elsevier Ltd: 453–58. DOI: 10.1016/j.watres.2008.12.001.

# Appendices

# Appendix A: Reviewed Treatment Methods

**Table A.1. Promising treatment techniques for PFOA and PFOS from literature review**

| Reactant | Reactant Details | Proposed Mechanism(s) | PFOA Conc. ($\mu g\ L^{-1}$) | PFOS Conc. ($\mu g\ L^{-1}$) | Matrix | Environmental Conditions | Source |
|---|---|---|---|---|---|---|---|
| Capture | | | | | | | |
| **Anion Exchange Resin** | 0.05 g $L^{-1}$ polyacrylic gel resin | Electrostatic attraction, hydrophobic adsorption, and diffusion into pores; Multi-layer, Freundlich isotherm | - | 200,000 >63 % removed | Aqueous | pH = 3 T = 25 °C Time = 50 h 150 rpm | (Deng et al. 2010) |
| **Anion Exchange Resin** | 0.01 g $L^{-1}$ macroporous polystyrenic resin | | 3 >99 % removed | - | Aqueous | T = 20 °C Time = 11 d 150 rpm | (Rahman 2014) |
| **Chemisorption** | 1 g $L^{-1}$ PAC with 10 mM PS | Covalent bonding onto PAC following reaction with PS | 207 70 % removed | - | Aqueous | pH = 8.2 T = 80 °C Time = 3 h | (Sun, Ma, and Sedlak 2016) |
| **Complexation** | 20 g $L^{-1}$ palladium coated zero valent iron nanoparticles | Formation of PFOS-Fe complex | - | 2898 ~35 % removed | Aqueous | pH = 3.6 T = 70 °C Time = 6 d | (Park et al. 2017) |
| **Constructed Wetland** | Constructed wetlands using four different aquatic plants | Uptake by plant roots, some sorption to organic matter in soil | 5000 (PFC mix) >90 % removed (PFOS) >70 % removed (PFOA) | | Aqueous | pH = 5.91 T = 28 – 32 °C Time = 15 d Aerobic | (Chen et al. 2012) |
| **Electro-Microfiltration** | Microfilter with 58 V $cm^{-1}$ and cross-flow of 0.18 m $s^{-1}$ | Electrophoretic and electrostatic attraction | 100 >84 % removed | 100 >84 % removed | Aqueous | pH = 10 P = 49 kPa Aerobic | (Tsai et al. 2010) |
| **Electro-Sorption** | Multi-walled carbon nanotubes with 0.6 V | Electrostatic attraction to charged electrode and diffusion to internal sites; some hydrophobic adsorption | 100 93 % removed | 100 96 % removed | Aqueous | pH = 6.5 – 7 T = 25 °C Time = 3 h | (Li et al. 2011) |

| Reactant | Reactant Details | Proposed Mechanism(s) | PFOA Conc. ($\mu g\ L^{-1}$) | PFOS Conc. ($\mu g\ L^{-1}$) | Matrix | Environmental Conditions | Source |
|---|---|---|---|---|---|---|---|
| Capture (Cont'd) | | | | | | | |
| Nanofiltration | Nanofilter operating at 1.37 L min$^{-1}$ | Diffusion into membrane; electrostatic self-repulsion prevents cake formation | - | 10,000 90 % removed | Aqueous | pH = 4 P = 1379 kPa Aerobic | (Tang et al. 2007) |
| Reverse Osmosis | Reverse osmosis (RO) | Size exclusion | 0.015 – 0.027 Removed BDL (0.0009) | 0.023 – 0.039 Removed BDL (0.0005) | Aqueous Effluent | Aerobic | (Thompson et al. 2011) |
| Reverse Osmosis | Thin-film composite polyamide RO membrane operating at 1.37 L min$^{-1}$ | | - | 500 – 1,600,000 >99 % removed | Aqueous | pH = 4 T = 25 °C P = 1380 kPa Aerobic | (Tang et al. 2006) |
| Sorption | 0.01 g L$^{-1}$ coal-based granular activated carbon (GAC) | | 3 >90 % removed | - | Aqueous | T = 20 °C Time = 16 d 150 rpm | (Rahman 2014) |
| Sorption | 0.025 g L$^{-1}$ powdered activated carbon (PAC) | Attraction to surface functional groups, diffusion into pores | 1.4 88 % removed | 1.4 97 % removed | Aqueous | pH = 6.7 T = 20 °C Time = 10 m 100 rpm | (Hansen et al. 2010) |
| Sorption | 2 g L$^{-1}$ PAC | | 1.15 > 80 % removed | 145 >80 % removed | 1:20 Soil: Ultrapure water | Time = 14 d | (Kupryianchyk et al. 2015) |
| Sorption | 0.005 g L$^{-1}$ nano-Fe3O4 embedded in fluorinated vermiculite | Selective adsorption due to fluorophilicity of sorbent material | | 25,000 23 % removed | 25,000 1127 mg/g | pH = 6 T = 25 °C Time = 4 h 150 rpm | (Du et al. 2017) |
| Sorption | 0.1 g L$^{-1}$ chitosan-based PFOS-imprinted polymer | Electrostatic attraction to protonated amino groups, diffusion into selective imprinting sites | - | 50,000 >99 % removed | Aqueous | pH = 3 T = 25 °C Time = 36 h 130 rpm | (Yu et al. 2008) |

| Reactant | Reactant Details | Proposed Mechanism(s) | PFOA Conc. ($\mu g\ L^{-1}$) | PFOS Conc. ($\mu g\ L^{-1}$) | Matrix | Environmental Conditions | Source |
|---|---|---|---|---|---|---|---|
| | | | Capture (Cont'd) | | | | |
| **Sorption** | 0.6 mg $L^{-1}$ magnetic mesoporous carbon nitride adsorbent | Electrostatic attraction and hydrophobic adsorption | 280,000 >79 % removed | 280,000 >97 % removed | Aqueous | pH = 3.25 T = 25 °C Time = 180 m Stirred | (Yan et al. 2014) |
| **Sorption** | 10 g $L^{-1}$ aerobic activated sludge | Hydrophobic interaction with organic carbon, some electrostatic attraction | 576 (PFAS mix) >95 % removed (PFOS) >80 % removed (PFOA) | | Aqueous | pH = 3 T = 25 °C Time = 11 h 150 rpm | (Zhou et al. 2010b) |
| **Sorption** | 1 g $L^{-1}$ sterilized wastewater treatment sludge with 100 mM $Ca^{2+}$ | | 0.2 – 5 (PFAS mix) 49 % removed (PFOS) 14 % removed (PFOA) | | Aqueous | pH = 6 T = 25 °C Time = 48 h Aerobic | (Arvaniti et al. 2014a) |
| **Sorption** | 165 mM $H_2O_2$, 3 mM Fe(III), and 600 mg $L^{-1}$ humic acid | Humic acid oxidized by Fenton's reagent creates structure for chemical sorption | 41,410 >99 % removed No DF | - | Aqueous | pH = 2.7 T = 25 °C Time = 30 m | ( Santos et al. 2016) |
| **Sorption** | Organo-montmorillonites with hexadecyltrimethyl-ammonium bromide (HDTMAB) | Hydrophobic interaction and diffusion, followed by electrostatic interaction with HDTMAB | - | 100,000 >95 % removed | Buffered Aqueous | pH = 4.3 T = 5 °C Time = 32 h 150 rpm | (Zhou et al. 2010a) |
| **Sorption** | 0.05 g $L^{-1}$ nano-Fe3O4 embedded in fluorinated vermiculite | Selective adsorption due to fluorophilicity of sorbent material | 25,000 >99 % removed | 25,000 >99 % removed | Aqueous | pH = 6 T = 25 °C Time = 4 h 150 rpm | (Du et al. 2017) |

| Reactant | Reactant Details | Proposed Mechanism(s) | PFOA Conc. ($\mu g\ L^{-1}$) | PFOS Conc. ($\mu g\ L^{-1}$) | Matrix | Environmental Conditions | Source |
|---|---|---|---|---|---|---|---|
| **Oxidative** | | | | | | | |
| **Alkaline Ozonation** | Ozone injected at 4.2 L min$^{-1}$ | Direct electron transfer between ·OH, formed by ozone with optional $H_2O_2$ catalyst, and PFAS to form perfluorinated radicals; undergoes hydrolysis chain reaction | 50 85 % removed | 50 90 % removed | Aqueous | pH = 11 T = 25 °C Time = 4 hr Aerobic | (Lin et al. 2012) |
| **Alkaline Ozonation + $H_2O_2$** | Ozone injected at 4.2 L min$^{-1}$ with 20 % $H_2O_2$ | | 50, 5000 >99 % removed | 50, 5000 >99 % removed | Aqueous | pH = 11 T = 25 °C Time = 4 hr Aerobic | (Lin et al. 2012) |
| **Alkaline Persulfate (PS) + Heat** | 60 mM PS with heat | Thermal activation of PS forms sulfate radical ($SO_4^{\cdot-}$), which forms ·OH at high pH to oxidize PFASs | High conversion of PFASs precursors; negligible removal of PFOA/ PFOS | | Buffered Aqueous | pH = 12 T = 85 °C Time = 6 hr | (Houtz and Sedlak 2012) |
| **Alkaline Photolysis** | 68 mM NaOH with 32 W Hg lamp (254 nm) | Photodecomposition by removal of functional group, followed by direct removal of $CF_2$ groups or hydrolysis chain reaction | - | 20,004 92 % removed | 2-Propanol | T = 38 – 50 °C Time = 10 d Anoxic ($N_2$) | (Yamamoto et al. 2007) |
| **Electrochemical Degradation** | Boron-doped diamond anode | Kolbe electrolysis releases fluorine radicals as PFOA binds to electrode surface | 993,840 Fluoride produced | - | Aqueous Electrolyte Solution | Time = 360 min | (Guan et al. 2007) |
| **Electrochemical Degradation** | Ti/$RuO_2$ anode (2.5 mA cm$^{-2}$) | Direct electron transfer at anode, adsorption to anode surface | 13 >90 % removed 58 % DF | 18 90 % removed 98 % DF | Aqueous Electrolyte Solution | pH = 7.4 T = Room Time = 500 m Aerobic | (Schaefer et al. 2015) |

| Reactant | Reactant Details | Proposed Mechanism(s) | PFOA Conc. ($\mu g\ L^{-1}$) | PFOS Conc. ($\mu g\ L^{-1}$) | Matrix | Environmental Conditions | Source |
|---|---|---|---|---|---|---|---|
| **Oxidative (Cont'd)** | | | | | | | |
| **Fe(III) + H₂O₂** | 500 µM Fe(III) and 1 M $H_2O_2$ | Production of hydroperoxyl ($HO_2\cdot$) and superoxide ($O_2^{-}\cdot$), ·OH needed for propagation Nucleophilic attack | 100 89 % removed High DF | - | Aqueous | pH = 3.5 T = 20 °C Time = 150 m | (Mitchell et al. 2014) |
| **Fe(III) + Sunlight** | 480 µM Fe(III) with sunlight | Electron transfer between Fe(III) and PFAS, forms Fe(II) and fluorinated radical; ·OH released from UV excitement of $H_2O$ to oxidize PFASs; hydrolysis chain reaction | 20,000 98 % removed 13 % DF | - | Aqueous | pH = 4.6 T = Ambient Time = 28 d Aerobic | (Liu et al. 2013) |
| **Fe(III) + UV** | 100 µM Fe(III) and 23 W Hg lamp (254 nm) | | - | 10,000 Removed BDL (20) 58 % DF | Aqueous | pH = 3.6 T = 25 °C Time = 48 h Oxygenated | ( Jin et al. 2014) |
| **Fe(IV)** | Excess $Fe^{IV}O_4^{4-}$ | Oxidization of PFASs | 4515 – 7022 17 % removed No DF | 779 – 1252 34 % removed No DF | Buffered Aqueous | pH = 9 Time = 5 d | (Yates et al. 2014) |
| **Fenton's Reagent + UV** | 30 mM H₂O₂ and 2.0 mM Fe(II) with 9 W UV lamp (254 nm) | ·OH and/or Fe(II)-PFOA complex creates PFOA radical; hydrolysis chain reaction | 8282 95 % removed 53 % DF | - | Aqueous | pH = 3 Time = 5 h | (Tang et al. 2012) |
| **Fungal Degradation** | Fungal degradation in microcosm | Biodegradation | 100,000 Some F | 100,000 28 % removed Some F | Aqueous | Time = 28 d Aerobic | (Quinnan et al. 2013) |
| **H₂O₂ + Manganese Dioxide** | 3 M H₂O₂ with manganese dioxide | Breakdown via superoxide radicals, nucleophilic attack | ~80 ~47 % removed | - | Aqueous | pH = neutral to slightly basic | (Geo-Cleanse International Inc. 2017) |

| Reactant | Reactant Details | Proposed Mechanism(s) | PFOA Conc. ($\mu g\ L^{-1}$) | PFOS Conc. ($\mu g\ L^{-1}$) | Matrix | Environmental Conditions | Source |
|---|---|---|---|---|---|---|---|
| **Oxidative (Cont'd)** | | | | | | | |
| **Heteropolyacid Photocatalyst + UV** | 6.68 mM of tungstic heteropolyacid (HPA) photocatalyst with 200 W Xe-Hg lamp (UV-visible) | HPA forms radical through UV excitement, electron transfer to form PFAS radical; photo-Kolbe hydrolysis to break C-COOH | 559,035 90 % removed 34 % DF | - | Aqueous | pH = 0.8 T = Room P = 0.48 MPa Time = 24 h Aerobic | (Hori et al. 2004) |
| **Nanozox™** | 1260 ppmV $O_3$ nano-bubbles with 10 % $H_2O_2$ | Formation of $HO_2\cdot$ and $O_2^{-\cdot}$, nucleophilic attack | 74 % removed | 82 % removed | Aqueous | Time = 3 h | (Strajin and Kerfoot 2012) |
| **Permeable Reactive Barrier** | Calcium peroxide mixed with granular activated carbon, clay, and humification enzymes | Enzyme-catalyzed oxidative humification | 67 Up to 85 % removed | - | Aqueous | Time = 6 d | (Huang 2013; Luo and Sidhu 2013) |
| **Photodegradation** | 185 nm vacuum ultraviolet (VUV) light | VUV creates PFAS radical, undergoes hydrolysis chain reaction | 25,000 62 % removed 17 % DF | - | Aqueous | pH = 3.7 T = 40 °C Time = 2 h Anoxic ($N_2$) | (Chen et al. 2007) |
| **Permanganate + Heat** | 8.4 µM permanganate with heat | Oxidation at C-S or C-C bonds to release $CF_2$ or $SO_4^{2-}$ | - | 100 47 % removed 5 % DF | Buffered Aqueous | pH = 4.2 T = 65 °C Time = 18 d | (Liu et al. 2012b) |
| **Persulfate (PS) + AC + Heat** | 60 mM PS with 10 g/L AC | Oxidative degradation of PFOA after pre-concentration by AC; chain reaction producing shortened perfluorinated radicals | 49,940 ~85 % removed 80 % DF | - | Aqueous | T = 45 °C Time = 12 h | (Lee et al. 2013) |

| Reactant | Reactant Details | Proposed Mechanism(s) | PFOA Conc. ($\mu g\ L^{-1}$) | PFOS Conc. ($\mu g\ L^{-1}$) | Matrix | Environmental Conditions | Source |
|---|---|---|---|---|---|---|---|
| **Oxidative (Cont'd)** | | | | | | | |
| **PS + Heat** | 200 mM PS | Thermal activation of $S_2O_8^{2-}$ forms $SO_4^{\cdot-}$, electron transfer to produce PFAS radical; hydrolysis chain reaction with $O_2$ to produce perfluoroperoxy radicals See above. | 100,005 Removed BDL (180) 98 % DF | - | Aqueous | pH = 2.5 T = 40 °C Time = 218 h Aerobic | (Lee et al. 2012a) |
| **PS + Heat** | 2 mM PS | | 8,282 90 % removed 24 % DF | - | Aqueous | pH < 3 T = 50 °C Time = 100 h | (Yin et al. 2016) |
| **PS + Heat** | 10 mM PS | | 207 94 % removed 44 % DF | - | Aqueous | T = 85 °C Time = 30 h | (Liu et al. 2012a) |
| **PS + Heat** | 42 mM PS | | 500 ~95 % removed 13 % DF | No removal | Aqueous | T = 50 °C Time = 31 h | (Park et al. 2016a) |
| **PS + Heat** | 50 mM PS | | 154,873 Removed BDL (629) 78 % DF | - | Aqueous | T = 80 °C P = 0.8 MPa Time = 6 h Aerobic | (Hori et al. 2008) |
| **PS + Heat** | 18.5 mM PS | | - | 100,000 26 % DF | Aqueous | Heated pH = 3.11 Time = 12 h | (Yang et al. 2013) |
| **PS + Heat** | 50 mM PS with heat from 70 W microwave power | | 105,099 Removed BDL (180) 80 % DF | - | Aqueous | pH = 3.6 T = 90 °C P = 18 psi Time = 6 h Aerobic | (Lee et al. 2009) |
| **PS + Heat** | 10 mM PS with heat from 70 W microwave power | | 105,181 >80 % removed 30 % DF | - | Aqueous | pH = 2.5 T = 90 °C P = 18 psi Time = 4 h Aerobic | (Lee et al. 2012b) |

123

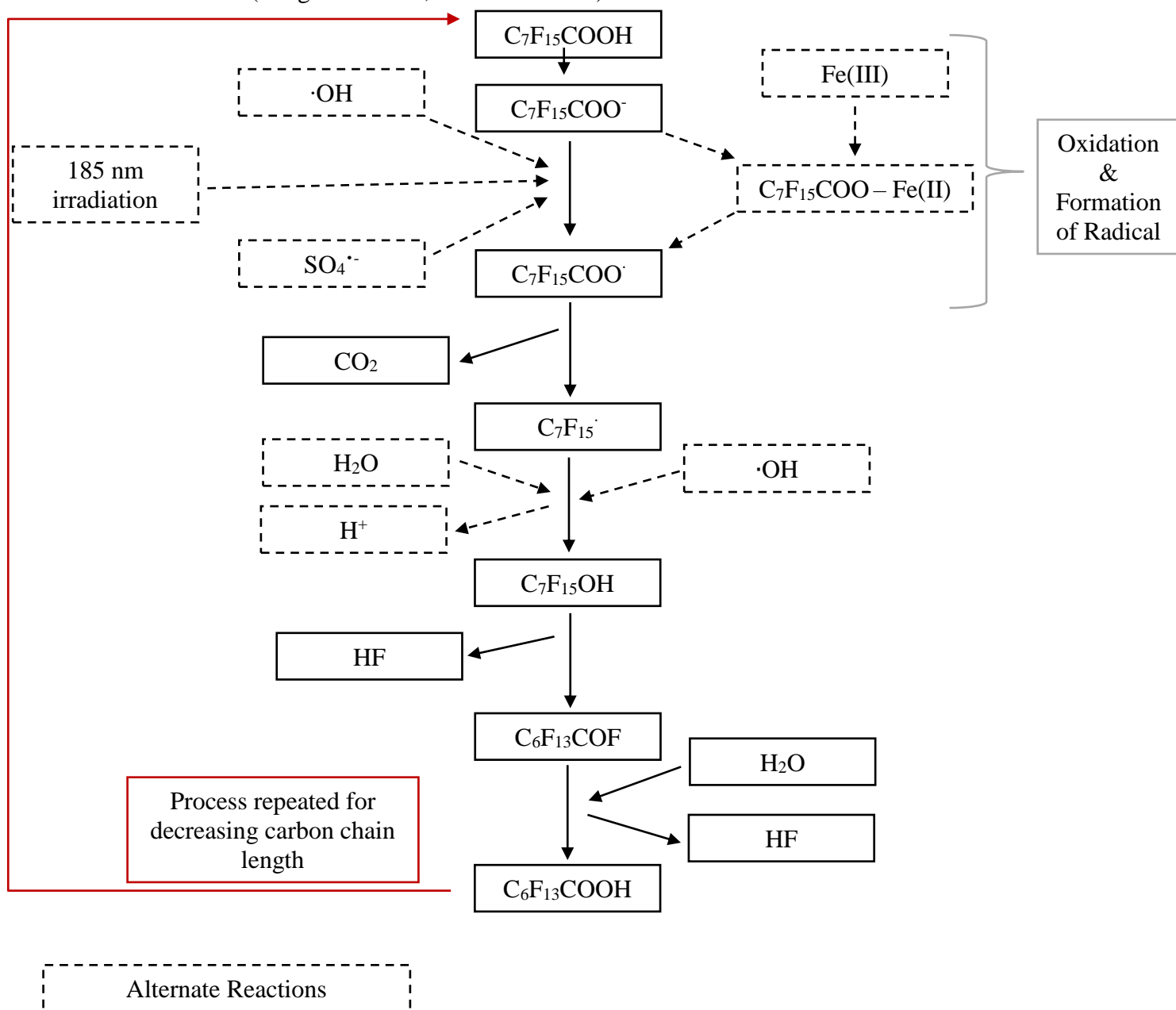| Reactant | Reactant Details | Proposed Mechanism(s) | PFOA Conc. ($\mu g\ L^{-1}$) | PFOS Conc. ($\mu g\ L^{-1}$) | Matrix | Environmental Conditions | Source |
|---|---|---|---|---|---|---|---|
| **Oxidative (Cont'd)** | | | | | | | |
| **PS + Heat** | 100 mM PS | | 41,410 Removed BDL >95 % DF | - | Aqueous | pH = 2.9 T = 70 °C Time = 20 h | ( Santos et al. 2016) |
| **PS + Heat + ZVI** | 5 mM PS and 3.6 mM ZVI with heat from 70 W microwave power | ZVI assists generation of $SO_4^{\bullet-}$, same mechanism as PS + Heat | 99,674 68 % removed 23 % DF | - | Aqueous | T = 90 °C P = 18 psi Time = 2 h Aerobic | (Lee et al. 2010) |
| **PS + UV** | 50 mM PS with 200 W Xe-Hg lamp (254 nm) | Photolysis of $S_2O_8^{2-}$ forms $SO_4^{\bullet-}$ and produces PFAS radical; undergoes hydrolysis chain reaction | ~560,000 Removed BDL (630) 74 % DF | - | Aqueous | pH = 3 T = 25 °C P = 480 kPa Time = 12 h Aerobic | (Hori et al. 2005) |
| **PS + UV** | 1.5 mM PS with 23 W Hg lamp (185 nm & 254 nm) | Direct photolysis or reaction with $SO_4^{\bullet-}$ to form PFAS radical, hydrolysis chain reaction | 25,000 87 % removed >42 % DF | - | Aqueous | T = 25 °C Time = 120 m Aerobic | (Chen and Zhang 2006) |
| **SCISOR** | Peroxysulfur (10-1000 mM), permanganate (1-10 mM) | Oxidation by both peroxysulfur and permanganate | 5 > 50 % removed | 30 >75 % removed | Aqueous or Soil Mixture | pH = 5 – 9 T = 10 – 15 °C | (Pancras et al. 2013) |
| **TiO$_2$ Photocatalyis** | 2.0 g $L^{-1}$ TiO$_2$ added with 1500 W $L^{-1}$ (310 – 400 nm) | Adsorption and oxidation by TiO$_2$ electrode | 1,822,040 50 % DF | - | Aqueous | pH = 1 Time = 60 d Oxygenated | (Vecitis et al. 2009) |
| **Reductive Methods** | | | | | | | |
| **B12 + Heat + Ti(III)-Citrate** | 260 $\mu$M B12 and 36 mM Ti(III)-citrate with heat | B12-carbon centred radical, creates reductive dehalogenation | - | 27,005 71 % DF (branched); 166,033 18 % DF (linear) | Buffered Aqueous | pH = 9 T = 70 °C Time = 7 d Anaerobic Dark | (Ochoa-Herrera et al. 2008) |

| Reactant | Reactant Details | Proposed Mechanism(s) | PFOA Conc. ($\mu g\ L^{-1}$) | PFOS Conc. ($\mu g\ L^{-1}$) | Matrix | Environmental Conditions | Source |
|---|---|---|---|---|---|---|---|
| **Reductive Cont'd** | | | | | | | |
| **B12 + Ti(III)-Citrate + Cu** | 200 μM B12, 45 mM Ti(III)-citrate, and 2 g $L^{-1}$ copper | Catalyzed reductive defluorination, in addition to direct electron transfer from Ti(III)-citrate | 50,000 65 % removed | - | Aqueous | pH = 9 T = 70 °C Anoxic | (Lee et al. 2017) |
| **H₂O₂ + PS + Fe-diatomite** | 0.5 M H2O2 with 0.3 M PS and 8.3 g $L^{-1}$ Fe-modified diatomite | Superoxide radicals used for reductive degradation | 9938 65 % removed | - | Aqueous | pH = 9 T = Room Time = 6 h | (da Silva-Rackov et al. 2016) |
| **Mg-Aminoclay + nZVI** | 1000 mg $L^{-1}$ Mg-aminoclay coated nZVI | Electrostatic attraction to coating, reduction by ZVI through dehydrohalogenation | 200 (PFC mix) ~96 % removed (PFOS) 38 % removed (PFOA) | | Buffered Aqueous | pH = 3 T = 20 °C P = Atm. Time = 1 h Anaerobic | (Arvaniti et al. 2015) |
| **Sulfite + UV** | 20 mM sulfite ($SO_3^{2-}$) with 10 W Hg lamp (254 nm) | Generation of hydrated electrons (photolysis of $SO_3^{2-}$ in N₂), defluorination closest to functional group | 8282 100 % removed 89 % DF | - | Aqueous | pH = 10.3 T = 25 °C Time = 24 h Anoxic (N₂) | (Song et al. 2013) |
| **Zero-Valent Metal Reduction + B12** | Pd/Fe, Mg, or Pd/Mg synthesized within clay interlayers with B12 | Abiotic reduction to defluorinate PFASs | SERDP Grant | | Aqueous | pH = 4 – 9 | (Lee 2009) |
| **ZVI + Heat** | 9.6 mM ZVI and heat | Sorption onto ZVI and mineralization on surface | - | 186,037 Removed BDL (1100) 51 % DF | Aqueous | T = 350 °C Pressurized Time = 6 h Anoxic (Ar) | (Hori et al. 2006) |

| Reactant | Reactant Details | Proposed Mechanism(s) | PFOA Conc. ($\mu g\ L^{-1}$) | PFOS Conc. ($\mu g\ L^{-1}$) | Matrix | Environmental Conditions | Source |
|---|---|---|---|---|---|---|---|
| **Thermolytic** | | | | | | | |
| **Calcium + Heat** | 1:1 (molar) Ca:F with heat | Defluorination from reaction with $Ca(OH)_2$, CaO provides additional reduction sites | ~50 % DF | 90 % DF | Solid Waste Mixture | T = 900 °C Time = 15 m Aerobic | (Wang et al. 2015) |
| **Sonochemical Degradation** | Ultrasonic irradiation (6.36 W cm$^{-2}$) | Pyrolysis at bubble interface splits at functional group, small potential for ·OH oxidation | 99 >99 % removed >89 % DF | 100 >91 % removed >82 % DF | Aqueous | pH = 7 – 8 T = 10 °C Time = 180 m Anoxic (Ar) | (Vecitis et al. 2008) |
| **Sonochemical Degradation** | Ultrasonic irradiation (3 W cm$^{-2}$) | Pyrolysis at interface, removes functional group, some oxidation of fluorinated radicals by ·OH | 10,000 85 % removed 64 % DF | 10,000 60 % removed 51 % DF | Aqueous | pH = 4.8 T = 20 °C Time = 60 m Anoxic (Ar) | (Moriwaki et al. 2005) |
| **Sonozone** | 2.5 % (v/v) ozone/ oxygen at 0.5 L min$^{-1}$ and 250 W L$^{-1}$ | Interfacial pyrolysis, ·OH destroys scavengers | 100 >98 % removed | 100 >93 % removed | Site ground-water | T = 10 °C Time = 140 m | (Cheng et al. 2008) |

# Appendix B: Schematics of Removal Mechanisms

Oxidation of PFOA (Tang et al. 2012; Hori et al. 2008)



$C_7F_{15}COOH$

$\cdot OH$

$C_7F_{15}COO^-$

Fe(III)

185 nm irradiation

$C_7F_{15}COO - Fe(II)$

Oxidation & Formation of Radical

$SO_4^{\cdot-}$

$C_7F_{15}COO^\cdot$

$CO_2$

$C_7F_{15}^\cdot$

$H_2O$

$\cdot OH$

$H^+$

$C_7F_{15}OH$

HF

$C_6F_{13}COF$

$H_2O$

HF

Process repeated for decreasing carbon chain length

$C_6F_{13}COOH$

Alternate Reactions

Reduction of PFOA (Song et al. 2013)



```
                          C₆F₁₃CF₂COOH
                                │         e_aq⁻ ┐
                                │ ◄──────────── │
                                ▼                ├── Reduction &
                                      ──► F⁻      │   Dehalogenation
                          C₆F₁₃CFHCOOH            │
          e_aq⁻ ──────────►    │
             F⁻ ◄──────────    │
                                ▼                ┘
                          C₆F₁₃CH₂COOH
                   ┌────────────┼────────────┐
                   ▼            ▼            ▼
              C₆F₁₃·          CH₂          ·COOH     ┐
                   │                         │        │
   ┌───────────────┼──┐                      │        ├── Radical
   │ Process repeated  │                     │        │   Degradation
   │ for decreasing    │      C₆F₁₃COOH      │        │   (Unknown
   │ carbon chain      │      (C₅F₁₁CF₂COOH) │        │   Catalysis)
   │ length            │                              ┘
   └───────────────────┘
```

$C_6F_{13}CF_2COOH$

$e_{aq}^-$

$F^-$

Reduction & Dehalogenation

$C_6F_{13}CFHCOOH$

$e_{aq}^-$

$F^-$

$C_6F_{13}CH_2COOH$

$C_6F_{13}\cdot$

$CH_2$

$\cdot COOH$

Radical Degradation (Unknown Catalysis)

Process repeated for decreasing carbon chain length

$C_6F_{13}COOH$
$(C_5F_{11}CF_2COOH)$

Oxidation of PFOS (Yamamoto et al. 2007; Jin et al. 2014; Lee et al. 2012a)

# Appendix C: Supplementary Information for Chapter 4

Table C.1. Concentration ($\mu g\ L^{-1}$) of C4 – C7 PFCAs in the C-PS/60°C and C-BLANK/60°C controls systems for OSS, BS, and SRS

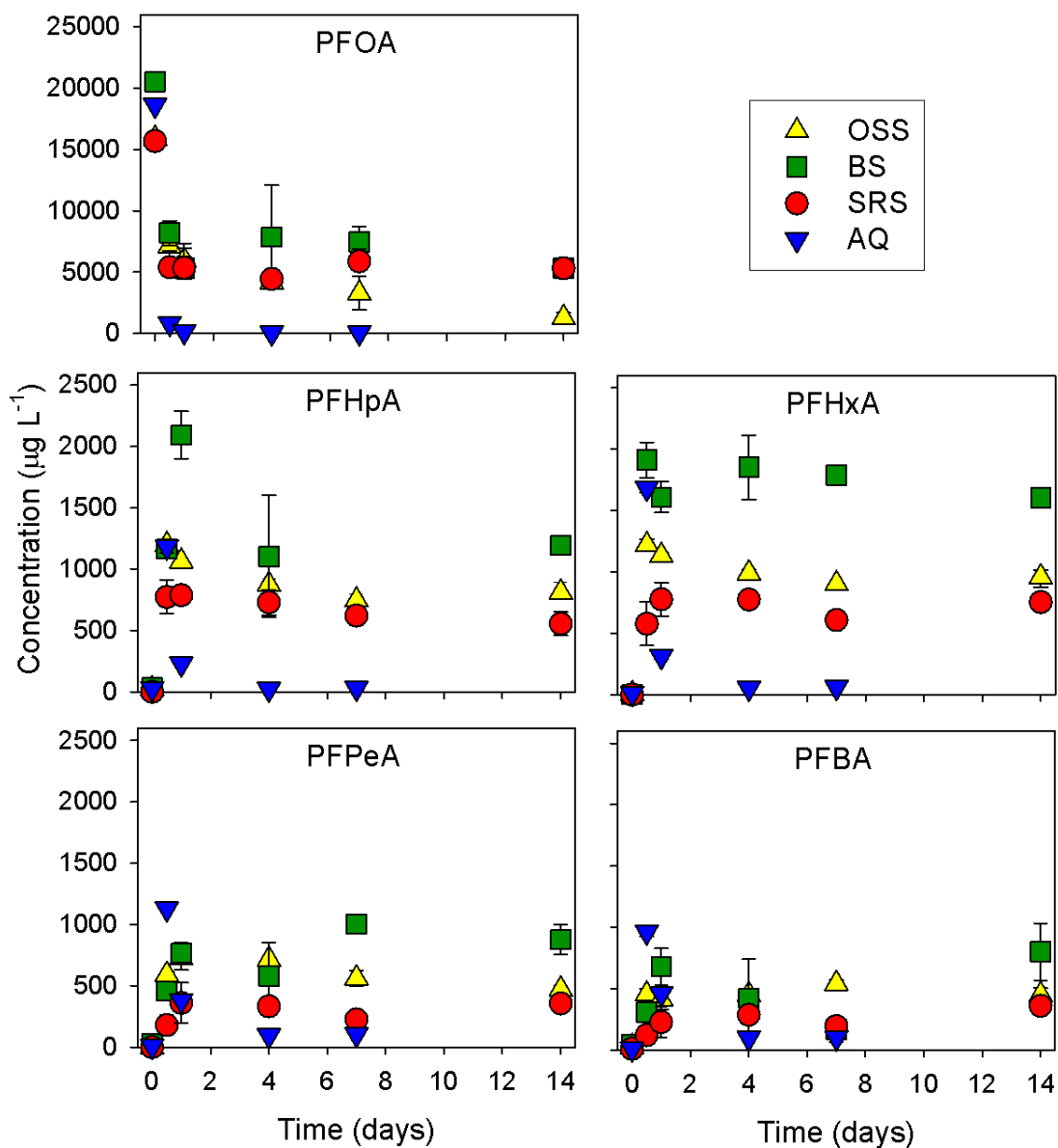| Sediment | Control | Concentration ($\mu g\ L^{-1}$) | | | | | | | |
|---|---|---|---|---|---|---|---|---|---|
| | | Day 0 | | | | Day 7 | | | |
| | | PFHpA | PFHxA | PFPeA | PFBA | PFHpA | PFHxA | PFPeA | PFBA |
| **OSS** | C-PS/60°C | 0.86 | 4.63 | 2.82 | 15.07 | 0.00 | 15.74 | 0.00 | 2.23 |
| | C-BLANK/60°C | 0.29 | 1.29 | 0.64 | 3.33 | 0.00 | 3.84 | 0.00 | 5.27 |
| **BS** | C-PS/60°C | 5.65 | 0.00 | 14.04 | *22.10* | 0.00 | 6.83 | 0.00 | *25.98* |
| | C-BLANK/60°C | 3.23 | 0.00 | 7.11 | *52.78* | 0.00 | 1.04 | 0.00 | *13.00* |
| **SRS** | C-PS/60°C | 0.00 | 0.00 | 0.17 | 35.02 | 0.00 | 1.88 | 3.52 | 3.66 |
| | C-BLANK/60°C | 0.00 | 0.00 | 0.03 | 3.81 | 0.00 | 0.49 | 0.96 | 7.20 |

Figure C.1. Aqueous PFOA, PFHpA, PFHxA, PFPeA, and PFBA concentrations ($\mu$g L$^{-1}$) for all thermally-activated persulfate treatment experiments (T-PS/60°C) at a lengthened experimental period (14 days). Each point is the average of duplicated measurements, with maximum and minimum error bars.
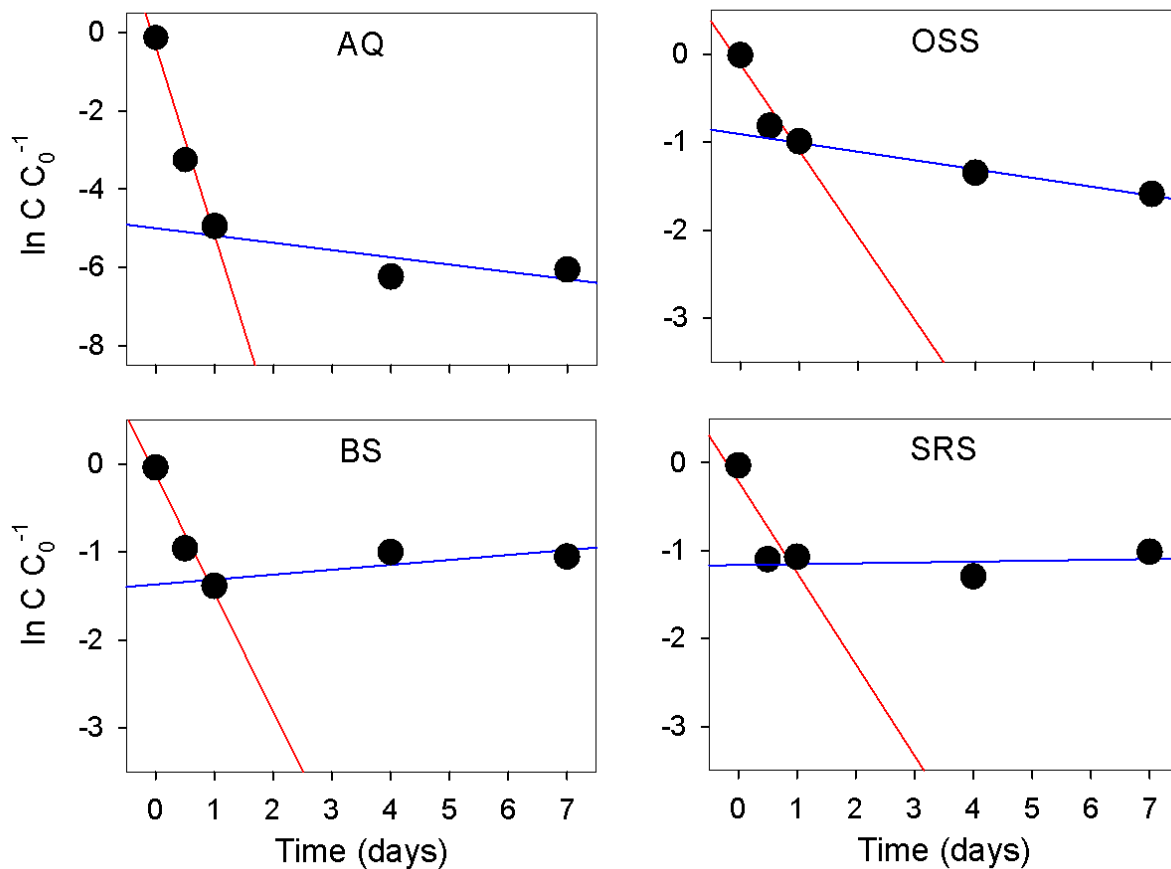
Figure C.2. Pseudo-first-order kinetic plots for the AQ, OSS, BS, and SRS T-PS/60°C systems. Removal of PFOA (theoretical initial concentration 15000 µg $L^{-1}$) was observed in the presence of thermally-activated (60 °C) PS (50 mM) in $NaHCO_3$ simulated groundwater. Kinetic behaviour was split into rapid degradation (0 – 1 days, red line) and slow degradation (1 – 7 days, blue line).

Table C.2. Concentration (µg g⁻¹) of PFOA and the sum of C4 – C8 PFCAs from the extraction process for sediments (OSS, BS, and SRS) in the treatment (T-PS/60°C, T-PS/20°C) and control (C-PFOA/60°C, C-PS/60°C, C-BLANK/60°C) systems.

| Sediment | Control | Concentration (µg g⁻¹) | | | | | | | | | |
| --- | --- | --- | --- | --- | --- | --- | --- | --- | --- | --- | --- |
| | | Day 0 | | Day 0.5 | | Day 1 | | Day 4 | | Day 7 | |
| | | Sum PFCAs | PFOA | Sum PFCAs | PFOA | Sum PFCAs | PFOA | Sum PFCAs | PFOA | Sum PFCAs | PFOA |
| OSS | T-PS/60°C | 0.45 | 1.60 | 1.84 | 2.00 | 0.75 | 1.63 | 0.33 | 1.33 | 0.00 | 1.07 |
| | T-PS/20°C | 0.45 | 1.60 | | | | | | | 1.25 | 2.35 |
| | C-PFOA/60°C | 0.38 | 1.49 | | | 0.70 | 1.85 | 1.74 | 2.88 | 1.01 | 2.03 |
| | C-PS/60°C | 0.24 | 0.39 | | | | | | | 0.00 | 1.17 |
| | C-BLANK/60°C | 0.15 | 0.31 | | | | | | | 0.00 | 1.06 |
| BS | T-PS/60°C | 1.16 | 1.19 | 2.61 | 2.61 | 1.77 | 1.82 | 0.98 | 1.07 | 1.06 | 1.11 |
| | T-PS/20°C | 1.16 | 1.19 | | | | | | | 2.10 | 2.10 |
| | C-PFOA/60°C | 1.12 | 1.13 | | | 1.46 | 1.48 | 1.52 | 1.54 | 1.39 | 1.42 |
| | C-PS/60°C | 0.26 | 0.27 | | | | | | | 0.28 | 0.29 |
| | C-BLANK/60°C | 0.42 | 0.43 | | | | | | | 0.27 | 0.28 |
| SRS | T-PS/60°C | 5.17 | 5.24 | 19.37 | 19.41 | 17.70 | 17.80 | 8.72 | 9.16 | 10.57 | 11.11 |
| | T-PS/20°C | 4.33 | 4.67 | | | | | 12.09 | 12.51 | 14.77 | 15.19 |
| | C-PFOA/60°C | 2.49 | 2.55 | | | 3.91 | 4.00 | 0.00 | 0.03 | 0.42 | 0.42 |
| | C-PS/60°C | 0.05 | 0.10 | | | | | | | 0.07 | 0.13 |
| | C-BLANK/60°C | 0.08 | 0.14 | | | | | | | 0.10 | 0.15 |
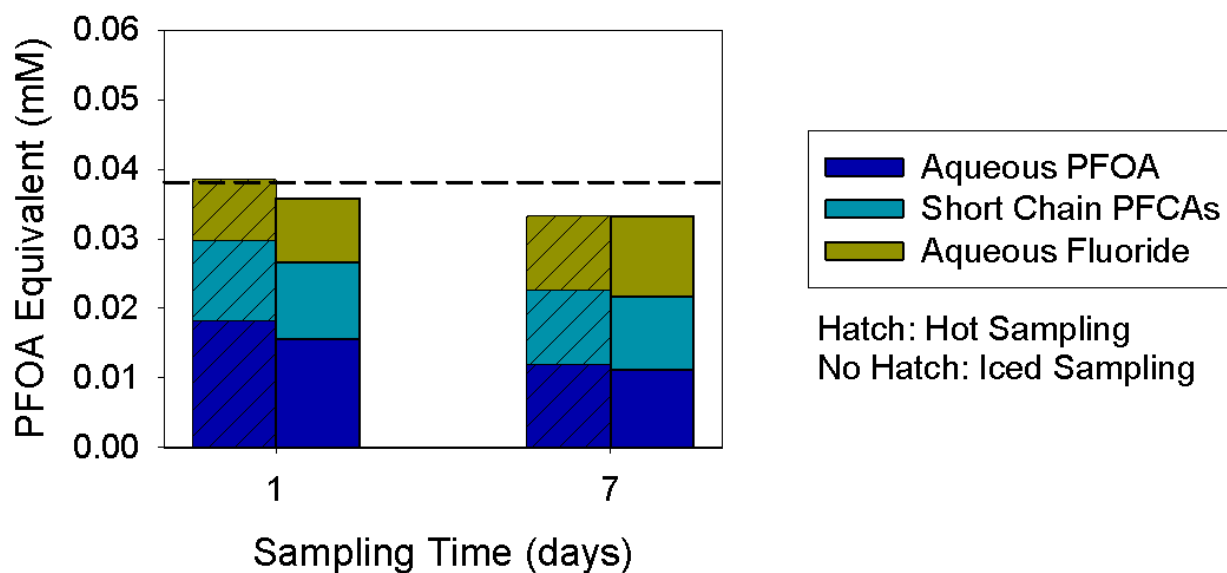
Figure C.3. The effects of sampling temperature on calculated mass balances (mM) for OSS thermally-activated persulfate treatment (T-PS/60°C). Duplicated reactors were created with identical conditions (60 °C, 50 mM PS, 20 g sediment: 30 mL aqueous phase). The data from hot sampling is hatched, while the data from sampling after ice-quenching has no hatch. The theoretical PFOA spike was 0.0381 mM, shown on the graph as a dashed line.